The Elastocoast® system
A study of possible failure mechanisms

MSc. Thesis report of E. Bijlsma

September 2008

Elastogran

BASF Group

ARCADIS
Infrastructure, environment, facilities

TUDelft
Delft University of Technology

The Elastocoast® system
A study of possible failure mechanisms

Report

MSc. Thesis of E. Bijlsma

Graduation committee:
Prof. drs. ir. J.K. Vrijling
Ir. H.J. Verhagen
Ir. J.A. den Uijl
Dr. ir. H.G. Voortman

Delft University of Technology
Faculty of Civil Engineering and Geosciences
Section Hydraulic Engineering

Preface

In this report research is done after the possible failure mechanisms of an experimental, polymer based dike revetment: Elastocoast. Elastocoast is a product of the German company Elastogran GmbH (subsidiary of BASF), which is specialized in the development and application of polyurethane products. Elastogran has approached the Delft University of Technology (DUT) and the Dutch engineering company ARCADIS for further research of the product, in order to introduce it to the Dutch market.

The thesis work actually comprises two separate parts, for which also separate reports have been produced. For ARCADIS work was done in the field; two pilot tests with a total area of 875 m^2 were monitored from the moment of their construction throughout the storm season. Useful information about the damage and behaviour of the prototypes in 'real life' conditions was obtained and presented in a separate report "Elastocoast pilots in the Netherlands, storm season 2007/2008" (Bijlsma, 2008). The setup of the Dutch pilot tests, however, did not give further insight into macro scale failure mechanisms.

Parallel to the field work, a desk study was done for the DUT, investigating the possible failure mechanisms of an Elastocoast revetment. Findings of this study are presented in the present thesis report. This report makes use of the results from the field work, and from a previous study into the mechanical properties of Elastocoast at the DUT (Gu, 2007a and 2007b). With these results combined, theoretical research is done after the behaviour and limitations of an Elastocoast revetment under extreme conditions.

A new temporary committee ("*klankbordgroep*") is planned to be erected in the near future, within the framework of the Dutch Expertise Network for Flood Protection (ENW). An objective of this committee will be to create a Technical Report, which will give guidelines for the design and construction of polymer revetments. With the present thesis study preliminary work is done, that can aid in the development of this Technical Report.

Egon Bijlsma

September 2008
e.bijlsma@gmail.com

Table of contents

Summary

Introduction

Elastocoast is a new type of revetment system for use as a cover layer on dikes. It consists of granular material (rocks), which is fixed together with a two-component polyurethane adhesive. In the Elastocoast system each individual rock is covered with a thin film of polyurethane. When the adhesive is cured, this film fixes the rocks together only on their contact points, creating a highly permeable, open structure.

From 2004-2007 several Elastocoast pilot tests were performed along the North-Sea islands in the most northern part of Germany. After the pilots in Germany, ARCADIS and Delft University of Technology have been involved in further research which is necessary for the introduction of Elastocoast on the Dutch market. Two pilot tests were constructed in the Netherlands in September and October of 2007.

The application of polymers as a binding material in dike revetments is new to the hydraulic engineering community. Design criteria or construction guidelines for these revetments, including the Elastocoast system, are therefore not readily available. Now, for Elastocoast such a set of design criteria and construction guidelines must be developed.

Objectives

The purpose of this MSc thesis study is to make a first step in the development of design tools for the Elastocoast system (and implicitly for similar polymer bonded revetments). The following objectives are formulated:

- Make an inventory of possible failure mechanisms for Elastocoast revetments.
- Eliminate those mechanisms that are not dominant and quantify those that are.
- Make a proposal for design criteria and construction guidelines where possible.
- Make recommendations for further research into those mechanisms and parameters that could not be quantified.

Failure mechanisms

On basis of theoretical considerations and experience from the field a list failure mechanisms and their relevance were determined:

- Micro scale instability (erosion)
    - *By tidal flows (not relevant)*
    - *By orbital flow (not relevant)*
    - *By wave breaking combined with wave up- and down-rush (relevant and quantified)*
    - *By overtopping discharge (not relevant)*
- Mechanical failure
    - *Breakage by wave impact (relevant and quantified)*
- Macro scale instability
    - *Uplift by static head difference (not relevant)*
    - *Uplift by dynamic head difference, at maximum wave retreat (relevant and quantified)*
    - *Uplift by dynamic head difference, at wave impact (relevant but not quantified)*
    - *Shear plane or circular slip plane (not relevant)*
    - *Soil liquefaction under repeated wave impact (relevant but not quantified)*
- Material degradation
    - *Fatigue (relevant but not quantified)*
    - *Exposure to aggressive environment (relevant but not quantified)*

Detailed analysis

A detailed analysis was performed for three relevant mechanisms and also for the influence of clogging on the permeability of Elastocoast.

Instability of individual rocks (erosion)

The wave conditions that the Elastocoast revetment has proven to be able to withstand in the Dutch pilot tests are used as input for established stability formulae for loose rock, respectively: Hudson, Van der Meer and Pilarczyk. Thus upgrading factors can be back-calculated that take the structure coherence into account. Only the Pilarczyk formula allows the layer thickness to be used as characteristic system size instead of the nominal rock diameter.

Breakage by wave impact

The response of the plate structure at wave impact is schematized in a structural model as a semi-infinite, elastically supported beam under a constant, triangular shaped wave load (Figure 1). For this problem the static solution is found. The model includes the possibility of a cavity in the foundation right under the wave load. From the model values for the maximum stress and displacement in the middle under the load can be calculated. Figure 2 shows the minimum required layer thickness depicted as a function of wave height.
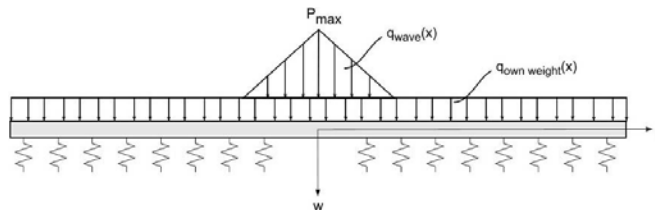
Figure 1 Schematization of a triangular wave load on a partially supported cover layer.
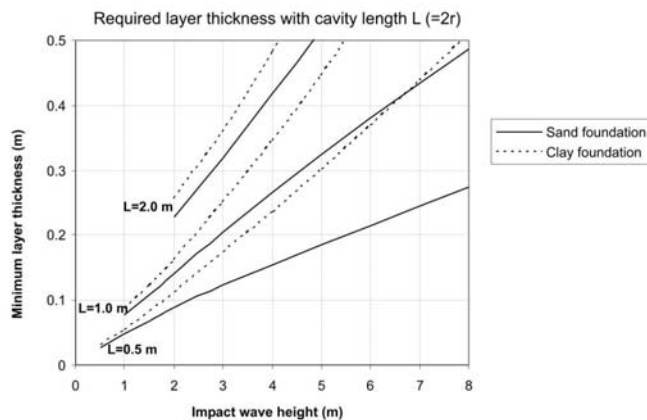
Figure 2 Required layer thicknesses as a function of impact wave height. Assumed are a Young's modulus of 2500 MPa and a flexural strength of 2.5 MPa.

Influence of clogging on the permeability of Elastocoast

The influence of clogging on the hydraulic conductivity of a porous structure is predicted theoretically. Standard filter rules are used to find the conductivity of the porous structure. Then the combined conductivity of the porous structure with clogging material in its pore space is calculated in analogy with an electric circuit with the electrical resistances put in a series. Thus, the joint conductivity is estimated.

Instability by uplift pressures

Once the hydraulic conductivity of the clogged Elastocoast structure is known, its stability is investigated with two separate approaches: 1) the leakage length theory, which takes into account flow through the cover layer but neglects structural coherence; and 2) a structural analysis, which neglects the reduction of pressure by leakage through the cover layer, but incorporates both the structure weight and moment capacity.
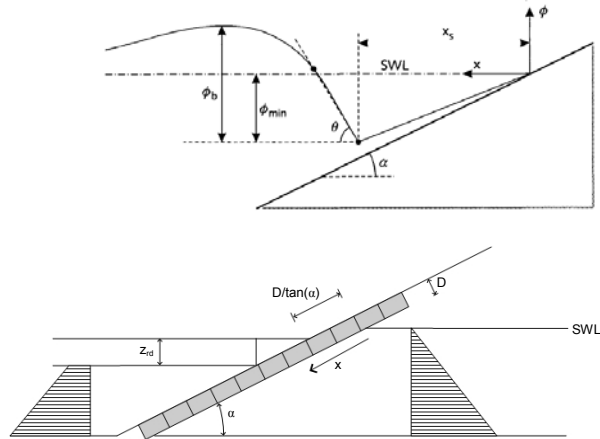
Figure 3 Two different approaches of the stability of a cover layer at the moment of maximum wave retreat: the leakage length theory (above) and the structural analysis (below).

Figure 4 shows that the spread in the results from the leakage length theory is fairly high, especially for the case in which Elastocoast is placed on top of a sand bed. For design purposes the line described by structural analysis has the most practical value. Though overestimating the overpressures behind the cover layer, this method incorporates both the structure weight as the structure coherence in the stability function of Elastocoast. Concluding, a save way to assess the stability of a cover layer design is by using the following expression from structural analysis:

$$\frac{H_s}{\Delta D} = \frac{3\cos(\alpha)}{\xi} \cdot \left(2 + \sqrt[3]{\frac{\sigma \cdot \tan^2(\alpha)}{\Delta^3 \cdot \rho_w \cdot D \cdot g \cdot \cos(\alpha)}} \right)$$
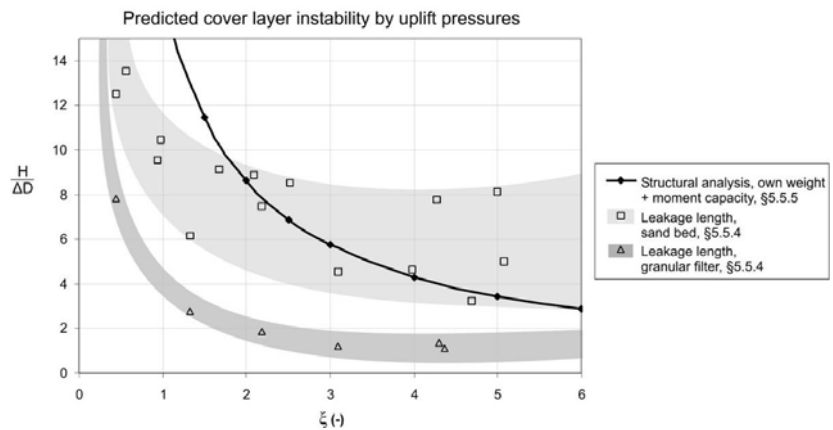
Figure 4 Stability of an Elastocoast cover layer under maximum wave retreat according to structural analysis and leakage length theory.

Conclusions

The conclusions from detailed analysis in this report are summarized below.

Micro scale instability by wave breaking (erosion)
Because of the polyurethane bonding, the stability of individual rocks in an Elastocoast cover layer is extremely high when compared to traditional rock based revetments. The physical processes that lie at the base of traditional stability formulas for rock armours are therefore not adequate to describe the stability of individual rocks in an Elastocoast cover layer. Thus, the use of these formulas for prediction of erosion is advised against. Based on this analysis, together with results from the Dutch pilot studies, erosion is not considered to be a problem for Elastocoast revetments.

Mechanical failure by wave impact
From calculations with a structural model, it is concluded that, in case of proper continuous support, the maximum tension in the bottom of the cover layer will not exceed the bending strength of the material. A lower compression constant of the foundation leads to higher stresses in the cover layer when loaded, but even on a soft clay foundation the maximum tension will not exceed the bending strength.

It appears that the maximum tension in the bottom of the loaded cover layer increases significantly when a cavity is present. Stresses increase when the cavity size increases, and also when the soil compression constant is lowered. Tensile strength is then easily exceeded, if the thickness of the layer is not sufficient.

The influence of clogging on the Hydraulic conductivity of Elastocoast
A calculation method that is developed for prediction of the hydraulic conductivity of granular filters is found to be also applicable to Elastocoast. Clogging of the open structure of Elastocoast strongly reduces its hydraulic conductivity. If the conductivity of the filling material is much smaller than the conductivity of the carrying material (which is the case for Elastocoast filled with sand), the joint hydraulic conductivity can be estimated with $k_v = k_s \cdot n_T$, which is the hydraulic conductivity of the filling material, multiplied by the porosity of the carrying material.

Macro scale instability by dynamic head difference at maximum wave retreat
When the Elastocoast structure retains its high permeability, instability by uplift under maximum wave retreat is not expected. Clogging of the open pore space gives the structure a higher weight but also strongly reduces the hydraulic conductivity. The net effect on stability is negative. Whether clogging can occur, depends on the local conditions and structure build up.

From the model according to the leakage length theory, it is concluded that the pressure leakage through the clogged cover layer is significant, so that the structure weight already provides a high stability. From the model based on structural analysis, it is concluded that the contribution of structure coherence (in this case defined by moment capacity) to stability is greater than that of structure weight. Of the two models, the structural analysis best describes the mechanisms that contribute to the resistance of an Elastocoast revetment against uplift pressures and is therefore considered to be most suitable for use in design tools.

Recommendations

After the analysis done in this study, some failure mechanisms remain still to be researched. Also, from the models presented in this report, a suggestion can be done where further research into system and structural parameters is useful.

Elimination or quantification of remaining mechanisms
As mentioned above, the failure mechanisms that need further research are:

- Macro scale instability
    - *Uplift by dynamic head difference, at wave impact*
    - *Soil liquefaction under repeated wave impact*
- Material degradation
    - *Fatigue*
    - *Exposure to aggressive environment*

Further research into material (strength) parameters

In the models presented in this report, both for the resistance to breakage as for the resistance against uplift a structural approach appeared to be valid. In a structural approach material parameters such as the stiffness and flexural strength play a key role in the resistance of the cover layer against loads. This means that it is important that representative values for the material parameters and their uncertainties are correctly described.

Effect of clogging on stability

It remains unclear, whether clogging can actually be expected to be present during extreme conditions, or if it will be simply flushed out, leaving the cover layer fully permeable again. Though further research into the clogging behaviour of porous structures is a very interesting topic, it is not necessarily useful in the development of design tools for Elastocoast. Improvements can be made to the structural model that predicts the resistance of the (clogged) cover layer against uplift pressures. The incorporation of a pressure leakage factor to the structural model will lead to a quick insight of how a certain amount of pressure reduction translates into increase of stability. Then, it can be determined whether further quantification of this factor is profitable.

Further research into loading parameters

The schematization of hydraulic loading has been very straightforward in this report. Little knowledge is available of wave impact pressures on open, permeable revetments. Improved insight would lead to more favorable results for the failure mechanism of breakage by wave impact.

Also, the wave load in the model for mechanical breakage is a stochastic parameter with a certain probability of occurrence. The choice of a normative impact wave height should therefore be the result of probabilistic considerations.

List of symbols

Symbol	Definition	Unit
a_f	Linear coefficient of resistance in the Forchheimer theory	s/m
A	Surface area	m²
b	1. Exponent in the Pilarczyk formula 2. Width	- m
b_f	Turbulent coefficient of resistance in the Forchheimer theory	s²/m²
c	Coefficient of compression of soil [per meter]	N/m²/m
c_{pl}	Factor for plunging waves in the Van der Meer formula for shallow water [=8.4]	-
c_s	Factor for surging waves in the Van der Meer formula for shallow water [=1.3]	-
C_n	Integration constant with n=1,2,3,4	depends
d	1. Depth of cavity under cover layer 2. Rock diameter	m m
d_F	Thickness of filter layer	m
d_T	Thickness of cover layer	m
D	1. Characteristic rock size or diameter of element 2. Specific size or thickness of protection unit 3. Layer thickness	m m m
D_{15}	Rock diameter where 15% of the rock mass has a smaller diameter	m
D_{85}	Rock diameter where 85% of the rock mass has a smaller diameter	m
D_{n15}	Nominal rock diameter where 15% of the rock mass has a smaller nominal diameter	m
D_{n50}	Nominal rock diameter where 50% of the rock mass has a smaller nominal diameter	m
E	Young's modulus or E-modulus (stiffness)	N/m²
F_D	Drag force	N
F_F	Friction force	N
F_L	Lift force	N
F_S	Shear force	N
g	Gravitational acceleration	m/s²
h	Thickness	m
H	Wave height	m
$H_{2\%}$	Wave height exceeded by 2% of the waves	m
H_{m0}	Significant wave height determined from wave spectrum	m
H_s	Significant wave height [average height of 33% highest waves]	m
i	Hydraulic gradient	-
I	Electric current	Ampere
k	Hydraulic conductivity	m/s
k_F	Hydraulic conductivity of filter layer	m/s
k_T	Hydraulic conductivity of cover layer	m/s
k_s	Hydraulic conductivity of filling material [sand]	m/s
K	Bending stiffness of a thin plate $[=Eh^3/(12(1-v^2))]$	Nm

K_D	Stability coefficient in the Hudson stability formula	-
K_u	Upgrading factor in the Hudson stability formula	-
l	Length of cavity under cover layer	m
L	1. External load scale	m
	2. Length	m
M_{max}	Maximum value for bending moment [at x=0, per meter]	Nm/m
n	Porosity [=volume of voids/volume of total]	-
N	Number of incident waves	-
N_{od}	Damage percentage	%
N_s	Stability number	-
p	Pressure	N/m^2
P	1. Notional permeability	-
	2. Wave impact force	N/m
	3. Uplift pressure	N/m^2
P_{max}	Maximum impact pressure	N/m^2
q	1. Load function [q(x)]	N
	2. Empirical impact factor	-
	3. Rate of flow	m/s
Q	Rate of flow	m^3/s
R	Electrical resistance	Ω
S_d	Damage level parameter	-
T	Wave period	s
$T_{m-1,0}$	Energy wave period	s
T_p	Peak wave period	s
U	Flow velocity	m/s
V	Difference of electric potential	Volt
w	Deflection	m
w_{max}	Maximum value for deflection [at x=0]	m
W	1. (Submerged) rock weight	N
	2. Area moment of inertia [per meter]	m^4/m
	3. Weight component	N/m^2
x	Distance along horizontal axis	m
z	1. Half the base width of triangular load	m
	2. Half the length of cavity [$= 0.5l$]	m
$z_{2\%}$	2% wave run-up level	m
z_{rd}	wave run-down	m
α	1. Slope angle in degrees	°
	2. Slope angle in radians	-
β	Calculation parameter [$= \sqrt[4]{c/4K}$]	1/m
γ_b	Reduction factor for the presence of a (horizontal) berm in the dike profile	-
γ_f	Reduction factor for the roughness of the slope surface	-
γ_β	Reduction factor for the angle of approach for incoming waves	-
δ	Phase angle	°
Δ	Relative density [$= (\rho_r - \rho_w)/\rho_w$]	-
Δ_m	Relative density of a system-unit	-
ν	1. Constant of Poisson	-
	2. Kinematic viscosity	m^2/s
ε	Strain (relative elongation)	-

θ	Slope of wave front	°
Λ	Leakage length	m
ξ_0	Surf similarity (Irribarren) parameter	-
$\xi_{s-1,0}$	Surf similarity (Irribarren) parameter, using the energy wave period $T_{m-1,0}$	-
ρ_{ec}	Own (bulk) weight of cover layer [Elastocoast]	kg/m^3
ρ_r	Mass density of rock	kg/m^3
ρ_w	Mass density of water	kg/m^3
σ	Stress	N/m^2
σ_{max}	Maximum value for stress [at x=0]	N/m^2
ϕ, Φ	1. Stability factor or stability function for incipient of motion	-
	2. Hydraulic head difference	m
ψ_u, Ψ_u	System-determined (empirical) stability upgrading factor in the Pilarczyk formula	-

1 Introduction

1.1 The Elastocoast system

Elastocoast is a new type of revetment system for use as a cover layer on dikes. It consists of granular material (rocks), which is fixed together with a two-component polyurethane adhesive. In the Elastocoast system each individual rock is covered with a thin film of polyurethane. When the adhesive is cured, this film fixes the rocks together only on their contact points, creating a highly permeable, open structure.

Figure 1.1 Impression of the polyurethane coating and bonding of rocks (BASF, 2006).

The chemical components of the polyurethane adhesive are produced by the German company Elastogran, which is a subsidiary of BASF. Besides their main facility at Lemförde in Germany Elastogran has production facilities located all over Europe, including the UK, France, Spain and now also in The Netherlands.

Though it is a novelty in hydraulic structures, the use of polyurethane is not new. As a plastic it is widely spread in applications such as sport, leisure, in and around cars, living accommodation, and it is also established in professional fields such as mechanical engineering, medical technology and maritime applications (Elastogran, 2006a).

In the past years Elastogran has also aimed for the introduction of polyurethane in the field of hydraulic engineering. Pilot tests were performed in Germany and the Netherlands and results look promising for Elastocoast to claim its place next to established revetment types.

1.2 Prototype tests

1.2.1 Pilots in Germany

From 2004-2007 several Elastocoast pilot tests were performed along the North-Sea islands in the most northern part of Germany. The first commercial project has also been constructed in this area in September 2007, comprising a revetment with an area of 1500 m^2.

- Early 2004: Breakwater on the peninsula Hamburger Hallig, 120 m^2 on a core of granular material.
- September 2005: On the sand beach of Sylt Ellenbogen, 270 m^2 on top of a geotextile.
- July 2006: Wave breaker on the island of Hallig Gröde, 500 m^2 on a core of granular material.
- May 2007: Upgrading of pilot on Hallig Gröde to 3000 m^2.
- September 2007: Commercial renovation of an existing damaged revetment near the harbor of Munckmarsch on the island Sylt, 1500 m^2 on a slope.

Figure 1.2 German Elastocoast pilot on the island of Hallig Gröde. An Elastocoast cover layer has been placed on a breakwater on top of the revetment.

Figure 1.3 First commercial application of Elastocoast pilot at a harbour on the island of Sylt Munckmarsch.

1.2.2 Pilots in the Netherlands

After the pilots in Germany, Elastocoast is also being introduced to the Dutch market in 2007. ARCADIS and Delft University of Technology have been involved in further research which is necessary for this introduction. ARCADIS supervised the construction and monitoring of two pilot tests in the Netherlands:

- September 2007: Revetment on a rudimentary sea dike called 'Zuidbout' near Ouwerkerk in the Eastern Scheldt, 490 m^2 on a 1:3-1:4 slope.
- Oktober 2007: Covering of the head of beach groyne no. 20.9 near the Pettemer Zeewering along the North Sea coast, 385 m^2 on a horizontal bed.

These pilot tests were constructed in September and October of 2007 and their performance was frequently monitored during the storm season of 2007-2008, running from October 2007 to April 2008. More information about the pilot sites and their monitoring is given in Appendix I.

Figure 1.4 Dutch Elastocoast pilot at Ouwerkerk. The Elastocoast structure is placed on the slope of a rudimentary sea-dike in the Eastern-Scheldt.

Figure 1.5 Dutch Elastocoast pilot at Petten. The Elastocoast structure is located on the head of a beach groyne in the North Sea (upper right part of picture).

1.2.3   Overtopping test Rijkswaterstaat

In April 2008, a strip of Elastocoast was constructed at Kattendijke in Zeeland to be subjected to overtopping tests. A simulator, specially designed for this purpose, was put on the crest of a dike to test the inner slope at high overtopping quantities. For the Elastocoast revetment the capacity of the simulator was upgraded to 125 l/s/m. No considerable damage was observed. Flow velocities were estimated at 6-12 m/s (Provoost, 2008).

Figure 1.6 Overtopping test at Kattendijke (NL). Waves were simulated to create overtopping volumes of up to 125 l/s/m.

1.3   Research activities

1.3.1   Introduction

Apart from the research done by the manufacturer Elastogran, studies for the behaviour of Elastocoast were performed in the Netherlands at the Delft University of Technology, the engineering company ARCADIS and the University of Amsterdam. Below a short description is be given of these studies. For detailed results is referred to their consecutive reports.

1.3.2   Preceding thesis work at Delft University of Technology

In 2007 Dehua Gu finished his MSc thesis work on Elastocoast at the Delft University of Technology. Gu investigated the mechanical properties of Elastocoast by conducting a variety of laboratory tests. In these tests, among others, the porosity, permeability, viscosity and bending strength were investigated. The results of these investigations are of key importance for the analysis done in the present report and will therefore be further discussed in Chapter 3.

Figure 1.7 Three point bending test on an Elastocoast beam (Gu, 2007).

1.3.3   Damage monitoring at Dutch pilot tests

Parallel to the thesis work presented in this report, monitoring work was done in the field for ARCADIS. The two pilot locations in the Netherlands were monitored, starting from their construction, during the storm season of 2007/2008. The damage development at the pilots was related to the loading conditions that were present during the storm season. A separate report was created, of which an abstract

is given in Appendix I. One of the conclusions of this study was that the erosion of Elastocoast during the storm season remained negligibly small (Bijlsma, 2008).

Figure 1.8 Damage monitoring of the Dutch pilots. The figures show a monitoring area in which the development of surface erosion was quantified.

1.3.4 Biological recovery in field and laboratory study

Another field study was performed on the Dutch Elastocoast pilots to monitor the recovery of the biological community after construction of the revetment. The presence and growth of algae and other forms of life on the Elastocoast was quantified during the first months after construction. Also a laboratory study was performed at the University of Amsterdam, where the development of bio-mass on different substrates was monitored. From these studies it was concluded that Elastocoast proves to be a suitable substrate for algae attachment and that the availability of moisture plays a key role in recovery of the biological community (Lock, 2008).

Figure 1.9 Study for ecological redevelopment on Dutch Elastocoast pilots (left) and laboratory study (left) (Lock, 2008).

1.4 Purpose of this study

1.4.1 Problem analysis

The application of polymers as a binding material in dike revetments is new to the hydraulic engineering community. Design criteria or construction guidelines for these revetments, including the Elastocoast system, are therefore not readily available. Design criteria are needed to prescribe a certain minimum layer thickness for specific loading conditions. Construction guidelines give information on how a structure should be built-up, including support and transition to surrounding structures. Together they form a set of design tools that, if followed, should ensure the adequate performance of a structure during its lifetime.

Now, for Elastocoast such a set of design criteria and construction guidelines must be developed. Only then the Elastocoast system can be taken along in revetment designs as an alternative to existing solutions. Goal is acceptance of the material in the (Dutch) hydraulic engineering community, eventually leading to its commercial application.

1.4.2 Objectives

In this thesis study a first step is made in the development of design tools for the Elastocoast system (and implicitly for similar polymer bonded revetments). The results of this study can serve as a basis for the development of a technical report (in 2008/2009), in which design criteria and construction guidelines will be presented.

To provide a good basis for this future technical report it is of importance to make the inventory of failure mechanisms as complete as possible. By doing so, the dominant mechanisms can be determined that should at least be incorporated in the technical report, whereas insignificant mechanisms can be left out. Also, this study can serve as an indication of where further research into mechanisms or material parameters is necessary or advantageous (i.e. in reduction of layer thickness).

The objectives of this MSc thesis study are as follows:
- Make an inventory of possible failure mechanisms for Elastocoast revetments.
- Eliminate those mechanisms that are not dominant and quantify those that are.
- Make a proposal for design criteria and construction guidelines where possible.
- Make recommendations for further research into those mechanisms and parameters that could not be quantified.

To reach these objectives a theoretical approach is followed. For this, the results from preceding research activities are combined with the field experience from prototype tests. Analogies with existing revetments are made to determine the possible failure mechanisms that apply to Elastocoast. Then, existing calculation methods are derived from these analogue revetments and, if necessary, modified for use with Elastocoast.

The design criteria that follow from the quantification of dominant failure mechanisms must give a safe approximation of the loads that work on the revetment and prescribe a layer thickness that ensures stability under the input conditions. Besides, they must be easy to use in practice. Therefore schematizations and simplifications are chosen in such a way that they resemble the worst possible scenarios.

1.5 Structure of this report

The structure of this report is as follows. First, in Chapter 2 an overview is given of the many types of revetments that are in use in the Netherlands. The historical development of revetment systems is described as well as their main characteristics application areas. Chapter 2 concludes with a list of common damage causes observed on revetments.

Next, in Chapter 3 the material Elastocoast is presented as a new type of revetment. Its composition and construction method are described. Then a summary is given of the present knowledge on system characteristics and mechanical properties, which have been investigated in preceding studies.

Chapter 4 describes possible mechanisms that could lead to the failure of an Elastocoast revetment. These failure mechanisms are derived from analogies with existing revetment types and engineering insight.

Then, in Chapter 5, a detailed analysis for a selection of the mechanisms described in the previous chapter is worked out to provide more insight and a first quantification. Cases that are chosen to be further analyzed:

- Micro scale erosion – instability of individual rocks (section 5.2)
- Mechanical breakage by wave impact (section 5.3)
- Theoretical prediction of the hydraulic conductivity of (clogged) Elastocoast (section 5.4)
- Macro scale instability by uplift pressures (section 5.5)

In Chapter 6 a set of design criteria and construction guidelines will be proposed.

Finally Chapter 7 concludes with a summary of the main results from the performed analysis and recommendations for further research are proposed.

2 Revetments

2.1 Introduction

A dike has a 'soft' core of sand or clay and is covered with a revetment. The revetment can be built up out of several layers; the most outer layer is called the cover layer. The main function of a dike revetment is to serve as protection against erosion of the dike body

The outer shell of a dike must be strong enough to withstand attacks from waves, currents and other loads in order to protect the soft core from eroding. Material from the core has to be kept in place and may not be transported through the cover layer. Protection against loads does not necessarily mean that the revetment needs to have a 'hard' cover layer. For small loads a simple, cohesive cover layer of clay and/or grass can be sufficient. If the loading is more severe, the cover layer has to be made harder, heavier or more cohesive in order to fulfill its function.
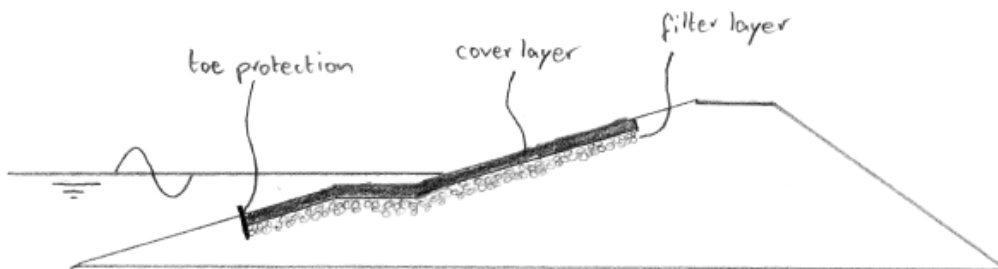
Figure 2.1 Typical cross section of a sea dike.

In the following sections, a short history is given of the development of revetments in the Netherlands. Then an overview of 'modern' revetments is given and a categorization of these revetments is made according to their degree of bonding. Finally a new type of revetment, the Elastocoast system, is introduced along with its possible applications.

2.2 A short history of dike protection in the Netherlands

Already thousands of years ago, in the era of the Mesopotamians, revetments were used to protect water reservoirs. These revetments consisted of a primitive type of asphaltic mastic (Pilarczyk, 1990). It was not until the 8th century A.D. that the first dikes were constructed in the early Netherlands with the function of preventing rising waters from reaching farmlands and settlements. These were simple mounts of compacted clay sometimes reinforced with grass or straw. At first the dikes were constructed directly at edge of the bank, at the mercy of the water. Later on they were built further away, thus creating a foreland. It was soon discovered that the seaward faces of the dikes were heavily damaged during storms. Consequently this side was protected with a construction of straw, reed or wicker. These forms of dike protection remained the best practice for the following five centuries (Dibbits, 1950).

As from the 14th century more sophisticated methods were devised for the protection of dikes. A so-called *slikkerdijk* was made, consisting of mud, silt and seaweed (*wierdijk)*. The *wierdijken* were later on further reinforced with wooden pole fencing (figure 2.2). Reed was sometimes used instead of seaweed, but this proved to be less durable and had to be replaced every five years.
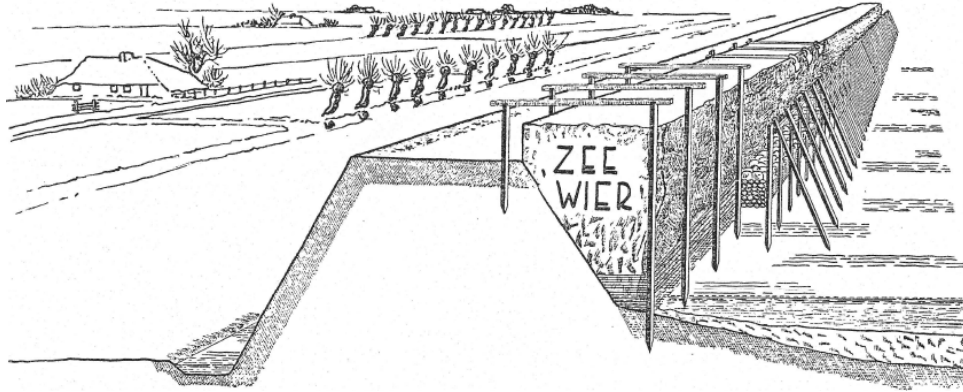
Figure 2.2 The 'wierdijk': a dike protection made out of seaweed and wooden poles (Dibbits, 1950).

Parallel to the development of the *wierdijk*, in the 15th century the application of revetments consisting of dumped or placed stone was slowly beginning to spread, but was relatively expensive. The introduction of the wood eating pole-worm in the 18th century finally marked the era of stone revetments. Stones were dumped on fascine mattresses and the first hand-placed stone pitchings from natural blocks were constructed and are still in use today (Dibbits, 1950).

In the 19th century experiments were done with concrete blocks, but these proved to be hardly durable. Slowly reinforced concrete was being developed for application in hydraulic structures. The application of concrete in plate structures appeared to be suitable for dike protections; several types of concrete cover layers were invented by De Muralt at the beginning of the 20th century. These *Muralt glooiingen* (slopes) and *Muralt muren* (walls) were relatively cheap and seemed to have survived the storm surges of 1906 and 1911, but it was later discovered that there was considerable damage under the water level (Bosch, 1998).

The beginning of the 20th century was a time in which a large part of Netherlands' present dikes were built. Pitchings were constructed out of natural stone (basalt columns) and experiments were done with concrete columns. However, these types of revetments required large amounts of skilled labourers and these were not always available. About 120 km of *Muralt muren* was applied along the coastline of Zeeland. These performed well, but were heavily damaged during the disaster flood of 1953 and mostly removed afterwards. It was time for a new type of revetment.

In the late thirties the tar-like material bitumen was already used for the filling of joints between blocks. It was not before the Second World War had ended in 1945 that asphalt was first applied for the grouting of dumped rock revetments (Dibbits, 1950). After the flood of 1953 asphalt was used on a large scale to repair damaged revetments. Asphalt was ideal for this purpose since it could be applied fast and with less manpower than other types of dike protection. Knowledge and experience on the area of asphaltic revetments needed to be built up and guidelines were unavailable. After years of research and experiences from the field, the first manual for the use of asphalt in hydraulic engineering was published in 1984 (TAW, 1984). Since then, asphalt revetments have become widely used.

Figure 2.3 Application of an asphalt revetment on a dike (Verhagen, 2008).

The development in placed block revetments had also continued throughout these years. Availability of natural rock columns and blocks became scarce and therefore expensive. Fabrication of artificial concrete elements became more and more attractive. Until the 1960's blocks were still placed by manual labour, but with the development of these new artificial blocks new placement methods became available. The constant shape and size of the blocks enabled them to be placed mechanically in large amounts at a time. Extensive research for the stability of blocks was done in the 1980's. With the first large scale assessment of block revetments on the Dutch dikes in 1995 many turned out to be insufficient and needed to be repaired, replaced or upgraded. In 1999 the first design manual for block revetments was published (Dorst, 2007).

Figure 2.4 Mechanical placement of concrete blocks on a dike slope (Dorst, 2007).

2.3   Modern revetment systems

As a result of centuries of development a great variety of dike revetments exists, some of which have become outdated and others that are still used in present-day applications. Since insight of hydraulic loads and structural behaviour is still expanding and new materials become available, new revetment types are constantly developed, sometimes by improvement of existing types with new techniques.

Figure 2.5 on the next page gives an overview of commonly used revetments in the Netherlands. The fourth degree of subdivision distinguishes between the ways in which the individual elements in the revetment are connected to each other. The level of bonding between the elements is an important factor

in the structure's interaction with hydraulic loads. Further on, this structure property will be used to make a specific categorization of revetments.

In figure 2.5 also a new, experimental type of bonding has been introduced in the form of polymer bonding. Possible applications for polymer bonding have also been depicted in figure 2.5. This is where a new type of revetment, the subject of this report, can be placed; namely the Elastocoast system. The Elastocoast system will be discussed at the end of this chapter.
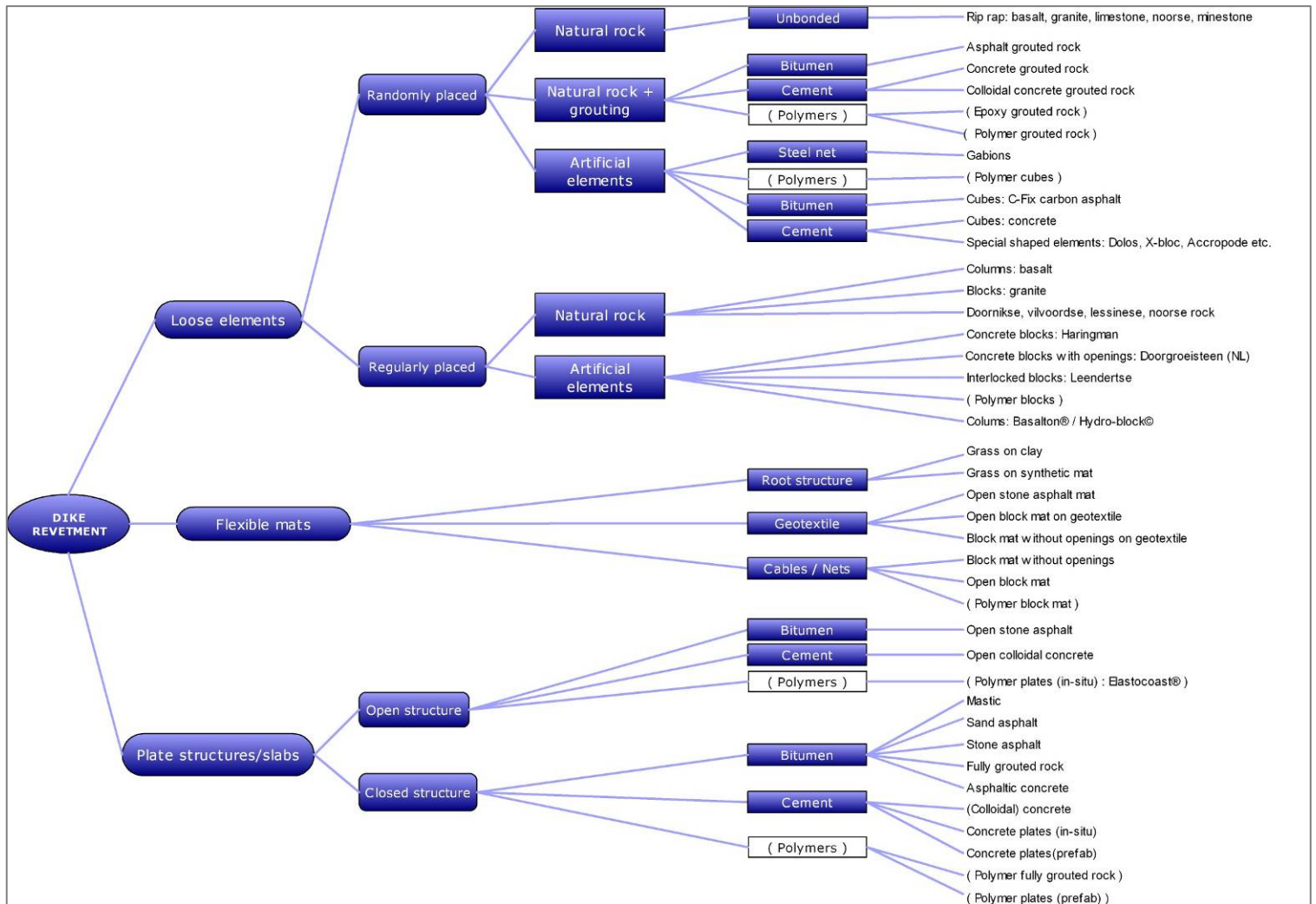
Figure 2.5 Overview of modern dike revetment types. An experimental type of bonding, namely with polymers has been added, together with its theoretical applications.

2.4 Categorization according to the degree of bonding

2.4.1 Introduction

In this section a categorization will be made of revetment types according to their degree of bonding. Ranging from least to most bonding the following categories are distinguished:

- No bonding: randomly placed rocks
- Element coherence: regularly placed blocks
- Grouped elements: gabions and mats
- Bonded elements: grouted rocks
- Bonded aggregate: open plate structures
- Bonded aggregate: closed plate structures

Aggregate is the name for natural sands, gravel and crushed stones that are used in the manufacture of for instance concrete and asphalt. For the last two categories this label is given to the rock elements because their individual size is less important as together they form a whole with the structure.

2.4.2 No bonding: randomly placed rocks

Randomly placed elements are mostly transported in bulk and dumped on site. The elements can either be natural rock from a quarry or prefabricated artificial elements. Together one or two layers of elements create a very open protection structure, which purpose it is to break down wave forces before the weaker underlying layer is reached. The extent to which this is successful depends mainly on the ratio between wave height, element size and element grading.

Figure 2.6 Dumped rock revetment (Verhagen, 2008).

Characteristics and structure classification
A characteristic of loose elements is that they are still moveable after placement. Forces exerted by wave action can cause movement and rocking of individual elements. This is not necessarily a bad thing. Under extreme conditions the structure reforms, adjusting itself to the wave loads. However if the movement is too large, elements can be removed from the structure. Also the rocking of artificial units can cause them to break into pieces.

The single most important factor providing stability to rocks is their weight, which depends on rock type (limestone, basalt etc.) and size. Therefore, for dumped rock structures under wave attack an important parameter is often used, which gives a relationship between wave height and unit weight. This parameter is the dimensionless stability number, N_s (-):

$$N_s = H_s / \Delta D$$

Where N_s = stability number (-), H_s = significant wave height (m), Δ = relative density (-) and D = characteristic element size (m). High values of N_s indicate that the structure is dynamic and constantly

reshaped by wave action. A classification of structures according to the stability number is given in the following table:

Table 2.1 Structure classification according to the stability number N_s (CUR/CIRIA, 2007).

Structure type	N_s
Caissons or seawalls	<1
Statically stable breakwaters	1-4
Dynamic/reshaping breakwaters	3-6
Dynamic rock slopes	6-20
Gravel beaches	15-500

Application area

Because of the placement method and the potentially unlimited size of the individual units this type of revetment is often applied under the water line and in locations where extreme waves have to be withstood. However, increase in unit size often results in a double increase in placement costs because of the heavy equipment that is needed for both transport to and placement on site.

2.4.3   Element coherence: regularly placed blocks

Stone pitchings are protections for banks, dams and dikes, consisting of individual elements, mostly of natural stone or concrete, which are regularly placed instead of dumped. There are many types of stone pitchings. Pitchings from former days were usually made of natural stone elements, such as hexagonal basalt columns or square granite blocks. Because of the natural irregular shape these stones were placed by hand. Nowadays pitchings consist mostly of concrete blocks, sometimes with modifications to reduce wave run-up. New stone pitchings consist of reinforced concrete elements. There is a wide variety of element shapes and sizes, ranging from simple blocks to fish-shaped columns. They are all designed to be placed mechanically. Shapes are sometimes designed to improve clamping force or to enable placement around bends.
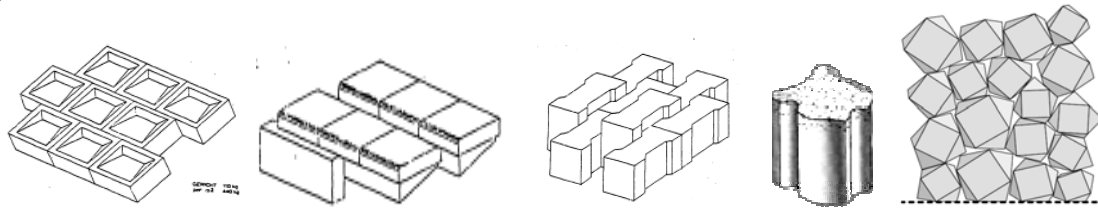
Figure 2.7 Several shapes of concrete blocks. From left to right: Haringman-, Leendertse-, Ipro- (CUR-VB, 1984), Hydro-block© (Haringman) and plan view of Basalton® (Holcim).

Characteristic unit interaction

In a correctly placed stone pitching there is interaction between the individual elements. Apart from the weight of the element, there is also a shear force between the elements contributing to stability. A third important factor, which is unique to stone pitchings, is the clamping force. Clamping behaviour contributes to the resistance of a single element of being pushed or pulled out of the revetment. The result of these factors is that an individual element in a pitching is more stable than a rock of the same weight in a dumped rock protection. This also shows in a slightly higher value for the stability number N_s, with block height as characteristic element size.

Table 2.2 Stability number N_s for regularly placed blocks.

Structure type	N_s
Regularly placed blocks	3-6

Since a stone pitching derives a large part of its strength from unit interaction, it is important that all units are properly in place. Locally, unit interaction will be lost if an element is missing (i.e. pushed out of the revetment by overpressure) or if the space between the elements becomes too large (for instance by partial sliding).

Application area

Stone pitchings are always placed above the water surface. Usually there is a granular filter or geotextile underneath the pitching top layer. Placing of the elements can to be done by manual labour, but is nowadays mostly done with use of mechanical equipment.

2.4.4   Grouped elements: gabions and mats

A step further in the bonding of elements is to bind them together with a mesh of steel wires. Loose rocks can be put in closed steel wire frames, called gabions. Artificial elements can be connected together with steel wires or a geotextile to form a mat. The advantage of grouping loose elements in such a way is that their individual weight becomes less important. It is the weight of the group that defines their stability, while the open structure remains intact. Therefore the characteristic element sizes are taken equal to the size of the entire gabion or the thickness of the mat. Resulting stability numbers are typically approximately the same as for regularly placed blocks (table 2.3). The effect of unit interaction has been replaced by connection with wire frames.
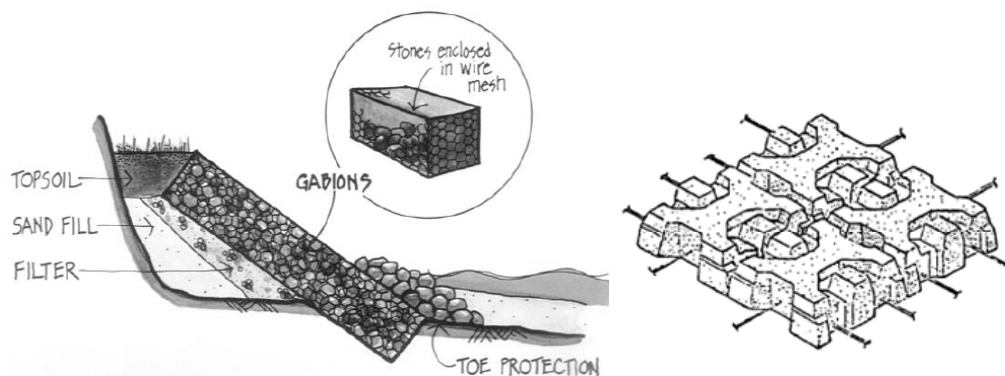
Figure 2.8 Elements grouped by a steel wire frame in gabions (Klein Breteler, 1998) and elements connected by steel wires to form a mat (CUR-VB, 1984).

Table 2.3 Stability number N_s for gabions and mats (Klein Breteler, 1998).

Structure type	N_s
Gabions (*D=size of gabion*)	2-6
Block mat (*D=thickness of mat*)	3-6

Application area

Gabions are used throughout the world to protect river banks, dikes and other slopes. The slope protections are usually constructed by placing the empty cells on the slope and connect them. Then they are filled with rock and closed (Klein Breteler, 1998). Mats are usually prefabricated and placed on the dike slope as a whole.

2.4.5   Bonded elements: grouted rocks

An existing or new dumped rock revetment can be strengthened by pouring a bonding material over the rocks. The individual units are then bonded together with for instance cement or bitumen, providing extra stability by coherence.

A layer of dumped rock can be grouted in several ways (figure 2.9):

- Surface grouting or 'fixation of rocks'
- Pattern grouting
- Full grouting
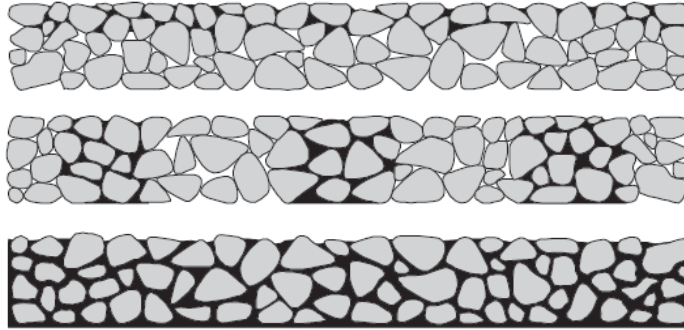
Figure 2.9 Three methods for grouting of a dumped rock revetment: surface grouting 'fixation of rocks', pattern grouting and full grouting (TAW, 2002).

The effect of surface and pattern grouting of rocks is a higher stability number, yet the spreading is larger because not all rocks are fixated by grouting (table 2.4). A full grouted layer of rocks can become completely impervious and will even show the same behaviour as an asphalt plate revetment. For this type of revetment the thickness of the layer instead of the size of the individual rocks can be taken as the characteristic element size. The result is a relatively high stability number, when compared to the previous revetments (table 2.4).

Table 2.4 Stability number N_s for grouted rock.

Structure type	N_s
Surface grouted rock ($D=D_n$)	1-6
Pattern grouted rock ($D=D_n$)	5-20
Fully grouted rock ($D=thickness$)	≈ 10

Application areas
Grouting with asphalt needs always to be done above water level, since the hot asphalt may not come in contact with water. Grouting with concrete can be performed under water, if special 'underwater concrete' is used: colloidal concrete. Colloidal concrete contains additives that keep the mixture from falling apart when applied under water. Grouting is an easy and cheap way to upgrade or repair existing structures.

2.4.6 Bonded aggregate: open plate structures

In open plate structures the bonding between the rocks is high. There are two standard applications:

- Open stone asphalt
- Open colloidal concrete

In the Netherlands open colloidal concrete is rarely used, whereas open stone asphalt is very common. Open stone asphalt is a mixture of narrow graded aggregate that is encapsulated by mastic asphalt (figure 2.10). The mixing ratio is such that much of the open pore space of the aggregate is retained. The open pore volume of approximately 25% makes the structure permeable to water as well as sand. Therefore it is always applied in combination with a sand tight geotextile or granular filter.
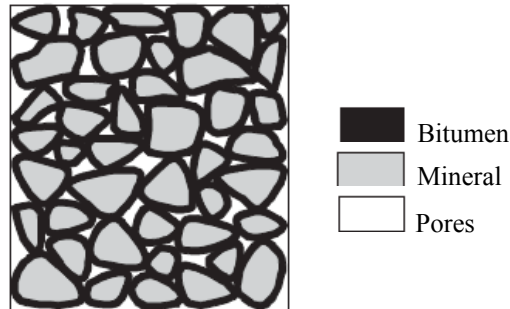
Figure 2.10 Structure of open stone asphalt (TAW, 2002).

After application, open stone asphalt forms a stiff plate that is well capable of withstanding hydraulic loads such as wave impacts (table 2.5). The viscoelastic nature of asphalt gives the plate some flexibility so that differential settlements in the subsoil can be slowly followed.

Table 2.5 Stability number N_s for open stone asphalt.

Structure type	N_s
Open stone asphalt (*D=thickness*)	≈ 8

2.4.7   Bonded aggregate: closed plate structures

The closed plate structure is the most extreme form of bonding of rocks. A common used plate revetment in the Netherlands is asphaltic concrete (Dutch: *waterbouwasfaltbeton*). It consists of a wide graded aggregate of gravel and sand the pores of which are filled with bitumen. The bitumen bonds the aggregate together and with an open pore volume of only 3-6% the mixture is impermeable to water and sand.
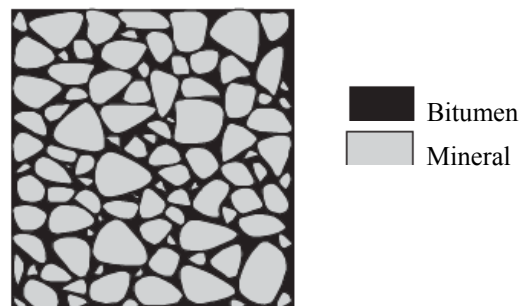
Figure 2.11 Structure of asphaltic concrete (TAW, 2002).

After application, asphaltic concrete forms a relatively stiff plate that is well capable of withstanding hydraulic loads such as wave impacts (table 2.6). The high amount of bitumen gives the plate some flexibility so that differential settlements in the subsoil are slowly followed.

Table 2.6 Stability number N_s for open stone asphalt.

Structure type	N_s
Asphaltic concrete (*D=thickness*)	≈ 10

Because an impervious plate is completely closed for transport of soil or water, no extra measures are needed to prevent loss of material from the sub layer, but also the release of excessive water pressures is prevented. The possibility of overpressures is an important characteristic that always has to be taken into account during the design of an impervious revetment (figure 2.12).
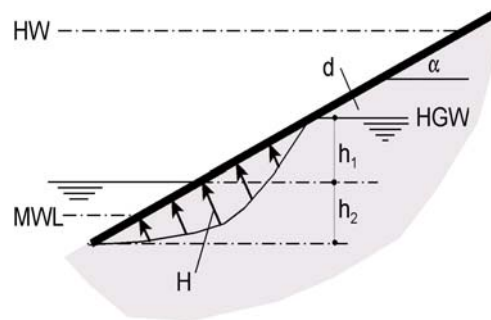
Figure 2.12 An important load case for impervious plate revetments is overpressure (Schiereck, 2001).

2.5 A new type of revetment system: Elastocoast

In Figure 2.5 an overview was given of modern revetment types, in which the last subdivision showed the different forms of bonding. Apart from the bonding of larger elements, two common used ways to bond aggregate are discerned, namely bitumen and cement.

Now, a new way of bonding is introduced: polymer bonding of aggregate. If this bonding is seen as a direct alternative to the bitumen and cement bonded appliances immediately several applications follow from figure 2.5, namely:

- Polymer (fully) grouted rock
- Polymer based large elements
- Polymer based blocks
- Polymer based blocks, connected with a mat
- **Polymer bond plate revetments (in-situ)**
- Polymer bond plate revetments (prefab)

The Elastocoast system is based on polymer bonding. The bonding polymer is in this case a two-component polyurethane adhesive. The main application of Elastocoast is in a plate revetment that is produced in-situ. In this form, the Elastocoast system combines the high permeability of a dumped rock structure with the stiffness and strength of a plate type revetment. This application is also the main subject of this study and from now on is referred to simply as 'Elastocoast'.

It should be kept in mind, however, that there are alternative ways to make use of the polymer bonding. Prefab plates or blocks could give way to new applications. In the development of Elastocoast, experiments have been done with polymer grouting of dumped rocks, but these were not successful.

3 Elastocoast properties

3.1 Introduction

The new revetment system Elastocoast consists of granular rock material, fixed together with a two-component polyurethane adhesive. In this system each individual rock is coated with a thin layer of polyurethane. The individual rocks are fixed together at the points of contact only. The resulting rigid structure has a high degree of open pore space, which depends on the choice of grading of the granular aggregate.

Aside from the introduction of the polyurethane adhesive, which is new to the hydraulic engineering sector, the novelty of the Elastocoast system is in its production process. At present, the production process of Elastocoast is a direct, yet up-scaled, copy of the method used in its laboratory development. The process is quite straightforward and is aimed to ensure the complete covering of each stone with a thin coating of the adhesive. This process is discussed later in this chapter, after introduction of the materials.

In this chapter an overview is given of the present knowledge on Elastocoast properties, based on interpretation of results from several sources.

3.2 Materials

3.2.1 Granular aggregate

For use in an Elastocoast system basically any type of granular material can be used. The adhesive bonding of polyurethane has been successfully tested on i.e. basalt stone, granite, limestone and iron slag. Provided that the surface of the rocks is dry and reasonably clean, a durable bonding with the rock is formed. The granular material can be either broken or rounded (gravel). Ultimately the application area and the production process define the type and grading of the rock used. However, the maximum useable stone size is limited by the production process.

Figure 3.1 Granular aggregate ready to be used for the Dutch Elastocoast pilot at Ouwerkerk.

The specific weight and the grading of the granular material define the bulk weight of the Elastocoast system and its open pore space. For instance, in the Dutch pilot tests (see Appendix I) limestone with a narrow gradation of 20-40 mm was used (this is the classification of the gradation, values obtained from the sieve cure are: D_{85}/D_{15}=34mm/22mm). In the end product Elastocoast retains the natural open pore

space of the material, which in this case is approximately 50%. The limestone had a specific weight of 2720 kg/m^3 and a bulk weight of 1340 kg/m^3. In similar tests performed in Germany larger stones were used. To give the structure extra weight, mostly heavier rock types were chosen, such as granite or iron slag.

Table 3.1. Armour stone grading width related to the uniformity (CUR/CIRIA, 2007).

	D85/D15
Narrow or *single-sized* gradation	< 1.5
Wide gradation	1.5 – 2.5
Very wide or *quarry run* gradation	2.5 – 5.0

Table 3.2 Specific weight of several rock types (CUR, 1999).

	Specific weight (kg/m^3)
Mining stone (coal)	2450-2650
Limestone	2650-2700
Granite	2600-2800
Basalt	2900-3000
Iron slag	3100-3400

The compression strength of natural rock material varies and is not always isotropic. It is mostly above 150 N/mm^2 (CUR, 1999).

3.2.2   Polyurethane adhesive

The polyurethane system as produced by Elastogran for use in hydraulic structures is *Elastocoast®* *6551/100*. This adhesive consists of two chemical components:

- Polyol-component: a mixture of *polyol* and additives
- Iso-component: a preparation containing *diphenylmethane-diisocyanat* (MDI) = IsoPMDI 92140

Figure 3.2 Chemical components for Elastocoast.

Once the A-component (polyol) and the B-component (isocyanate) are mixed together with a ratio of 2:1 (parts by weight) an exothermic chemical reaction or curing process begins, in which the material hardens to solid polyurethane. The processing time after mixing is about 20 minutes at 23°C. The speed of the chemical reaction and thus the processing time is dependent on temperature. Therefore processing time is longer at a low temperature and vice versa. The recommended processing temperature is between 10°C and 30°C (Elastogran, 2006b).

The material properties of the adhesive after having cured for 28 days are shown in the following table.

Table 3.3 Physical properties of cured Elastocoast® 6551/100 adhesive (Elastogran, 2006b).

	Measured value	
Hardness	70	Shore D
Tensile strength	22	N/mm^2
Elongation	20	%
Tear strength	33	N/mm
Density	1.1	g/cm^3

In order to give the rocks a complete coating, the mixing ratio of the polyurethane with the granular material needs to be adjusted to the grading of the stones. More small particles in the grading give a larger surface area to be covered. For the limestone 20-40 mm the mixing quantities are shown in table 3.4. In general a volume ratio of 100:3 is sufficient for completely covering the stones in a narrowly graded aggregate.

Table 3.4 Mixing quantities as used with the Dutch pilot tests (Bijlsma, 2008).

	Specific weight (kg/m^3)	Porosity (-)	Quantity (kg)	Quantity (m^3)	Mass percentage Elastocoast	Volume percentage Elastocoast
Limestone 20-40 mm	2720	0.51	670	0.50	2.4 %	2.9 %
Elastocoast 6551/100	1110	-	16.5	0.015		

Once cured, the polyurethane is hydrophobic (water repellent). Yet, the two components are moisture sensitive and therefore have to be stored in sealed, closed containers. When water comes in contact with an isocyanate group (component B) it reacts to form an unstable carbamic acid, which then decomposes to produce the corresponding amine and CO_2 gas (Oertel, 1985). This process is used to create the gas bubbles in the well known PU-foam.

For use in Elastocoast this behaviour is unwanted. As long as the mixed components have not sufficiently reacted with each other, contact with water must be avoided. The enclosed gas bubbles would lessen the bonding of the coating to the rock and perforate the important contact points between the rocks. In practice, this means that the aggregate must be dry before the fresh polyurethane mixture is added. After mixing of the aggregate with the polyurethane, the curing process has advanced enough to make the mixture hydrophobic and applicable in moist conditions.

3.3 Production process

Elastocoast, as being a new product, has a production process that is still under development, evolving from labour-intensive low volume production to large scale high volume production. The basic workflow however, stays the same (see also figure 3.4 on the next page):

- 11 kg of component A is mixed to a homogeneous substance in approximately 1 minute.
- 5.5 kg of component B is added and the two components are mixed for approximately 2 minutes.
- The mixture is added to 0.5 m^3 of limestone while tumbling.
- After tumbling for approximately 3 minutes the unhardened Elastocoast is dumped on the application area.
- Within approximately 20 minutes the Elastocoast is smoothened to profile height with help of a hydraulic crane and hand-rake.
- Shortly after the profiling dry sand is scattered over the hardening Elastocoast by hand to create a rough surface.
- The Elastocoast system hardens in several hours. It can be loaded after 24 hours and is almost fully cured (90%) after 2-3 days.

For construction in the pilot tests at Ouwerkerk and Petten respectively 90 m^3 and 75 m^3 of Elastocoast revetment were produced. A specially equipped shovel capable of tumbling and dumping was used.

With this production technique only a small quantity of 0.5 m^3 is dumped per cycle. This way in the order of 10 m^3 is produced per hour. To scale up the production to a higher capacity tests were done with standard concrete mixing trucks. With these trucks production volumes of 6-8 m^3 per cycle could be reached.

Figure 3.3 Specially equipped shovel capable of tumbling and dumping (left) and standard concrete mixing truck (right).

1 Homogenizing A and B

2 Mixing of components

3 Mixing with aggregate

4 Dumping on dike slope
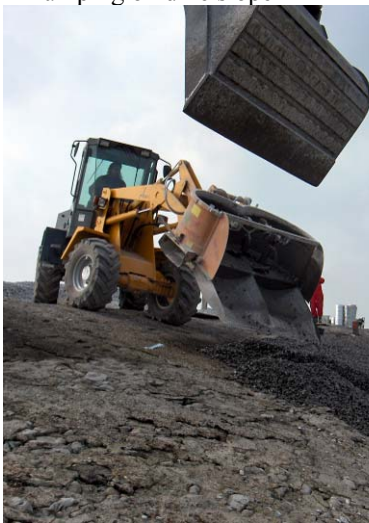
5 Profiling with crane
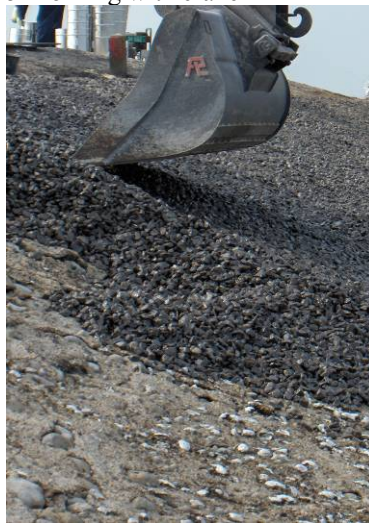
6 Covering with sand

7 Curing

Figure 3.4 Small scale production process of an Elastocoast revetment.

3.4 System properties

3.4.1 Open pore volume

The porosity of a granular material is defined as the volume of the open space between the rocks divided by the total volume of the bulk, often expressed as a percentage. Most natural granular materials (i.e. sand, gravel) have a porosity between 30-45%. A small value of the porosity indicates a dense packing, whereas a high open pore volume percentage indicates a loose packing (Verruijt, 1999).

The Elastocoast system consists of granular rock material mixed with polyurethane. The polyurethane creates a thin coating around each individual rock and fixes the rocks together on their contact points. The space between the rocks is not filled with polyurethane and remains open. Besides, the stickiness of the polyurethane film makes it more difficult for the rocks to slide into position, thus retaining a loose packing. The result is a highly permeable structure with a high open volume percentage.

The open volume percentage of Elastocoast is equal or even a little higher than the natural open space of the bulk rock material and therefore dependent on the rock grading. A rock grading with no or few small fractions present gives a high open pore volume. For the Elastocoast system a grading is chosen where the small fractions are not present. Thus the open space remains open and the open pore volume can be very high, 45-50% (Gu, 2007a).

3.4.2 Hydraulic conductivity

The hydraulic conductivity is a measure for the ease with which water can move through the pore spaces of a material. Because the open pore volume of Elastocoast is approximately equal to the natural open pore volume of the used aggregate its hydraulic conductivity should also be approximately equal to that of the aggregate.

The hydraulic conductivity of Elastocoast was investigated by Gu (Gu, 2007a) in a series of laboratory tests on specimens with varying thickness and with varying water pressures. A specific goal of his research was to determine the influence of superfluous polyurethane adhesive leaking on an underlying geotextile on its permeability. Figure 3.5 shows this effect on the bottom of an Elastocoast cube sample.

Figure 3.5 Leaking of superfluous polyurethane adhesive on the underlying geotextile of an Elastocoast cube sample (Gu, 2007).

After some modifications (see Appendix III) the results of Gu can be presented as in the following graph. This graph depicts the hydraulic conductivity k of Elastocoast samples in relation to the hydraulic gradient i.
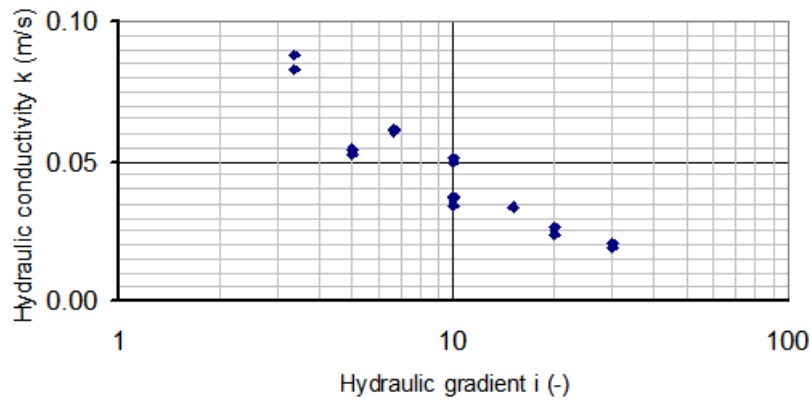
Figure 3.6 Hydraulic conductivity of Elastocoast samples with D_{n15}=22.5mm and n=0.5 (adapted from Gu, 2007a).

Based on the results of Gu, there is no indication for a strong negative influence of either clean or clogged geotextile on the total hydraulic conductivity. The values for the hydraulic conductivity of Elastocoast are similar to that of the used aggregate without the addition of polyurethane.

3.4.3   Reduction of wave loads

Wave run-up is the rush of water up a structure on the breaking of a wave on the surface of that structure. The amount of run-up is the vertical height above still water level that the rush of water reaches. An example of a commonly used design formula for the 2% wave run-up level $z_{2\%}$ (m), is (Van der Meer, 2002):

$$z_{2\%} = 1.75 \cdot \gamma_b \cdot \gamma_f \cdot \gamma_\beta \cdot \xi_0 \cdot H_{m0}$$

In which ξ_0 is the surf similarity parameter (-), H_{m0} is the significant wave height at the dike toe (m) and γ_b, γ_f and γ_β are dimensionless reduction factors to account for respectively, the presence of a (horizontal) berm in the dike profile, roughness of the slope surface and the angle of approach for incoming waves. The index 2% implies that that 2% of the incoming waves have a run-up of this level or higher. The roughness factor γ_f has been determined for many types of revetments, some of which are shown in table 3.5.

Table 3.5 Roughness factor of several revetment systems (Van der Meer,2002).

	γ_f
Smooth, impermeable (concrete, asphalt etc.)	1.0
Grass	1.0
Open stone asphalt	0.9
Vilvoordse stone	0.85
Rip-rap, single layer	0.77
Rip-rap, double layer	0.55

A model-scale study done by Gu shows that the open structure of Elastocoast gives a fairly high reduction of wave run-up. With a roughness factor γ_f of 0.7-0.9 the reduction effect on wave run-up is comparable to that of open stone asphalt.

Table 3.6 Roughness factor for Elastocoast (Gu, 2007a).

	γ_f
Elastocoast®	0.9

3.4.4   Stability of unhardened Elastocoast on a slope

In order to determine the stability of unhardened Elastocoast on a slope, simple tests were performed (Gu, 2007a). In these tests freshly produced Elastocoast was put on an adjustable plate, of which the slope was slowly increased. Two different types of geotextile were tested. The results of this test show that there is a better grip on geotextile that is woven and that it is best not to apply Elastocoast on slopes steeper than 1:3-1:4.

Table 3.7 Stability of unhardened Elastocoast on a slope (Gu, 2007a).

	Initiation of movement	Complete failure
Woven geotextile	1:3,7	1:2,7
Non-woven geotextile	1:1,9	1:1,5

3.4.5   Resistance to erosion by abrasion

A qualitative comparison has been made of the resistance to erosion by abrasion of fully cured Elastocoast (Gu, 2007a). For this comparison several samples were put in a tumbling machine together with abrasive material (sand and gravel). This resulted a qualitative ranking, in which Basalton was least damaged and open stone asphalt was damaged most. Elastocoast performed better than open stone asphalt, but showed more damage by abrasion than the smooth materials Basalton and colloidal concrete:

1. Basalton
2. Colloidal concrete
3. Elastocoast
4. Open stone asphalt

At the Dutch Elastocoast pilot tests, there was an important difference between the two pilot locations: the water at the location Petten contained significant amounts of sand, shells and other material, whereas the water at location Ouwerkerk was quite clean. Despite these characteristics, no significant difference was found in the amount of damage at both structures. At Petten the surface of the rocks showed more signs of weathering by abrasion, but this did not lead to extra damage (Bijlsma, 2008).

Figure 3.7 The Elastocoast pilot location Petten suffered from large amounts of sand and other abrasive material, but no extra damage was observed (Bijlsma, 2008).

3.5 Mechanical properties

3.5.1   Viscoelastic behaviour

Dynamic or oscillatory tests are performed to study the viscoelastic properties of a sample. Viscoelastic materials have both elastic (solid) and viscous (fluid) properties, the extremes of which are described by Hooke's law of elasticity and Newton's law of viscosity. Purely elastic materials do not dissipate energy when a load is applied and then removed. A viscoelastic material dissipates energy (produces warmth) through a cycle of loading and unloading (figure 3.8). The degree of viscous behaviour is an important property for revetment cover layers. Gradual viscous deformation tends to reduce internal stresses caused by i.e. imposed deformations (thermal expansion, differential settlement, etc).
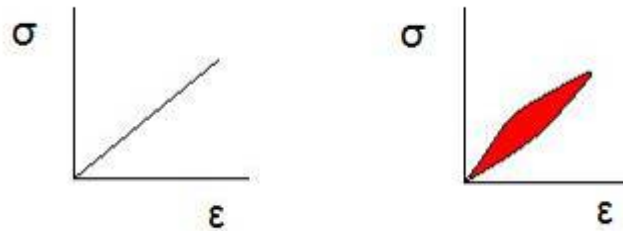
Figure 3.8 Stress-strain curves for a purely elastic material (left) and a viscoelastic material (right). The area in the right graph shows the amount of energy lost (as heat) in a loading-unloading cycle (wikipedia, 2008).

In example, a cover layer consisting of open stone asphalt is capable of slowly deforming under its own weight when a cavity is present under the cover layer. The viscous behaviour of the bitumen allows for relaxation, so that the stresses in the material are effectively 'reset' to zero in its new shape. This is a positive quality of the asphalt cover layer, since it retains its original strength even when deformed. In contrast, a non viscous material such as concrete in the same situation, would be stressed under its own weight, but does not deform to follow the shape of the cavity. The resulting span and internal stresses create a relatively unfavourable situation when the structure is loaded by external forces, such as impacting waves.

A frequency sweep test is a particularly useful test as it enables the viscoelastic properties of a sample to be determined as a function of timescale. A parameter that describes energy storage in structure loading and response is the phase angle δ. The phase angle is associated with the degree of viscoelasticity of the sample. A low value indicates a higher degree of elasticity (Akzo Nobel, 2004):

- $\delta = 90°$ indicates a viscous sample
- $\delta = 0°$ indicates an elastic sample
- $0° < \delta < 90°$ indicates a viscoelastic sample

A phase angle of zero indicates that the material has pure elastic behaviour; there is no energy storage. An angle between 0° and 90° means that the material has both elastic as viscous properties, in other words it has viscoelastic behaviour.

A four-point bending frequency sweep test was performed on small beams of 50x50x400 mm with limestone 10-14 mm as aggregate (Gu, 2007b). In this dynamic test both the sample stiffness and the phase angle were determined at different loading frequencies and temperatures.
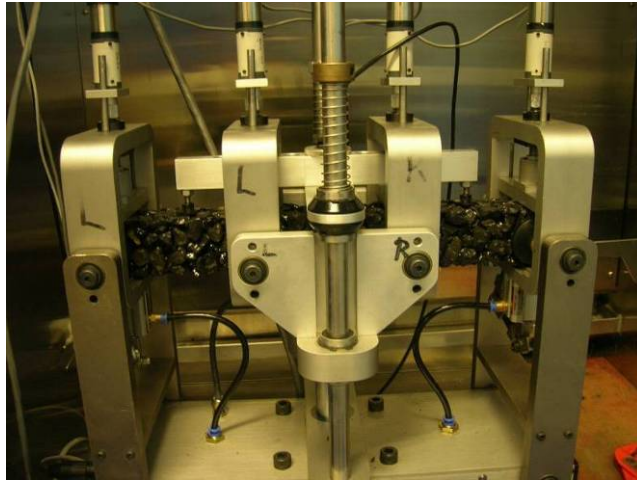
Figure 3.9 Setup for four-point bending frequency sweep test on a beam of Elastocoast (Gu, 2007b).

The following graph shows measured values of phase angle at different temperatures. The graph shows that Elastocoast phase angles are, at all temperatures, lower than those of open stone asphalt, indicating that the Elastocoast system behaves less viscous than open stone asphalt.
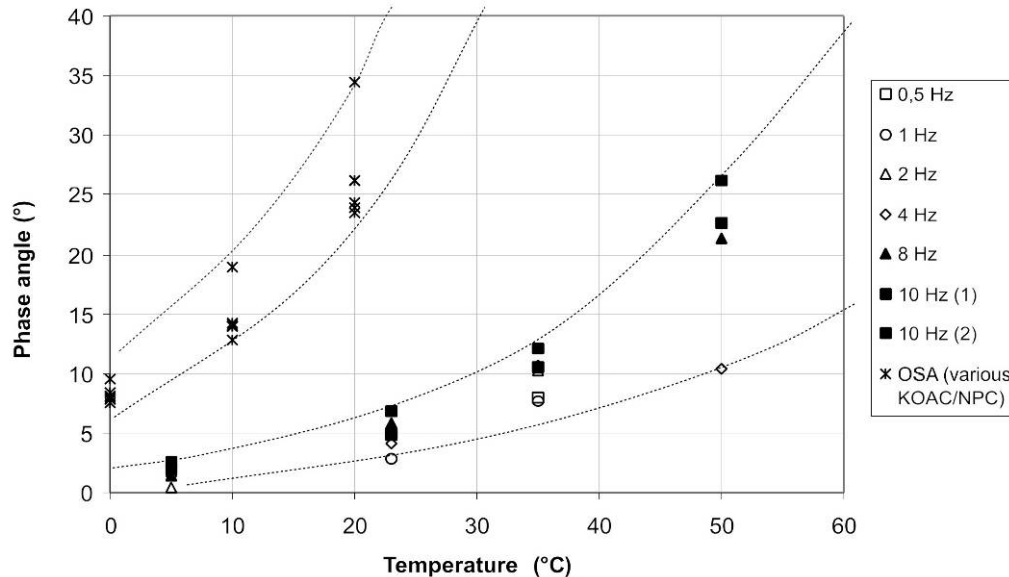
Figure 3.10 Results from frequency sweep test of Elastocoast (adapted from Gu, 2007b) compared to open stone asphalt (KOAC/NPC data adapted from DWW, 2006). Phase angle related to temperature.

It can clearly be seen from figure 3.10 that the phase angle is strongly related to the temperature. At higher temperatures the Elastocoast sample behaves more viscous, whereas at low temperatures it behaves almost completely elastic. Also an increasing deviation in phase angle is seen between different loading frequencies at higher temperatures. The material seems to behave more viscous at high frequencies of loading. One measurement at 50°C and 4 Hz has an atypical position in the graph, but since other measurements at 50°C for low frequencies (0.5-2.0 Hz) are missing it is not certain whether this is a measuring error or if there is more spreading between frequencies at high temperatures.

3.5.2   Young's modulus

From the frequency sweep test also the modulus of elasticity was derived as a material constant, expressed in the so-called Young's modulus or E-modulus. Young's modulus is a measure of the stiffness of a material. It describes the ratio between stress and strain and is expressed in MPa.

The following graph shows the development of the stiffness at different temperatures (assuming linear-elastic behaviour). There is a clear relation between the temperature and stiffness. When temperature rises, the stiffness decreases proportionally. There is only negligible deviation between the stiffness at different loading frequencies.
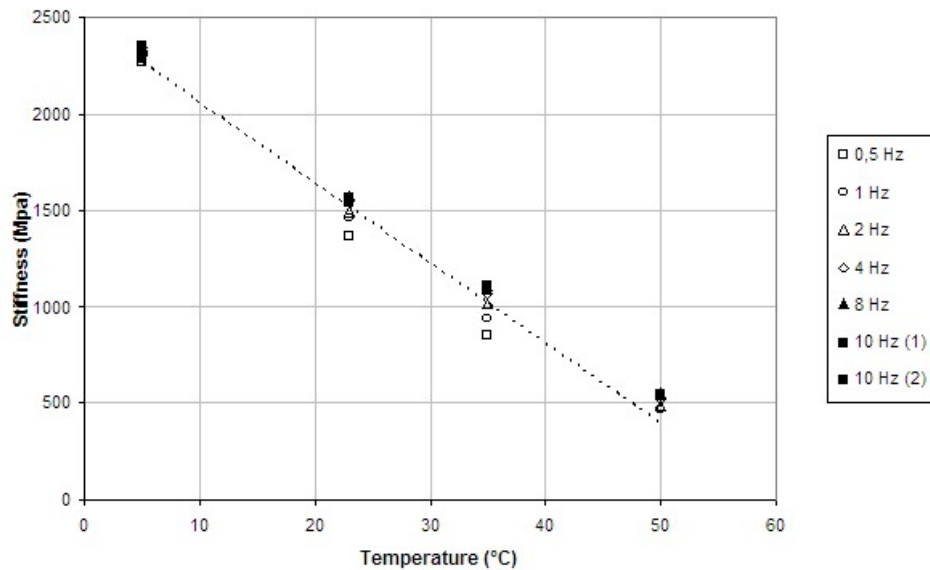
Figure 3.11 Stiffness of Elastocoast 10-14mm related to temperature (adapted from Gu, 2007b).

In comparison, the Young's modulus that is used for calculations with Open Stone Asphalt is 1.000 MPa, whereas for asphaltic concrete a value of 10.000 MPa is used (TAW, 2002).

Next, the average results for limestone samples with a 10-14 mm aggregate are set out against those of samples with 8-11 mm aggregate. This graph shows that a smaller stone size gives the sample a higher stiffness. There was no difference in open pore space or adhesive mixing ratio between the samples. The explanation probably lies in the number of contact points per volume, which is higher when the stone size is smaller.
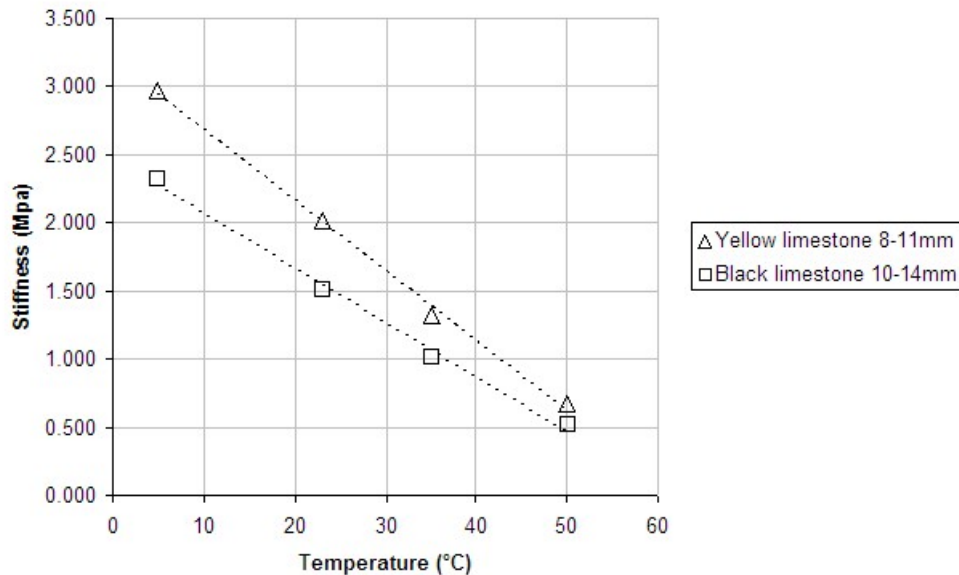
Figure 3.12 Stiffness of Elastocoast with two different gradings as a function of temperature (adapted from Gu, 2007b).

3.5.3 Bending strength

The flexural strength of Elastocoast beams was tested by Gu in a three-point bending test. From the maximum flexural moment just before failure and the beam dimensions the maximum tensile strength in the bottom part of the beam was derived. All tests were performed on 50x50x400 mm beams with 10-14 mm and 8-11 mm limestone aggregate. A total of twelve beams were tested at room temperature at two displacement rates: 50 mm/minute and 0.5 mm/minute.

The following figure shows two typical stress-displacement curves from the three-point bending test. At a lower displacement rate it can be seen that the Elastocoast beam does not behave completely linear elastic but slightly viscoelastic. The average results of all beams are given in table 3.8.
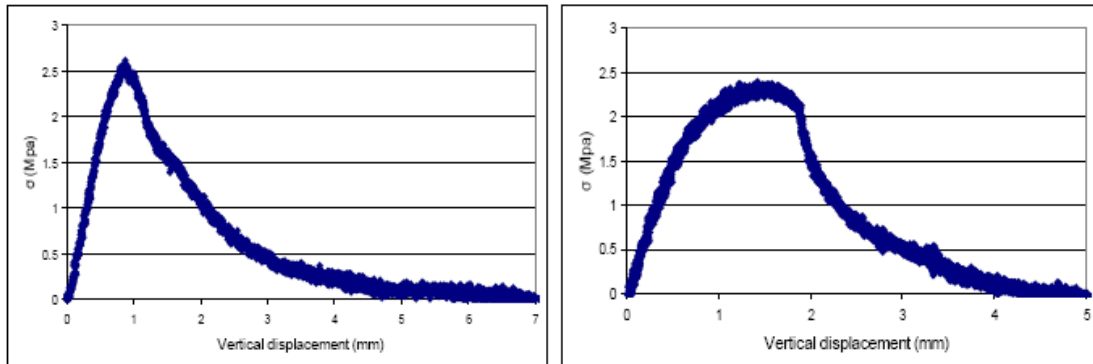
Figure 3.13 Two typical stress-displacement curves for Elastocoast. The graph on the left is for a beam loaded with a 50 mm/min displacement and the graph on the right with a 0.5 mm/min displacement (Gu, 2007b).

Table 3.8 Average results of three-point bending tests with Elastocoast beams (Gu, 2007b).

	Average flexural strength (MPa)	Standard deviation (MPa)
Elastocoast 10-14 mm	2.51	0.28
Elastocoast 8-11 mm	2.85	0.64

One has to keep in mind that this tensile strength is a measure for the bending strength of the beam, which not the same as the actual strength of the material itself. In reality the material is not distributed homogeneously over the cross section, but instead concentrated in certain points with open space in between. Since material stresses can not be transmitted through an open space, they are concentrated in and transmitted through the rocks and their contact points. Nonetheless, the bending strength parameter has a practical value as it can be directly used in mechanical analysis.

3.5.4 Compression strength of cube samples

During construction of the two Dutch pilots, samples were taken by Elastogran for the purpose of quality monitoring. On a regular basis, $150\times150\times150$ mm cubes of Elastocoast were produced on site and tested in a laboratory for compressive strength after a few days (fully cured).

These type of compression tests are normally performed on solid materials, such as concrete. Elastocoast has a very porous structure. Compression test results are therefore not directly comparable to those of other (solid) materials. Yet, the compression test has a highly practical value for qualitative comparison of separate Elastocoast productions. The method is simple and can be performed by any company involved in the construction of an Elastocoast revetment. In doing so, the results can be used to ensure a minimum quality of the product.

Figure 3.14 Compression test with an Elastocoast cube sample (Pasche, 2007).

The results of the compression tests taken from the Dutch pilots are shown in figure 3.15. Each value is averaged from five cube samples taken from the same moment during construction.
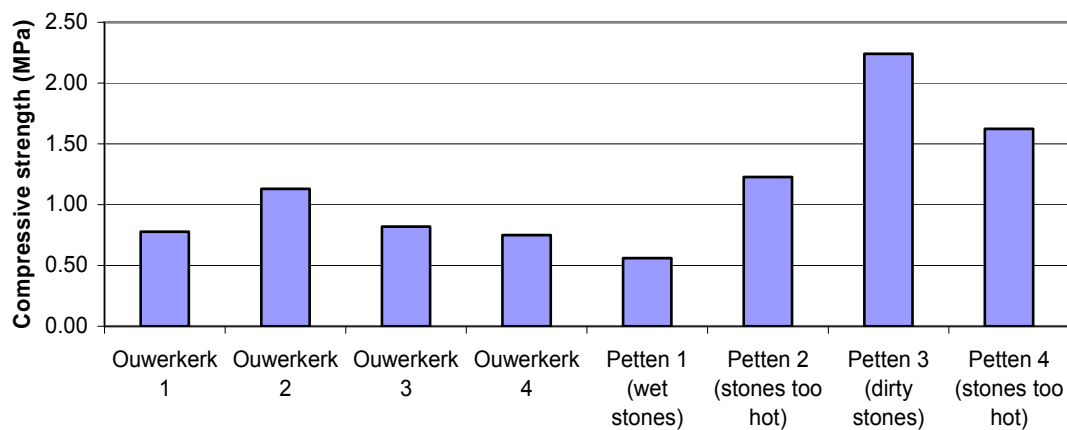
Figure 3.15 Results from compression tests with Elastocoast cube samples taken on different days of the construction of the Dutch pilots (adapted from Vugrek, 2007).

The figure shows that at the pilot location Ouwerkerk a reasonably constant quality was produced, with a minimum compressive strength of 0.75 MPa and an average of 0.87 MPa. The results from Petten however, show much more variability, from which interesting conclusions can be drawn regarding the influence of construction 'errors' on material strength:

- The samples from 'Petten 1' were taken at a moment that the aggregate had a very high content of moist. As explained in section 3.1.2, the presence of water on the surface of the rocks leads to formation of gas bubbles that weaken the bonding between the rocks and the polyurethane adhesive. This results in a lower strength of the end product, which is clearly visible in the compression test. A strength of only 0.56 MPa was reached.
- The samples from 'Petten 2' and 'Petten 4' were both taken at a moment that the stones were too hot (above 30°C). The high temperature was the result of the heating in an industrial dry tumbler, which was used to dry the previously too wet stones. Due to the rough tumbling process extra fine fragments were created by fracture of the rocks. These fine fragments increase the number of contact points in the end product, thus improving strength to an average of 1.43 MPa.
- A side effect of the heating however, is that the curing process is drastically accelerated. This decreases the time that is available for installation and profiling of the product. If incompletely cured Elastocoast is being shaped after the installation time has expired, the adhesive has become too much hardened to restore broken contact points or create new ones.
- The samples from 'Petten 3' had cooled long enough to a normal handling temperature, but still contained large amounts of dirt from the tumbling. These fine fragments increased the total surface area of the aggregate to such an extent, that extra polyurethane adhesive had to be added

to completely cover all rocks. The presence of fine fragments plus the extra adhesive produced relatively high strength samples (2.24 MPa).

Yet, this situation is depreciated, since the consumption of (costly) polyurethane adhesive is very high and the end product no longer has the clean and open structured look.

The main conclusion that can be drawn from above examples is that the strength and appearance of the end product is very dependent on the quality management and decisions that are made during construction. Heat and dirt are depreciated, but can be allowed to a certain extent. High moisture content however, has a significant negative effect on strength and should therefore be avoided at all times.

3.5.5   Durability (chemical degradation)

There are many ways in which external influences can cause cured polyurethane to chemically degrade in time. Some of these are (Gajewski, 1990):

- Hydrolysis – reaction with water
- Thermolysis – reactions which occur due to heat
- Oxidation – reaction with oxygen
- Photolysis – reactions caused by interaction with light (UV)
- Pyrolysis – reactions which occur due to burning
- Microbial – degradation caused by the attack of microorganisms
- Solvolysis – attack by solvents (i.e. alcohol)

Such degradation results in a loss of physical and mechanical properties and often visible discoloration. However, it is well possible to prevent or reduce this degradation by the use of stabilization systems during production, i.e. by addition of antioxidants or UV light absorbers to the compound (Michealis, 1997). In this way a polyurethane product can be designed to withstand aggressive influences from the environment in which it is applied.

The exact composition of the polyurethane system used for Elastocoast is a trade secret of Elastogran, but it is designed to withstand the harsh conditions that exist on the interface of sea and land. The type of polyurethane has been selected on, amongst others, the following criteria (Pasche, 2007):

- Resistance to abrasion
- Durability against hydrolysis
- Resistance to weathering
- Ecologically harmless (non-toxic)

Elastogran has tested the durability and strength of Elastocoast with intensive UV-radiation (simulating exposure to sunlight over many years). There were no signs of significant degradation found. Also, the first pilots that were constructed in Germany have remained undamaged under freeze-thaw cycles and salt water attack for almost five years now.

However, in order to give full certainty of the durability of Elastocoast these experiments should be combined with tests for material strength to determine whether the mechanical properties have not changed after exposure. This type of degradation cannot always be observed visually and is very important for the life expectancy of the Elastocoast system.

4 Possible failure mechanisms

4.1 Loading zones on a sea-dike

Not all parts of a dike body are exposed to the same hydraulic loads. The type of loading is important for a choice of revetment type and determination of possible failure mechanisms. Several zones can be discerned in a sea-dike profile. Each zone has its characteristic dominant type of hydraulic loading:

- I: Permanently submerged (below mean low water)
- II: Wave attack zone (between mean low water and mean high water + $\frac{1}{2}H_s$)
- III: Severe wave attack zone (between mean high water and design water level + $\frac{1}{2}H_s$)
- IV: Wave run-up zone (from design water level + $\frac{1}{2}H_s$ to design water level + $z_{2\%}$)

In the last years there is a trend of studies towards the application of wave-overtopping resistant dikes. This implies that the height of the dike is limited and overtopping by waves is allowed to a certain extent. An international project named ComCoast project has developed solutions to cope with the future increase of wave overtopping of dikes (by increasing water levels). One of these solutions is to make the dike itself more resistant to wave overtopping, by replacing the top of the dike and its inner slope with a revetment that will not wear away by severe overtopping (ComCoast, 2008).

In the present Dutch regulation the requirement for the crest and inner slope of an overtopping dike are simply met by an extension of the wave run-up zone (zone IV) to the back of the dike. Although comparable, the load conditions in the overtopping area are different (i.e. flow in only one direction instead of up and down). Anticipating on future developments, in this study a fifth loading zone is defined:

- V: Overtopping zone (crest of the dike and inner slope)

A special case, which is not limited to the previously defined loading zones, is the overpressure region. Overpressures can form a problem only with impermeable or semi-permeable revetments. The overpressure region can be defined as the part of the dike profile in which water overpressures could occur, namely ranging from below mean ground water level to the end of the cover layer. Mean ground water level is defined as halfway between mean water level and design water level (VTV, 2007).

- Water overpressure region (below mean ground water level).

With these five zones and the overpressure region the main hydraulic load cases that are present on a sea-dike can be described. Figure 4.1 gives a schematic representation of these loading zones on a sea-dike body.
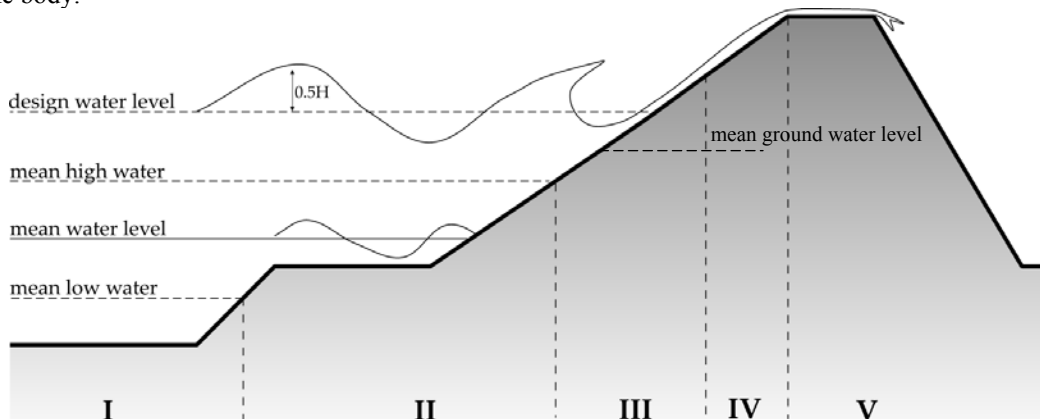
Figure 4.1 Schematization of loading zones on a sea-dike.

4.2   Common damage causes for revetments

In Chapter 2 a variety of modern revetment systems was described and categorized. These systems have been in use on the Dutch sea-dikes for extensive periods of time. The following table shows some common damage causes and critical failure mechanisms that have been derived from field experiences with existing revetments.

Table 4.1 Common damage causes, strength and critical failure modes for sea-dike revetments categorized by the extent of bonding (adapted from Pilarczyk, 1990 and Van der Meer, 1990).Situations that are well conceivable but have not (often) been seen in practice are indicated with 'o'.

	less bonding ← → more bonding					
	Dumped rock	Placed blocks	Mats, gabions	Grouted rock	Plates, open	Plates, closed
Damage cause						
Wave attack (max flow velocity)	x		x			
Wave attack (impact hammering)	x	x	x	x	x	x
Overpressure		x		x		x
Mechanical wearing (abrasion)	x	x	x	x	x	x
Climatologic influence (weathering)	x	x	o	x	x	x
Differential settlement of subsoil		x			x	x
Transport of material from sub layer	x	x	o	o	x	
Strength						
Structure/element weight	x	x	x	x	x	x
Mechanical strength				x	x	x
Bonding/interlocking		x	x	x	x	x
Friction	x	x				
Dynamic stability	x		x			
Porosity/permeability	x	x		x	x	
Critical failure mode						
Initiation of motion	x		x			
Breakage					x	x
Uplift / sliding		x	o			x
Erosion/abrasion			x	x	x	
Deformation	x	x	x	x	x	x

It should be noted that the above table is far from complete. Often the exact underlying mechanism of a revetment failure is hard to establish, simply because the 'evidence' has been washed away during the extreme conditions that led to the failure. Still, it gives a good first impression of the strengths and weaknesses of these revetment categories.

4.3   Characteristics of the Elastocoast revetment

The main characteristics of the Elastocoast system were presented in Chapter 3. They are of key importance for the prediction of the behaviour and critical failure mode of an Elastocoast revetment under extreme conditions. The main characteristics of the system are:

- Improved stability of individual rocks by polyurethane bonding
- Limited structure weight because of high porosity
- High hydraulic conductivity because of very open structure
- Plate type behaviour because of high bending stiffness and strong bonding

On basis of these characteristics a first investigation can be done into the failure mechanisms for an Elastocoast revetment. In the following section, the possible failure mechanisms will be discussed together with their relevance to Elastocoast.

4.4   Possible failure mechanisms for Elastocoast

In general, four main failure modes can be distinguished for the cover layers of sea-dike revetments:

- Micro instability
- Mechanical failure
- Macro instability
- Material degradation

The first failure mode, micro instability, refers to damage on the scale of individual rocks that are part of the cover layer. Removal of these rocks by instability or abrasion can lead to an intolerable material loss which, over time, results in a reduction of layer thickness and structure weight. This in turn could lead to exposure of the weak sub layer and also increases the risk of the failure modes mechanical failure and macro instability.

Second, mechanical failure means that the material strength is exceeded under loading. This is a typical mechanism that applies to plate type structures, in which loading perpendicular to the plate leads to bending of the plate. If the resulting stresses and strains exceed the strength and deformation capacity of the material it will break.

Macro instability stands for the loss of stability of the structure as a whole or a large part of it. This, for instance can be the uplifting of the structure by overpressure underneath, sliding down the slope by reduced friction at the interface with the sub layer or even the instability of a dike section as a whole (geomechanical failure). In the latter case the supporting soil under the cover layer turns instable and the structure collapses around a circular slipping plane or even subsides by loss of soil cohesion. Although macro instability can manifest in different ways, the mechanism is often caused by saturation of the supporting soil with water, which can strongly affect its stability.

Finally, the failure mode of material degradation comprises the change of physical or mechanical properties of the material in time. This can be the result of environmental attack such as was discussed in Section 3.5. Loss of material strength, stiffness or bonding is crucial for the performance of the revetment in the other failure modes. However, since the chemical change of materials is mostly in the field of expertise for material sciences, this failure mode is considered outside the scope of this thesis work. It should be always kept in mind though, that the material properties used in calculations should not always be taken for granted, especially when a design is made with a lifetime of multiple decades.

4.4.1   Micro instability (erosion)

Instability of individual rocks
Rocks can become unstable if attacked by waves or currents. Stabilizing forces that keep the rocks in place are its submerged weight, friction and interlocking with surrounding rocks. Also the degree of

exposure (neighbouring rocks provide sheltering) and rock shape play a role. If the destabilizing forces exerted by currents and waves are larger than the stabilizing forces the individual rocks will be loosened and removed from the cover layer.

The loading type depends on the location in the dike profile:

- Zone I: Permanently submerged (currents)
- Zones II and III: Wave impact zone (impact forces, wave run-up, wave run-down)
- Zone IV: Wave run-up zone (wave run-up, wave run-down)
- Zone V: Overtopping zone (overtopping discharge)

Possible load cases for structure interaction with currents and waves are:

- Tidal flows
- Orbital flow
- Wave breaking
- Wave up-rush and down-rush
- Overtopping discharge

Tidal flows are semi-constant currents that are caused by the propagation of tidal waves, which are very long waves with typical periods of 12 hours and wave lengths of several hundreds of kilometres (Schiereck, 2001). Currents can also be produced by wave action. Due to the dynamic nature of waves, these wave induced currents are highly variable (oscillatory) in velocity and direction and are called orbital flow.

Waves breaking on the slope of a dike can cause very high and local impact pressures. The air content of the water is very high and flow in this area is very turbulent. By the energy of impact part of the water is pushed up the slope with high speed (up-rush) to fall back again (down-rush) after having reached a certain run-up height.

When the water level and wave run-up are high enough for the up-rush to reach over the crest of the dike, water will flow over the crest and rush down the other side of the dike at high speed.

In the above only the forces exerted by clean water were considered. However, water may also contain hard particles carried along with the flow, such as loose grains (sand), rocks or shell material. The larger particles such as rocks can exert extra impact forces on a micro scale. Therefore the presence of abrasive material in the water can significantly increase the loads that work on the individual rocks (figure 4.2).
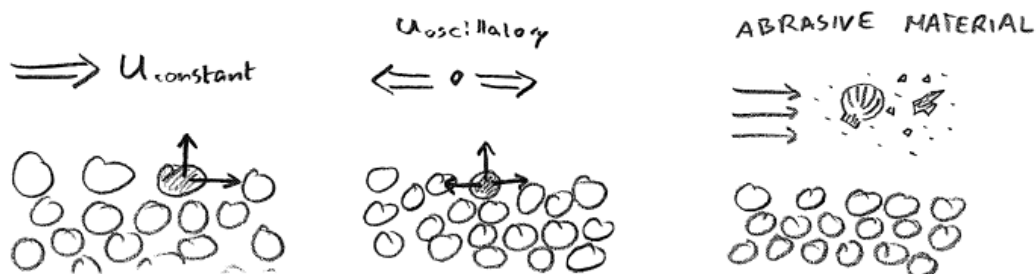
Figure 4.2 Destabilizing forces on individual rocks in a cover layer.

Relevance to Elastocoast

Loading by tidal flows plays only a small role on sea-dike revetments. These currents are often strongest in deeper water and velocities are in the order of 0.5-1.0 m/s with a depth of 10-15 m. It is possible for Elastocoast to be placed under the water level, but the underwater curing process results in a strong reduction of bonding strength (about 50%). Therefore Elastocoast will mainly be applied around mean

water level and above. In this region uniform and tidal flows will not be of importance compared to the other flow conditions.

Also orbital flow and overtopping discharge are assumed not to be normative for Elastocoast. A strong indication for this assumption is the excellent performance of a prototype Elastocoast revetment during overtopping tests in April 2008. These tests proved that Elastocoast is well capable of withstanding turbulent flow velocities of at least 6-7 m/s and perhaps even up to 12 m/s (Provoost, 2008). These are very high velocities that are seldom observed in natural conditions.

This leaves open the load cases of wave breaking and wave up- and down-rush or in other words: direct wave attack. At the Dutch prototype pilot 'Zuidbout' the Elastocoast revetment proved to be strong enough to withstand the attack of plunging and collapsing waves with a significant wave height of up to $H_s = 1.4\ m$ with a peak period of $T_p = 5.5\ s$. For the behaviour of Elastocoast under more extreme wave conditions additional research is necessary.

4.4.2   Mechanical failure

Breakage by wave impact
For hydraulic structures, the most important loads result from wave attack. Wave impact pressures cause high peak loads that work perpendicular to the dike slope. Forces perpendicular to a plate type cover layer lead to bending deformations in the plate. These deformations cause bending stresses in the layer's cross section. If these stresses exceed the bending strength of the material, mechanical breakage occurs.

The area on a dike slope around still water level is most prone to attack by waves:

- Zones II and III: Wave impact zone

Not all waves cause wave impact and not all impact loads are of the same size. First of all, waves with a plunging or collapsing breaker type are most likely to cause impacts. Wave impacts result from water mass of breaking waves hitting the dike slope with high velocity. The duration of a wave impact load is very short; i.e. 10-100 ms. Maximum impact pressure under extreme conditions can be as much as 100-150 kN/m^2, and locally (over small areas) pressures can be twice as high (Kolkman, 1996).

In case of a plate loaded perpendicular to its surface, there are two scenarios to be distinguished (figure 4.3):

- Loading of a plate that is fully supported by the underlying soil (ideal situation)
- Loading of a plate with a local absence of support
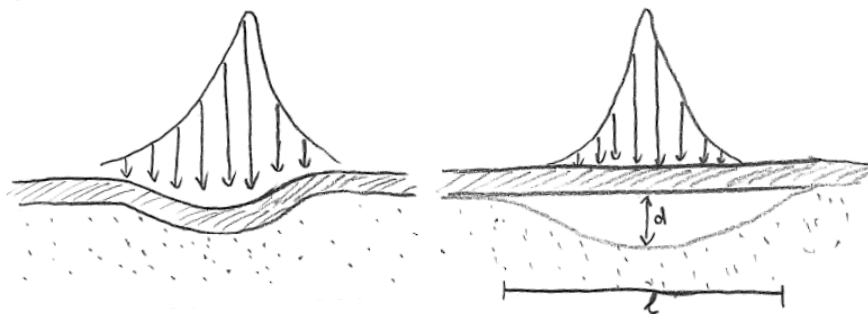
Figure 4.3 Two load scenarios: a fully supported plate and a local absence of support under the plate.

The local absence of support under the cover layer can be the result of:

- Formation of a cavity due to differential settlement
- Formation of a cavity due to material transport out of the supporting layer
- Loss of carrying capacity due to liquefaction of the soil

Differential settlement is probably one of the most common causes for the formation of cavities. A variable settlement of the subsoil along a dike body is almost inevitable in the construction of dikes, due to the natural spreading of subsoil properties. Human error by insufficient compacting during construction can also lead to uneven settlement. Differential settlement is the main cause of the failure of several plate revetments made out of concrete in the early 20th century. Concrete is a very stiff material and has very high compression strength, but is can only withstand relatively small tensile forces. Bending deformation therefore quickly leads to brittle failure of a concrete plate unless reinforcement measures are taken.

Formation of a cavity by material transport is most often the result of a bad design or construction error. A structure should be designed such that sand from the subsoil is prevented from washing out by application of a suitable granular filter or geotextile at the interface of the sand and the cover layer unless the cover layer can be considered completely sand tight. However, it can happen that for instance a geotextile is locally damaged for some reason, enabling sand from the sub layer to be washed out through a hole.

The last case is the most complex one. Soil liquefaction comprises the loss of carrying capacity of the grain skeleton. This may occur in undrained and saturated soil. The phenomenon of liquefaction is further discussed in section 4.4.3.

Relevance to Elastocoast
As shown in Chapter 3 the Elastocoast system has a bending stiffness of around 2500 MPa. A continuous cover layer consisting of Elastocoast is expected to behave as a stiff plate, which will bend under perpendicular loading. The high bending stiffness will result in a high tensile stress in the bottom of the plate when deformed. Calculations are necessary to define the limits to which an Elastocoast cover layer can be loaded.

An interesting and informative scenario is that of an Elastocoast cover layer with a local absence of support. At the German Elastocoast pilot at Sylt Ellenbogen breakage by formation of a cavity has actually already been observed in reality. Here on a sandy beach the Elastocoast was applied under water on top of a geotextile. The construction was bordered on each side by steel sheet piles. Now a hypothesis of what happened was that sand from underneath the structure was washed away through a crevice in the sheet piles. The foundation was washed away, but the geotextile remained hanging on the top of the sheet piles. A large cavity formed under the structure and consequently it collapsed under its own weight and the loading of impacting waves. Figure 4.4 shows a schematization of the process.
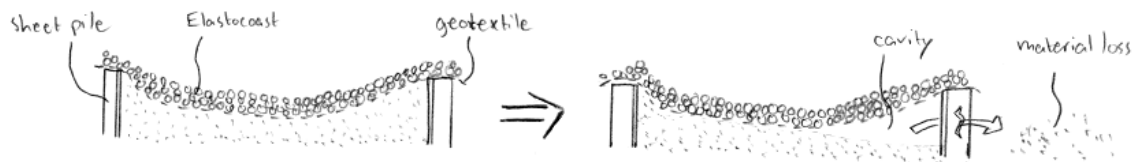
Figure 4.4 Hypothesis for the mechanical breakage of the Elastocoast pilot at Sylt Ellenbogen.

4.4.3   Macro instability

Overpressures
Macro instability is the overall instability of the whole structure or a large part of it. The main cause of macro instability is the buildup of water pressure inside the dike body. Head differences between the inside and outside water level lead to groundwater flow. If this flow is obstructed in some way pressure will build up, which may lead to a variety of problems.

Overpressures under a cover layer can occur in the zone starting at the level of the revetment toe to the level of the groundwater inside the dike body:

- Water overpressure region

Three failure modes will be discussed in this section:

- Uplift
- Shear and slip
- Soil liquefaction

Uplift
If there is a difference in water level under and above the cover layer of a dike a pressure gradient exists over the thickness of that layer. In case the water flow resulting from this pressure gradient is obstructed by for instance limited hydraulic conductivity of the cover layer, or in the most extreme case complete impermeability, an upward force works perpendicular to the dike slope.

There are three basic situations in which a head difference between the outside water level and the groundwater level in the dike can occur:

- Static
- Dynamic, during maximum wave retreat
- Dynamic, during wave impact
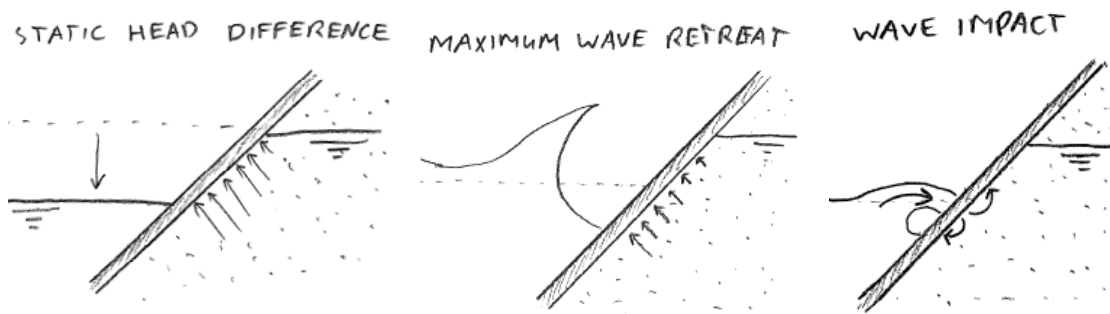
Figure 4.5 Three cases in which overpressures can occur under the cover layer of a dike.

A static head difference occurs when the outside water level drops, for instance after a period storm with high wind setup. According to the law of communicating vessels, the groundwater level in the dike will follow, but this happens only slowly. The result is a situation of a relatively constant head difference, causing overpressure. The time scale of this process is quite long, the water level usually needs several hours to have dropped significantly.

A dynamic head difference can be the result of the water level moving up and down the slope over the length of a wave period, or by wave impact. The time scale of these processes is respectively seconds and milliseconds. Pressure variations are therefore present only for a short period of time, but can be very significant in size.

If the cover layer is pushed up from the dike body an open space is created underneath, in which groundwater can flow freely and transport of core material takes place. By this transport cavities and bumps are formed under the cover layer, preventing it from returning to its original position after the upward pressures have gone. The cavities can then lead to breakage of the revetment as described before.

Shear and slip

A high groundwater level inside the dike body can not only lead to uplift pressures, but also the structural coherence of the soil can change. Water overpressures in the open pore space of the soil lead to reduction friction forces between the individual grains. When the friction between grains is reduced, a shear force can cause them to slide over each other. Two distinctive forms of such as sliding plane are (figure 4.6):

- Shear plane between two layers of the structure (i.e. between the cover layer and the soil)
- Circular slip plane over the dike cross section
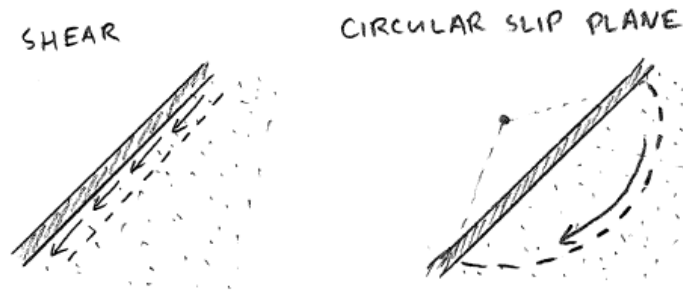
Figure 4.6 Instability of the cover layer by formation of a shear plane or slip circle.

The mechanism of sliding becomes of importance when the gravity component parallel to the slipping plane is higher than the shear resistance over the slipping plane. The shear resistance decreases when the perpendicular gravity component decreases. Only in very steep slopes, the parallel gravity component is much greater than the perpendicular component. Therefore, only in very steep slopes geomechanical instability by slipping can be expected. For slopes milder than 1:2.5 it is very unlikely to occur (Klein Breteler, 2007a).

Soil liquefaction

The most extreme form of loss of structural coherence in the soil is liquefaction. The strength of a soil mass is determined by the transfer of the forces from grain to grain. Water overpressures in the open pore space of the soil lead to reduction of friction forces between the individual grains. This leads to loss of coherence and possible liquefaction of the soil. Liquefaction may occur in fully saturated loosely packed sand. A vibration or shock can initiate a flow slide, in which the fluid mass of water and cohesionless sand behaves like a heavy liquid (quicksand).

Wave impact has a twofold effect on the occurrence of liquefaction. First, repeated wave pressure penetration through the cover layer leads to a step-by-step increase of water pressure inside the dike body. Then, the shock of impact propagates through the cohesionless soil and can initiate liquefaction (figure 4.7).
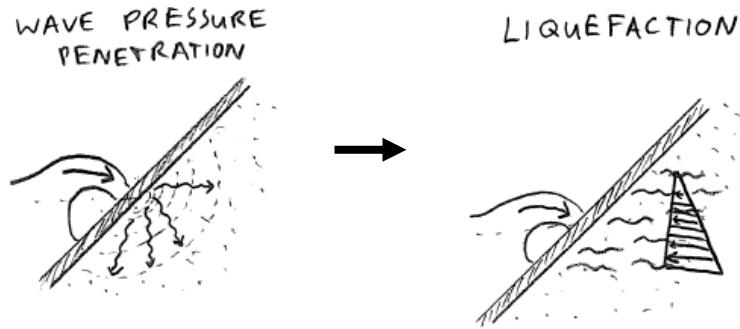
Figure 4.7 Repeated wave pressure penetration leads to a step-by-step increase of water pressure and can initiate liquefaction.

Unlike the above mechanism of a shear or circular slip plane, liquefaction will result in a flow slide even with very gentle slopes (d'Angremond, 2001).

Relevance to Elastocoast
Uplift by static head differences is not to be expected with an Elastocoast revetment, simply because of its high permeability. Even a low permeability would be enough for the water pressures to be able to diminish before high uplift pressures could build up. Normally, uplift by dynamic head differences is unlikely for the same reason of high permeability. However, if the permeability of the Elastocoast revetment is reduced by, for instance, clogging of its pores with fine sediment some overpressures might occur. This depends on the extent of the reduction of hydraulic conductivity of the material when clogged.

It can be argued that the failure modes of shear and slip are not relevant to an Elastocoast revetment. First, the high permeability of Elastocoast provides a good drainage, which should reduce the chance of water pressures leading to loss of soil coherence. Second, if the soil is reasonably compacted, the danger of shear or slip is only likely to be present on steep slopes (Klein Breteler, 1998), whereas the Elastocoast system can only be placed on relatively gentle slopes (see also Chapter 3).

Liquefaction can take place under pressure penetration of wave impacts on sand bodies that are insufficiently compacted and saturated with water. The open structure of Elastocoast offers a good way for impact pressures to penetrate to the underlying layers. It is conceivable, that repeating wave impact pressures lead to such an increase of saturation and water pressure inside the dike body that liquefaction becomes a danger.

Concluding, uplift by dynamic head differences should be investigated for unfavourable conditions in which the permeability of Elastocoast is reduced. Subsoil liquefaction is a complex phenomenon that is difficult to predict, but fairly simple to prevent. To reduce the risk of liquefaction it is of great importance that a good compaction of the subsoil is ensured, prior to construction of the cover layer.

4.5   Choice of mechanisms for further analysis

This chapter started with an introduction of loading zones on a sea-dike and common damage causes known for existing revetments. Then the possible failure mechanisms that could apply to Elastocoast were summed up and discussed. Some of these mechanisms were already ruled out by the system characteristics of Elastocoast. The remaining mechanisms need further analysis to determine their relevance to and implications for an Elastocoast cover layer.

Chosen to be further analyzed in this report are:

- Micro scale instability (erosion) under wave attack
- Breakage of an Elastocoast plate under wave impact
- Uplift under dynamic head differences

In order to assess the extent of uplift pressures also the hydraulic conductivity of Elastocoast under non-ideal conditions needs to be determined:

- Hydraulic conductivity of clogged Elastocoast

Not all relevant mechanisms will be further analyzed in this report. The failure mechanism of material degradation was found to be more of a material science problem and lies outside the scope of this study. The specific type of macro failure by liquefaction under wave impact might be relevant to Elastocoast but is also chosen to be left out, since this is a complex phenomenon for which no adequate models are yet available and its probability of occurrence can be significantly reduced by adequate compaction of the subsoil.

Relevant but outside the scope of this report:

- Material degradation
- Liquefaction under wave impact

5 Detailed analysis

5.1 Introduction

In this chapter a detailed analysis will be performed for some of the cases discussed in Chapter 4. These cases are:

- Micro scale erosion – instability of individual rocks (section 5.2)
- Mechanical breakage by wave impact (section 5.3)
- Theoretical prediction of the hydraulic conductivity of (clogged) Elastocoast (section 5.4)
- Macro scale instability by uplift pressures (section 5.5)

5.2 Failure mechanism: Instability of individual rocks

5.2.1 Introduction

Instability of individual rocks may lead to their removal from the cover layer. This loss of material is called erosion. When the erosion is persistent, the loss of material causes the actual thickness of the cover layer to decrease in time. This can eventually lead to failure by either loss of top layer macro stability because of the reduction in structure weight or by formation of gaps in the cover layer which cause the vulnerable underlying layer to be exposed to hydraulic loads.

Erosion is caused by hydraulic forces such as wave action and current velocities. Impact, shear, drag and lift are destabilizing forces, trying to lift individual rocks from the structure's surface. Stabilizing forces that keep the rocks in place are its submerged weight, friction and interlocking with neighbouring rocks. Also the degree of exposure (neighbouring rocks provide sheltering) and rock shape are important.

The following figure shows the forces that theoretically act on an individual rock in an armour layer (Schiereck, 2001):
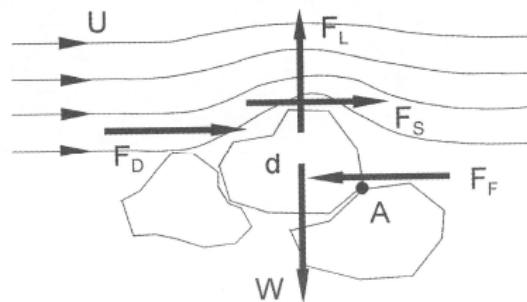
Figure 5.1 Hydraulic forces exerted on an individual rock under influence of flow (Schiereck, 2001).

Stability formulas

To predict the stability of loose rocks in dumped armour layers under wave attack a wide variety of stability formulas has been developed. The structure-wave interactions however are so complex, that the models mostly have a limited theoretical basis (which is illustrated in figure 5.1). They are empirical, based on laboratory or full scale research. A few commonly used stability formulas that have proved their value over time have been found by Hudson (1953, 1959), Van der Meer (1988, 2004) and Pilarczyk (1990). They are all used to find a minimum element weight that should be stable or on the edge of movement at the input wave parameters and structure properties.

5.2.2 Expected stability of Elastocoast on a micro scale

Apart from the attachment of the individual rocks to each other by polyurethane, the Elastocoast structure is very similar to a dumped rock armour layer. The destabilizing forces on rocks in the Elastocoast structure are equal to those that would occur on loose dumped aggregate of the same size, but then without the polyurethane addition. Therefore it can be argued that the general stability formulas for dumped rock structures are, to a certain level, applicable to Elastocoast.

The polyurethane bonding provides an extra stabilizing force. In the Hudson and Pilarczyk stability formulas empirical upgrading factors have been introduced, in which such extra stability can be taken into account. The upgrading factors extend the applicability of the formulas to cases where the stability of loose rock is improved by for instance grouting or steel nets. In fact, the Pilarczyk formula is designed with this purpose in mind.

Now, it is supposed that the general stability formulas for loose rock structures can be applied to an Elastocoast revetment if a suitable upgrading factor is chosen. The upgrading factor for Elastocoast can be determined by filling in its system properties and loading conditions in which Elastocoast has proven to be stable.

5.2.3 Stability of dumped rock structures

Structure classification

For rock slopes and rock breakwaters under wave attack an important parameter, which gives a relationship between the structure properties and the wave conditions is the dimensionless stability number N_s (-) (CIRIA/CUR, 2007). High values of N_s indicate that the structure is dynamic and constantly reshaped by wave action.

The stability number is defined as:

$$N_s = \frac{H}{\Delta D}$$

With:

H = wave height (m), this is usually the significant wave height H_s

$\Delta = \dfrac{\rho_r - \rho_w}{\rho_w}$ = relative buoyant density of stone (-)

ρ_r = mass density of rock (kg/m^3)

ρ_w = mass density of water (kg/m^3)

D = characteristic size or diameter (m), depending on the type of structure

The characteristic size for natural rocks is their median nominal diameter D_{n50}. In some cases the thickness of the cover layer can be used instead as a characteristic size D. In the latter case the relative buoyant density is defined as $\Delta = (1-n)\Delta$ where n (-) is the porosity of the cover layer.

Hudson formula

Hudson (1953, 1959) developed a simple formula, based on model tests with regular waves on non-overtopped rock structures with a permeable core. The Rock Manual 2007 (CIRIA/CUR, 2007) suggests a notation of the Hudson formula in a practical form, related to the stability number N_s with the use of H_s. An upgrading factor K_u is added to take into account improved coherence of the rock material in special cases.

The Hudson formula can be written as follows:

$$N_s = \frac{H_s}{\Delta D_{n50}} \le K_u \frac{(K_D \cot\alpha)^{1/3}}{1.27}$$

With:

K_D = stability coefficient (-)
K_u = upgrading factor (-)
α = slope angle (°)

The K_D values suggested for design correspond to the *no damage condition* of 0-5%. The Rock Manual 2007 gives $K_D=2.0$ for breaking waves and $K_D = 4.0$ for non-breaking waves. The upgrading factor K_u was suggested in a Dutch technical report (TAW, 2002) for application of the Hudson formula on rock structures that are partly penetrated with asphalt. Values for the upgrading factor are given in the following table:

Table 5.1 Upgrading factors for the Hudson formula in case of grouting.

Revetment system	Upgrading factor K_u (-)
Surface grouting	1-1.5
Pattern grouting	5-6

Van der Meer formulas for shallow water conditions
Van der Meer (1988) derived from a series of tests empirical formulae to predict the stability of rock armour layers on slopes in deep water. An extension for application in shallow water conditions was proposed by Van Gent et al (2004). The result is four separate formulas in which discrimination is made between plunging and surging waves in both deep and shallow water conditions. In The Rock Manual 2007 the Van der Meer formulas for shallow water are given as follows.

For plunging waves in shallow water:

$$N_s = \frac{H_s}{\Delta D_{n50}} \le c_{pl} P^{0.18} \left(\frac{S_d}{\sqrt{N}}\right)^{0.2} \left(\frac{H_s}{H_{2\%}}\right) \left(\xi_{s-1,0}\right)^{-0.5}$$

For surging waves in shallow water:

$$N_s = \frac{H_s}{\Delta D_{n50}} \le c_s P^{-0.13} \left(\frac{S_d}{\sqrt{N}}\right)^{0.2} \left(\frac{H_s}{H_{2\%}}\right) \sqrt{\cot\alpha} \left(\xi_{s-1,0}\right)^{-P}$$

With:

c_{pl} = 8.4 (-) with a standard deviation of $\sigma = 0.7$
c_s = 1.3 (-) with a standard deviation of $\sigma = 0.15$
P = notional permeability of the structure (-), the value of this parameter should be: $0.1 \le P \le 0.6$. For structures with a geotextile as part of the filter $P=0.1$ is recommended.
S_d = damage level parameter (-), $S_d=2$ for no damage condition
N = number of incident waves at the toe (-), which depends on the duration of the wave conditions
$H_{2\%}$ = wave height exceeded by 2% of the incident waves at the toe (m)
$\xi_{s-1,0}$ = surf similarity parameter (-), using the energy wave period $T_{m-1,0}$ (-)
$T_{m-1,0}$ = the (spectral) mean energy wave period (s)

Compared to the Hudson formula the Van der Meer formula for plunging waves in shallow water conditions requires a significantly more comprehensive data set of the wave conditions, containing the number of waves, 2% wave height and the mean energy wave period.

Pilarczyk formula for wave attack

For practical design of revetments consisting of loose aggregate, placed blocks or related structures a general (empirical) formula was derived by Pilarczyk (1990):

$$N_s = \frac{H_s}{\Delta_m D} \leq \psi_u \phi \frac{\cos(\alpha)}{\xi^b} \text{ with } \cot \alpha > 2$$

With:

Δ_m = relative density of a system-unit (-)

D = specific size or thickness of protection unit (m)

Ψ_u = system-determined (empirical) stability upgrading factor (-), Ψ_u = 1.0 for riprap as a reference and $\Psi_u > 1$ for other revetment systems

Φ = stability factor or stability function for incipient of motion (-), defined at $\xi = 1$

α = slope angle (°)

$\xi = 1.25 \, T_p H_s^{-0.5} \tan \alpha$, surf similarity index on a slope (-)

T_p = peak wave period (s)

b = exponent related to the interaction process between waves and revetment type (roughness, porosity/permeability etc), $0.5<b<1$ (-). For rough and permeable revetments as riprap, $b = 0.5$. For smooth and less permeable placed-block revetments it can be close to $b = 1$.

An important difference between Hudson and Van der Meer is that Pilarczyk intended his formula to be used with a wide variety of revetment systems including loose aggregate, rip-rap, placed blocks, gabions and mattresses and even open stone asphalt. This is possible because of the system-determined stability upgrading factor Ψ_u and the possibility to give the relative density Δ_m and characteristic size D in terms of submerged bulk density and cover layer thickness. The result is a formula that is easy in use but highly flexible in application. A downside is that the formula is a crude simplification of reality and the choice of a suitable upgrading factor has to be made on basis of expert insight.

Pilarczyk defined the stability number Φ using Van der Meer's formula for loose rock. A value of $\Phi = 2.25$ was found for incipient motion (no damage condition). It is used as a reference value for comparison with alternative revetment systems.

In the following table the upgrading factor Ψ_u is given for several revetment systems:

Table 5.2 Upgrading factors for the Pilarczyk formula for different types of revetment systems.

Revetment system	Upgrading factor Ψ_u (-)
Rip-rap	1.0-1.3
Pitched stone	1.0-1.5
Pattern grouting	1.5
Surface grouting	1.0
Open stone asphalt (D=d)	2.0-2.5
Gabion baskets and mattresses (D=d)	2.0-3.0

5.2.4 Calculations

Input parameters

In order to apply the rock stability formulas to Elastocoast it is required to know the conditions at which movement of the rocks in the Elastocoast system is initiated. The results from the damage monitoring by Bijlsma (2008) at the Elastocoast Zuidbout pilot will be used for this. It is assumed that during the most extreme conditions measured at the pilot, the rocks in the Elastocoast structure were only just on the edge of stability. This means that the damage caused by these conditions did not exceed the *no damage condition* ($S_d = 2$ or $N_{od} = 0\text{-}5\%$).

The figure below shows the damage development as was observed at the Zuidbout. There is an increase in damage during each storm event (storms are not shown in the figure). In determining the damage percentage N_{od} only the top $2D_{n50}$ of the layer thickness was taken into account. It is clear that the damage percentage remains very small and well within the definition of the *no damage condition*. Therefore the assumption made above can be considered a safe one.
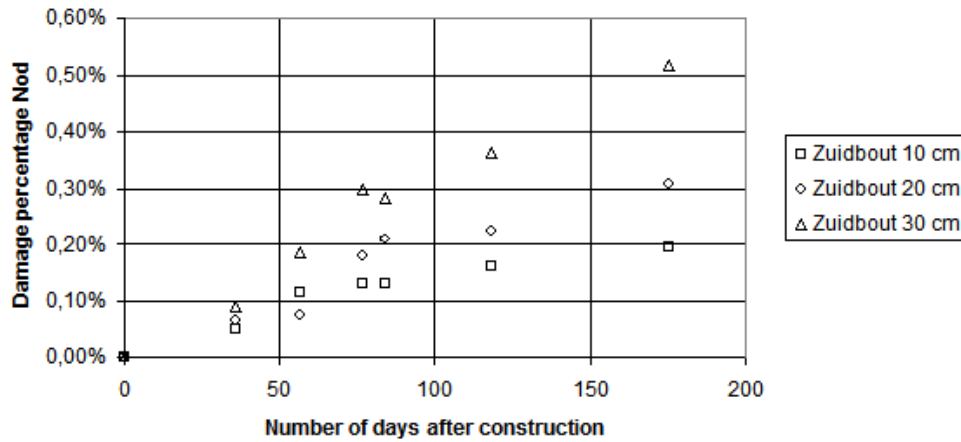
Figure 5.2 Damage development at the Elastocoast Zuidbout pilot during the storm season of 2007-2008 (Bijlsma, 2008).

The characteristic structure properties of the Zuidbout pilot location are as follows:

Table 5.3 Structure properties at the Zuidbout pilot location (Bijlsma, 2008).

Parameter	Description	Value	
D_{n50}	Rock diameter	0.021	m
h	Layer thickness	0.1	m
ρ_r	Mass density	2720	kg/m^3
n	Porosity	0.50	-
$\cot(\alpha)$	Slope angle	3	-

The parameters presented in the following table have been obtained from the original dataset for the pilot location Zuidbout (Bijlsma, 2008). The wave conditions are the most extreme that were measured during the storm of March 12th in the storm season of 2007-2008. The wave conditions during this storm were:

Table 5.4 Wave conditions at the Zuidbout pilot during the storm of March 12th, 2008 (Bijlsma, 2008).

Parameter	Description	Value	
H_s	Significant wave height	1.4	m
$H_{2\%}$	2% wave height	2.1	m
T_p	Peak wave period	4.5	s
$T_{m-1,0}$	Mean energy wave period	4.1	s
ξ	Surf similarity index	1.6	-
$\xi_{m-1,0}$	Surf similarity index calculated with $T_{m-1,0}$	1.4	-

Rock diameter as characteristic system size

First, calculations will be made with the median nominal rock diameter D_{n50} as the characteristic system size. For each of the three stability formulas a minimum rock size can be derived that would be needed for a rock armour layer to remain stable under the circumstances described above. A rip-rap revetment with this rock size could be seen an equivalent alternative to the Elastocoast revetment (remains stable under the same conditions). Also the value for an upgrading factor is determined that would be needed to make the formula applicable to Elastocoast.

The stability number is:

$$N_s = \frac{H_s}{\frac{\rho_r - \rho_w}{\rho_w} D_{n50}} = \frac{1.4m}{1.654 \cdot 0.021m} = 40$$

The following table shows the resulting equivalent rock size and the upgrading factor for the stability formulas of Hudson, Van der Meer and Pilarczyk applied to Elastocoast.

Table 5.5 Equivalent rock diameters and upgrading factors for Elastocoast according to the stability formulas with D_{n50} as characteristic system size.

$N_s=40$	Elastocoast rock diameter	Equivalent rock diameter	Upgrading factor for Elastocoast
Hudson	0.021 m	0.59 m	28
Vd Meer	0.021 m	0.52 m	25
Pilarczyk	0.021 m	0.50 m	24

Layer thickness as characteristic system size

Now, the calculations will be repeated, but in this case with the cover layer thickness as the characteristic system size. This method is not allowed for the formulas of Hudson and Van der Meer, which are specifically based on calculations with the rock diameter. Therefore only the Pilarczyk formula will be applied. For comparison a cover layer of open stone asphalt ($\Psi_u=2.5$) will be used to derive an equivalent layer thickness.

$$N_s = \frac{H_s}{(1-n)\Delta \cdot h} = \frac{1.4m}{0.801 \cdot 0.1m} = 17$$

Table 5.6 Equivalent layer thickness in open stone asphalt and upgrading factor for Elastocoast according to the Pilarczyk stability formula with the cover layer thickness as characteristic system size.

$N_s=17$	Elastocoast layer thickness	Equivalent layer thickness in open stone asphalt ($\Psi_u=2.5$)	Upgrading factor for Elastocoast Ψ_u
Pilarczyk	0.10 m	0.41 m	10

5.2.5 Evaluation

Structure classification

The stability numbers N_s for Elastocoast are very high. According to the classification of structures based on the stability number (section 2.4.2), the dynamic behaviour of the Elastocoast revetment would be in the range of a gravel beach. A gravel beach is constantly in movement and reshapes to adjust to the varying wave conditions. Although trivial, the fact that the Elastocoast revetment remains completely stable despite of the high stability number shows that the polyurethane bonding has a significant effect on the stability of the individual rocks. The bonding keeps the rocks in place under conditions where there would normally be movement.

When the stability number is based on layer thickness instead, the resulting value of $N_s=17$ is still high when compared to the other structures from section 2.4, where layer thickness was used (fully grouted rock, open stone asphalt and asphaltic concrete) and stability numbers ranging around $N_s=8\text{-}10$.

Stability formulas

When the rock diameter is used as the characteristic system size, the stability formulas give an equivalent rock size of approximately 0.5 m. The upgrading factor that is needed for Elastocoast is around 25, which is very high when compared to upgrading factors for other revetment systems. On the one hand this is an indication of the superiority of Elastocoast compared to, for instance, grouted rock, whereas on the other hand the high value of the factor gives thought about the applicability of the formulas.

The rock stability formulas have in common that the weight of the rock is the single most important factor contributing to stability. In the Elastocoast system the weight of an individual rock is relatively small and the contribution of the polyurethane bonding relatively high. Thus the premise that the individual rock weight is normative for stability is wrong in case of Elastocoast. This makes the stability formulas unsuitable for prediction of Elastocoast stability when rock diameter is chosen as a characteristic system size.

When, instead, the Pilarczyk formula is used with the layer thickness as characteristic system size, the upgrading factor derived for Elastocoast is $\Psi_u=10$. This is a factor 4 larger than the upgrading factor for open stone asphalt. Again, this can be seen as an indication of the superiority of Elastocoast over an open stone asphalt cover layer. The applicability of this formula seems reasonable.

Because of the strong polyurethane bonding it is more credible that the stability of Elastocoast depends on bulk weight rather than the weight of an individual rock. Strictly speaking the use of layer thickness instead of rock size no longer describes the stability of the individual rock on a micro level but that of a larger piece of the cover layer on a macro scale. The stability of such a larger piece will be discussed later on in this report (section 5.5).

5.2.6 Conclusion

The applicability of the stability formulas of Hudson, Van der Meer and Pilarczyk to an Elastocoast revetment is very limited. When the median rock diameter D_{n50} is used as characteristic system size, the upgrading factors for the stability formulas are very high, even too such an extent that the appliance of these formulas to Elastocoast is depreciated. The basic assumption of rock weight being the main stability parameter does not adequately describe the stability of rocks in an Elastocoast cover layer. The physical processes that lie at the base of stability formulas for rock armours are therefore not suitable to describe the stability of individual rocks in an Elastocoast cover layer.

The Pilarczyk formula has the option to choose the overall cover layer thickness as characteristic system size. The resulting upgrading factor of $\Psi_u=10$ implies that the required thickness of an Elastocoast cover layer would be four times less than that of an open stone asphalt cover layer under the same loading conditions. However, strictly speaking the use of layer thickness instead of rock size in the Pilarczyk formula no longer describes the stability of the individual rock on a micro level but that of a larger piece of the cover layer on a macro scale. On a macro scale the physical processes that determine a structure's stability are of a different order than those on the scale of an individual rock. The stability of such a coherent structure is examined in section 5.5 of this report.

5.3 Failure mechanism: Mechanical breakage by wave impact

5.3.1 Introduction

A plate type cover layer will fail by mechanical breakage when the internal stresses caused by loading of the structure exceed the material strength. Depending on the extent of the breakage this can lead to an impermissible exposure of the protected under layers.

Four basic load cases can be discerned. These can occur separately of each other, but also simultaneously:

- Tension/compression force
- Shear force
- Bending moment and shear force
- Torsional moment

Based on its mechanical properties such as the relatively high stiffness, an Elastocoast cover layer is expected to behave as a plate structure. Wave impact pressures cause peak loads that work perpendicular to the dike slope. Forces perpendicular to a plate lead to bending and shear deformations. Therefore bending and shear are assumed to be the normative load case for mechanical breakage by wave impact of an Elastocoast cover layer. Although the stress field in the cover layer is a combination of both bending and shear, for simplicity we assume here that the deformation and failure of Elastocoast is governed by bending moment and bending strength only. The consequences of this assumption are discussed in section 5.3.6.

Now, let's consider the basic scenario from section 4.4 in which an Elastocoast cover layer is placed on an elastically supporting soil, i.e. a sand or clay bed, with only a flexible geotextile at the interface. A wave impact load causes the cover layer to bend and consequently compresses the soil underneath. This results in an upward reaction force from the soil (Figure 5.3). The amount of resistance to bending thus depends on the bending stiffness of the cover layer, but also on the compressibility of the soil.

In the scenario above the cover layer is assumed to be continuously supported by an elastic foundation. As discussed in section 4.4 in reality it is possible for the support to be locally absent due to material loss, differential settlement or to lose its carrying capacity by liquefaction. In case a cavity is formed under the cover layer the amount of resistance to bending depends again on the bending stiffness of the cover layer and the compressibility of the soil along the edges of the cavity and of the dimensions of the cavity itself (Figure 5.3).
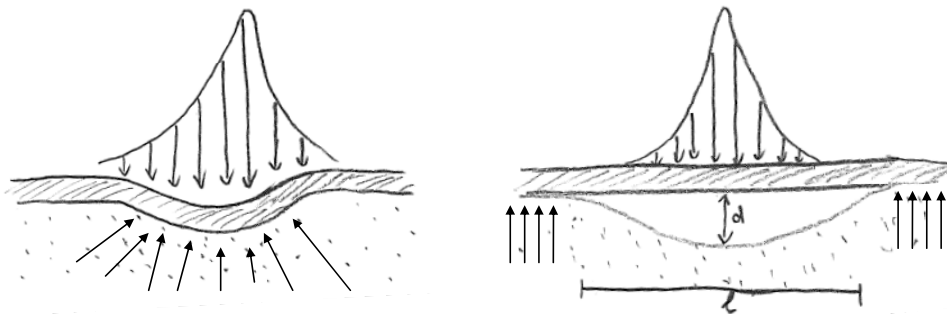
Figure 5.3 Scenario of cover layer continuously supported on elastic soil (left) and scenario of local absence of support (right).

Not only the horizontal dimension l of the cavity is an important factor in the bending deformation, but also the depth d, compared to the deflection of the plate. In a narrow and deep cavity bending deformation is governed by the bending stiffness of the cover layer, but in a wide and shallow cavity it is possible that, after a bending deformation equal to depth d, the cover layer finds support again on the bottom of the cavity. Thus the ratio d/l, bending stiffness and soil compressibility all determine the amount of bending deformation.

5.3.2 Schematization of an elastically supported plate structure under wave impact

The schematization of a structure must approach the real situation as much as possible. A straightforward schematization of an Elastocoast cover layer is that of a plate of finite dimensions lying on a damped elastic subsoil. The dynamic load of wave impact can be schematized as a distributed load of a repeating nature. Figure 5.4 shows a schematization with a spring-dashpot system to describe the soil reaction and a typical distribution in shape and time of the wave load.
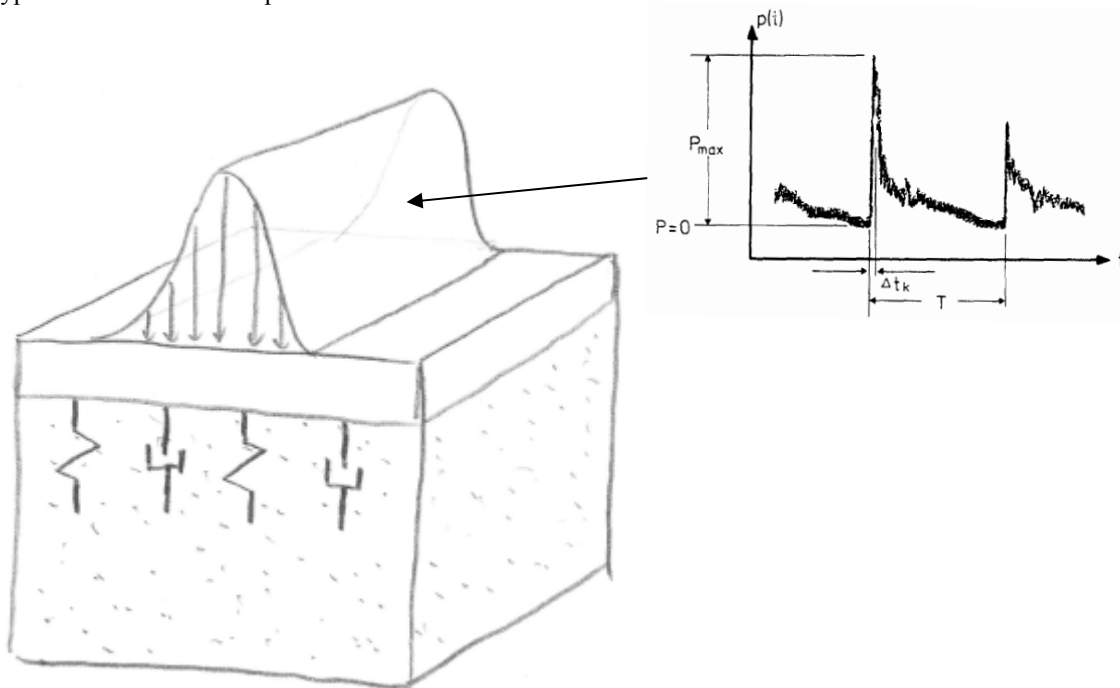
Figure 5.4 Schematization of mechanical system and shape of wave load, Q(x,y,t,) (Kolkman, 1996)

This schematization however results in a complex problem that could only be solved numerically with the help of a computer program. Therefore in this report a schematization is made that gives insight in the interactions between load, cover layer and support, but is still manageable analytically. Two scenarios are analyzed:

- Scenario 1: wave impact on continuously supported cover layer;
- Scenario 2: wave impact on only partially supported cover layer.

Although both scenarios basically describe the same system, the specific load case in each scenario requires a different approach in schematization.

Scenario 1: wave impact on continuously supported cover layer
The Elastocoast structure will be schematized as a plate on linear-elastic foundation. The plate is loaded by a wave impact, schematized as a triangular distributed load $q(x)$ with a maximum of P_{max} and a base width equal to H.
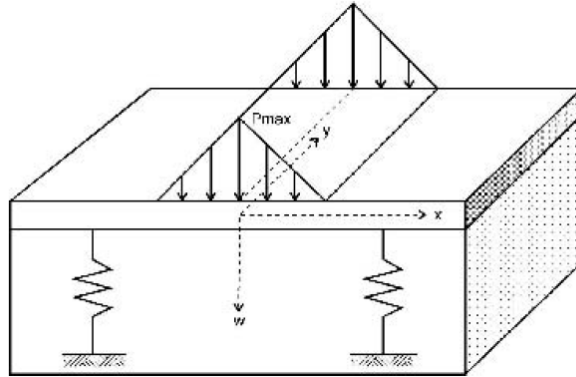
Figure 5.5 Schematization of the wave impact with a triangular load (TAW, 2002).

The deflection of the plate can be described with the following differential equation:

$$K \frac{\partial^4 w}{\partial x^4} + cw = q(x)$$

In which:

$K = \dfrac{Eh^3}{12(1-v^2)}$ is the bending stiffness of a thin plate

E = Young's modulus of Elastocoast (MPa)
h = thickness of the plate (m)
v = constant of Poisson of Elastocoast (-)
c = coefficient of compression of subsoil (MPa/m)
w = deflection of the plate (m)
$q(x)$ = load function
x = distance along horizontal axis (m)

The above differential equation is based on the assumption that the plate is infinitely long in y-direction, such that all derivatives in that direction are zero. The triangular wave load is also assumed to be infinitely long in y-direction.

Since the structure's own weight as well as the elastic support are continuously present over the entire length it is not necessary to incorporate the own weight in the load function $q(x)$. The deflection and therefore also the support reaction caused by the own weight are constant throughout the structure. The load function can now be defined as:

$$q(x) = \frac{P_{\max}(z - x)}{z} \qquad \text{for} \quad -z \le x \le z$$

$$q(x) = 0 \qquad \text{for} \quad x < -z \quad \text{and} \quad x > z$$

In which:

$P_{max} = \rho_w \cdot g \cdot q \cdot H$ is the maximum impact pressure (MPa)

ρ_w = density of water (=1025 kg/m^3)

g = gravitational acceleration (= 9.81 m/s^2)
q = empirical impact factor dependent on dike slope (=4.0)
H = wave height (m)
z = half the triangular load width (= 0.5 H)

Now, the assumptions are made that, first, the maximum pressure P_{max} takes place in the center of the plate $x=0$ and, second, that the length of the plate structure is enough to be considered infinite in x-direction.
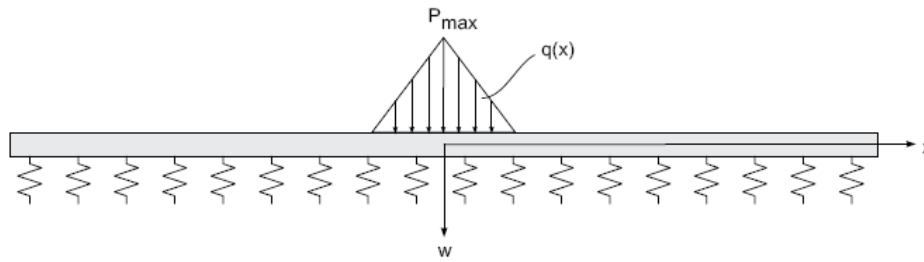
Figure 5.6 Mechanical schematization of problem.

The response to the loading is symmetrical, so that the schematization can be further simplified by considering one semi-infinite half.
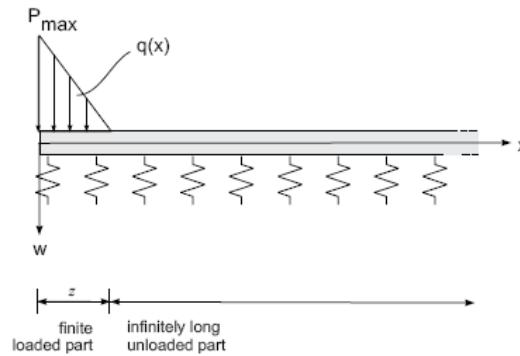
Figure 5.7 Mechanical schematization of problem as a semi-infinite beam.

In order to obtain the solution to the differential equation, the structure is split into two sections, 1) a finite part on which the distributed load $q(x)$ works; and 2) an infinitely long unloaded section.

Choice of the right boundary conditions makes sure that the interface between the sections is properly defined. A complete elaboration of the schematization and its solution is given in Appendix II.

For the maximum moment M_{max} per meter (Nm/m) in the center under the triangular load the following solution is found:

$$M_{max} = -K(2C_2\beta^2 - 2C_4\beta^2)$$

$$w_{max} = C_1 + C_3 + \frac{P_{max}}{c}$$

Where β is a convenient parameter introduced during calculation and C_1, C_2, C_3 and C_4 are integration constants (see Appendix II for details).

The maximum tension σ_{max} (MPa) in the bottom of the plate at this point can now be calculated with:

$$\sigma_{max} = \frac{M}{W} = \frac{M}{\frac{1}{6}h^2}$$

Scenario 2: wave impact on only partially supported cover layer
In case of a cavity under the cover layer, the analytical solution to the above schematization becomes more difficult to find. Therefore for this case the triangular wave load is further simplified to a constant line load.
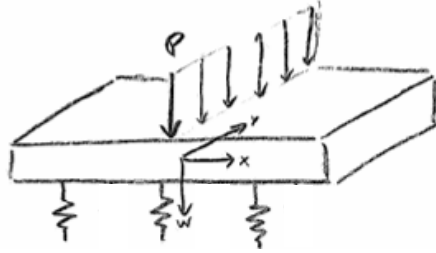
Figure 5.8 Schematization of the wave load as a line load.

The deflection of the plate is then again described with the differential equation:

$$K\frac{\partial^4 w}{\partial x^4} + cw = q(x)$$

In case of a cavity the support reaction to the structure's own weight is no longer constant in the x-direction. At the location of the cavity the support is completely absent. This means that the own weight of the cover layer ρ_{ec} now has to be taken along in the load function. It is represented as a constant distributed load over the entire length of the structure.

The load function now becomes:

$$q(x) = \rho_{ec}gh$$

In which:

ρ_{ec} = own weight of the cover layer (kg/m^3)
h = thickness of the cover layer (m)

The concentrated wave load at $x=0$ is defined as follows and will be introduced as a boundary condition.

$$P = p \cdot b$$

In which:

P = wave impact force (N/m)
$p = \rho_w \cdot g \cdot q \cdot H$ is the maximum impact pressure (N/m^2)
H = wave height (m)
q = empirical impact factor dependent on dike slope (=2.3)
b = the width over which the maximum impact pressure is schematized to represent the full wave load (= 0.4 H)

Analogous to scenario 1, the plate is further considered to be fully symmetrical around the loading point and infinitely long in the horizontal plane. The concentrated load P works at $x=0$.
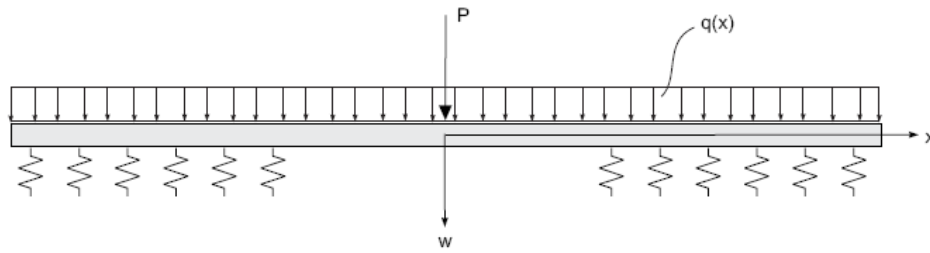
Figure 5.9 Mechanical schematization of the problem.

To find the solution to this problem, the structure is again cut in half and split into two sections: 1) a section of finite length, over which there is no support reaction, $c \cdot w = 0$ and a shear force of *0.5P* at x=0; and 2) a infinitely long unloaded section on elastic support. Half of the load *P* can now be applied as a boundary condition at *x=0*. A complete elaboration of the schematization and its solution is given in Appendix II.
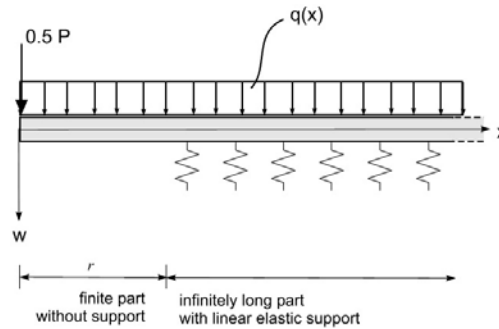
Figure 5.10 Mechanical schematization of the problem as a semi-infinite beam.

For the maximum moment M_{max} (Nm/m) in the center under the line load, *x=0*, the following solution is found:

$$M_{max} = C_2$$

$$w_{max} = -\frac{C_4}{K}$$

The solutions to the integration constants can be found in Appendix II. From the bending moment M_{max} directly under the line load, the maximum stress σ_{max} in the bottom of the plate can be easily derived in the same way as in scenario 1:

$$\sigma_{max} = \frac{M}{W} = \frac{M}{\frac{1}{6}h^2}$$

5.3.3   Assumptions made during schematization

Static solution to a dynamic problem

In the above schematizations a static linear solution is given for a problem that is in fact dynamic. The time-dependency of the load, support reaction and deflection is neglected. This approach is adopted from the Dutch *Technisch rapport asfalt voor waterkeren* (TAW, 2002) for determination of stresses in an asphalt cover layer. The effect of this schematization was investigated in its predecessor; the *Leidraad voor de toepassing van asphalt in de waterbouw* (TAW, 1984). The underestimation in the bending moment that is derived from the static solution is approximately 22%, which error is believed to be acceptable because the damping effect of the soil has not been taken along in the calculations. Damping would result in a reduction of the actual moment. Furthermore the effect on the final result for the layer thickness is very small.
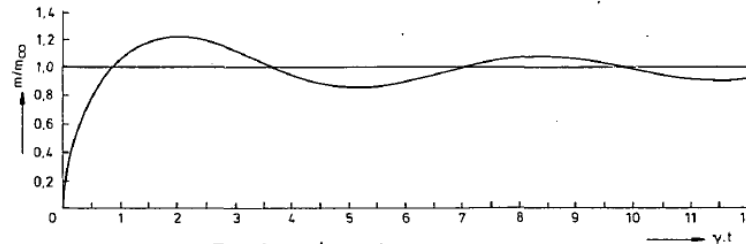
Figure 5.11 Bending moment for dynamic solution compared to the static solution (TAW, 1984).

Beam and plate theory

The plate structure has been simplified to a well known model in mechanics; the Euler-Bernoulli beam theory. The stiffness K is borrowed from plate theory for thin plates. These theories are valid under the following assumptions (Bouma, 2000 and Blaauwendraad, 2006):

- No extensional forces occur, so the beam axis is a neutral line. This is valid if $w \ll d$.
- A flat cross section remains flat after the load is applied. In fact, the cross section will undergo warping, but we can work with an average plane.
- The tension in y-direction is negligibly small and assumed to be zero. Due to a non-zero Poisson's ratio, some strains will occur in y-direction. Therefore the vertical displacement will vary a bit over the depth of the beam. We have neglected this.
- Shear deformation is small compared to bending deformation and therefore is neglected; this means that a plane cross section will remain plane.

With the schematization to a semi-infinite half space in x-direction, the assumption was made that the deflection *w* becomes zero at infinite distance. In reality, the cover layer has finite dimensions, which would introduce an edge effect. If this edge effect is to be neglected, the beam must be long enough for the effects of the load to have diminished before the end of the beam is reached. This assumption holds if the beam can be classified as a 'long beam' (Simone, 2007):

- The beam can be classified as long if the condition $\beta L > \pi$ is satisfied.

Poisson's ratio

The actual Poisson's ratio of Elastocoast is unknown. Most solid materials have a ratio between *0-0.50*. The Poisson's ratio for concrete is *0.15-0.20*, most steels are around *0.30* and rubber is almost *0.50*. In calculations with asphalt cover layers the Poisson's ratio is commonly assumed to be equal to *0.35*. Despite these values for the Poisson's ratio being meant for solid materials, the ratio for asphalt will now also be assumed for calculations with the porous structure of Elastocoast:

- The Poisson's ratio ν of Elastocoast is assumed to be *0.35*.

The possible error that is made with above assumption can be neglected, since the effect of the Poisson's ratio on the resulting maximum stress is quite small. An increase of the ratio leads to only a slight increase in stress.

Linear-elastic foundation

A continuous elastic support can be schematized according to the theory of Winkler, which states that the upward reaction force of the support is proportional to the compression of the supporting medium. The most simple form of this proportionality is linear: $p = c \cdot w$. In reality the relation between the reaction p and the compression of the soil w is non-linear. With increasing compression the soil stiffens and the reaction p increases more than proportional. The linearization of this relation is an approximation, which generally gives reliable results if the deflection is not too big (Bouma, 2000). This is implicitly already taken along in the earlier defined condition of $w \ll d$. Indicative values for the compression constant are *c=100 MPa/m* for a reasonably compacted sand bed and *c=30 MPa/m* for a foundation of clay.

5.3.4 Expected model outcome

On basis of the models presented above, it is expected that calculations will show the following results:

- Scenario 1: wave impact on continuously supported cover layer.
  With a continuous support it is expected that large part of the wave load is directly transferred to the elastic soil. The cover layer is thus relieved and will undergo only a small deflection. The maximum tension σ_{max} in the bottom of the plate will probably not exceed the bending strength of the material.
- Scenario 2: wave impact on only partially supported cover layer.
  With a cavity under the cover layer the ratio *d/l* will become important. If the depth of the cavity does not pose any constraints on the amount of deflection, the structures own weight and the line load will cause it to bend and possibly the bending strength of the material will be exceeded. On the other hand, with only a small depth and a large span, the deflected cover layer will find support on bottom of the cavity after all. Then the remaining burden will be transferred directly to the elastic soil and bending strength will not be exceeded.

The actual outcome according to the models will be analyzed in the next section.

5.3.5   Calculations

In the following calculations the maximum stress and the maximum deflection of the cover layer are determined as a function of the thickness of the cover layer. The wave load is varied to resemble waves between *H=1.0 m* to *H=6.0 m*. To get an impression of the influence of the soil compression constant for each case both a sand and a clay foundation are examined. The bending stiffness of the Elastocoast cover layer is set to *E = 2500 MPa* and the bulk density to ρ_{ec} = *1350 kg/m³*. The bending strength of Elastocoast is typically in the order of σ_{max} = *2-3 MPa*. Detailed calculations are given in Appendix II. Below only some typical results are given.

Scenario 1: wave impact on continuously supported cover layer
The following calculations represent a case of an Elastocoast cover layer supported by a relatively weak foundation consisting of clay. The cover layer is loaded by a wave with a height of *H=4 m*. The figure below shows the deflection of the cover layer along the x-direction. The triangular load has its peak at x=0, this is also where the maximum deflection is found.
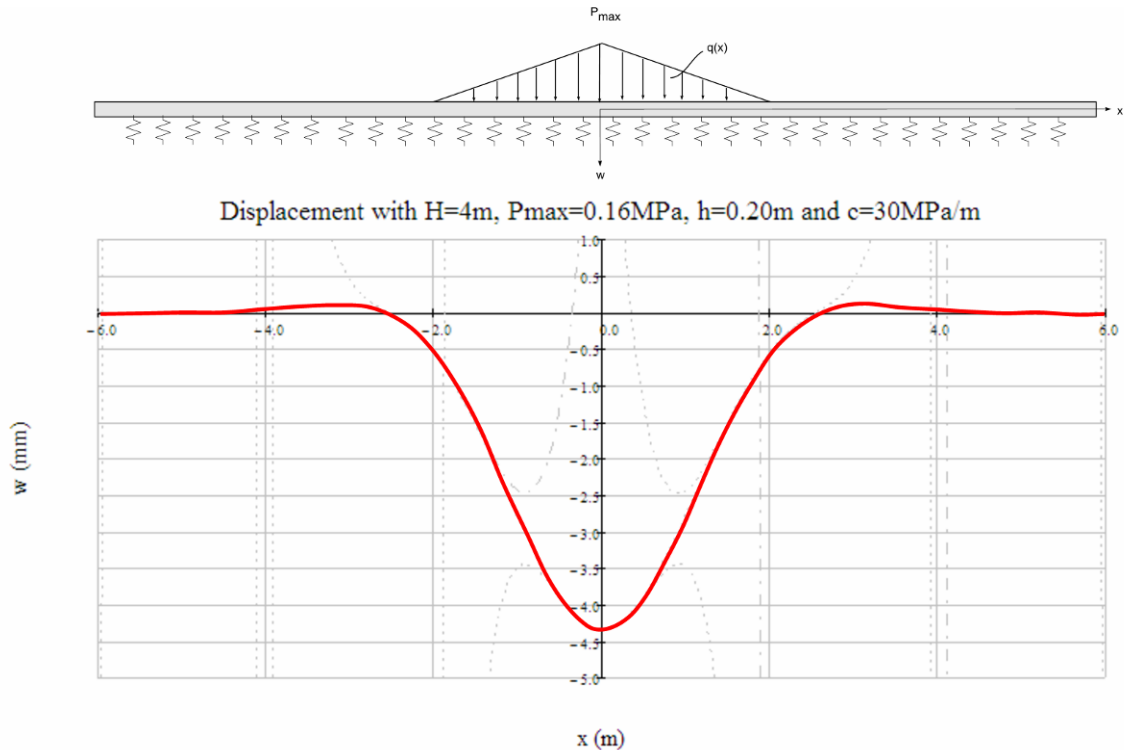
Figure 5.12 Displacement of the cover layer in scenario 1.

In the following figures, the maximum tensile stress σ_{max} and the deflection w_{max} at *x=0* are depicted as a function of the thickness of the cover layer, *h*. If read from right to left, it can be seen in the figures that the stress and displacement increase when the thickness of the cover layer is reduced. The stress then reaches a local maximum, after which a further reduction in the thickness results in a decrease in stress, whereas the displacement keeps on increasing. This point of maximum stress indicates that below a certain thickness, the cover layer starts to behave as a 'flexible' mat, which transfers the load directly to the elastic support.
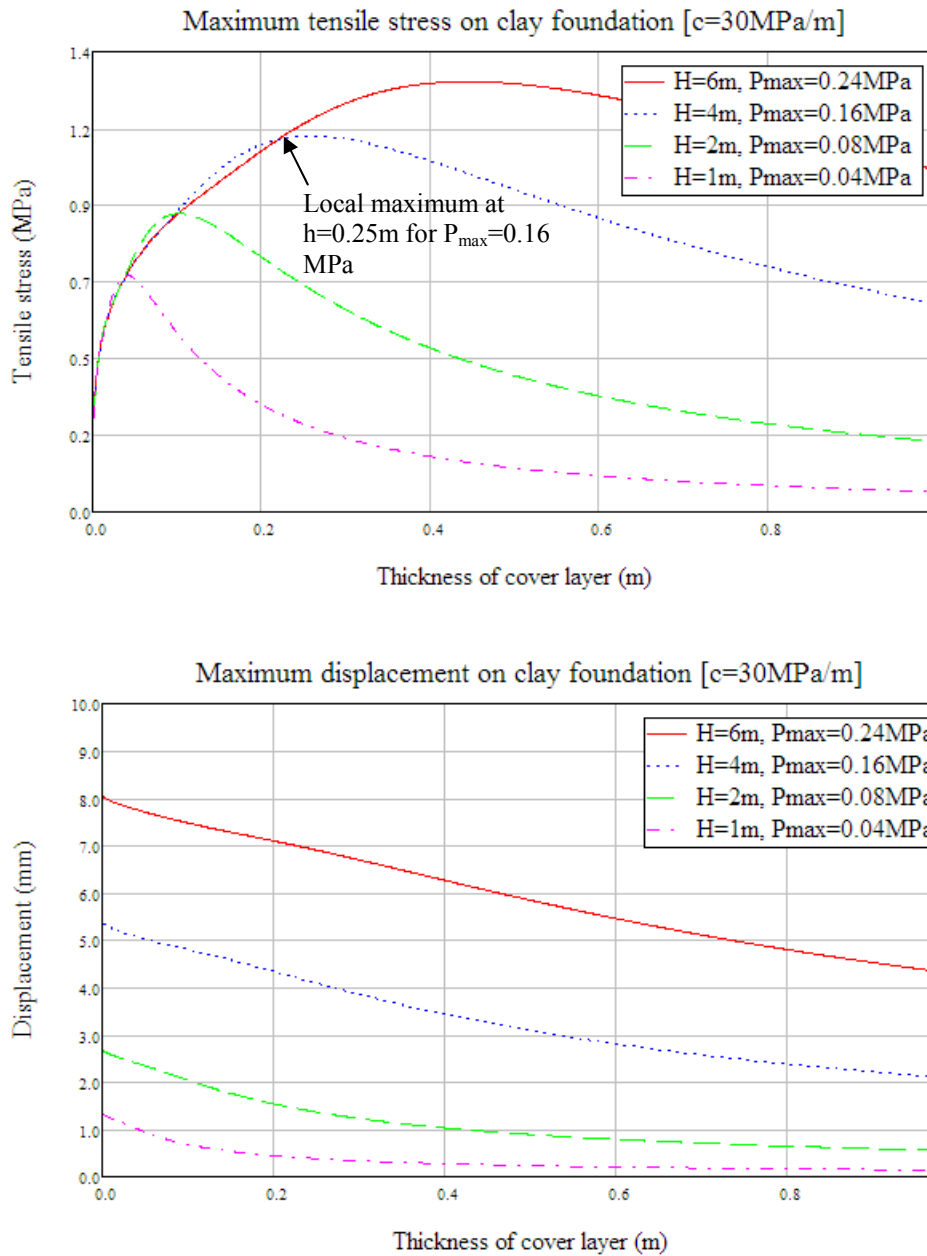
Figure 5.13 Maximum tensile stress and maximum displacement in scenario 1 as functions of cover layer thickness.

With a high loading of *H=4 m* or *P_{max}=0.16 MPa*, the maximum stress remains limited to values below σ_{max} *=1.2 MPa* (the approximate bending strength of Elastocoast is σ_{max} *=2-3 MPa*). In case the cover layer is supported by a firm sand foundation instead of clay, the stress with the same loading does not exceed σ_{max} *=0.6 MPa*.

Scenario 2: wave impact on only partially supported cover layer
The following calculations represent a case of an Elastocoast cover layer which is only partly supported by a foundation consisting of sand. The structure is loaded by a wave of *H=4 m*. The width of the cavity around x=0 is taken to be 2 m, so *z=1m*. The figure below shows the deflection of the cover layer along the x-direction. The concentrated wave load is located at x=0, this is also where the maximum deflection is found.

Displacement with H=4, P=148kN/m, h=0.20m, r=1m and c=100MPa/m
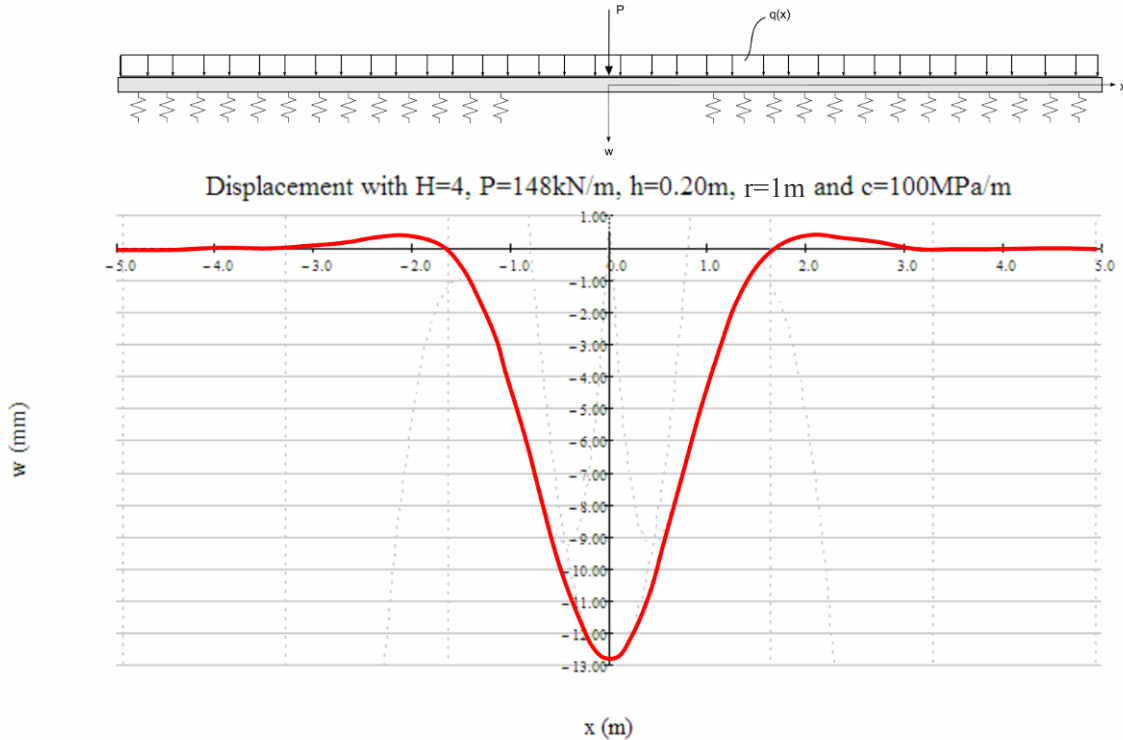
Figure 5.14 Displacement of the cover layer in scenario 2.

In the following figures, the maximum tensile stress σ_{max} and the displacement w_{max} at *x=0* are depicted as a function of the thickness of the cover layer, *h*. It can clearly be seen that both the maximum stress and the displacement grow exponentially when the thickness of the cover layer is decreased and approaches to infinity if the thickness approaches to *h=0 m*. The material strength of approximately σ_{max} = *2-3 MPa* is quickly reached at high loads and small thickness.
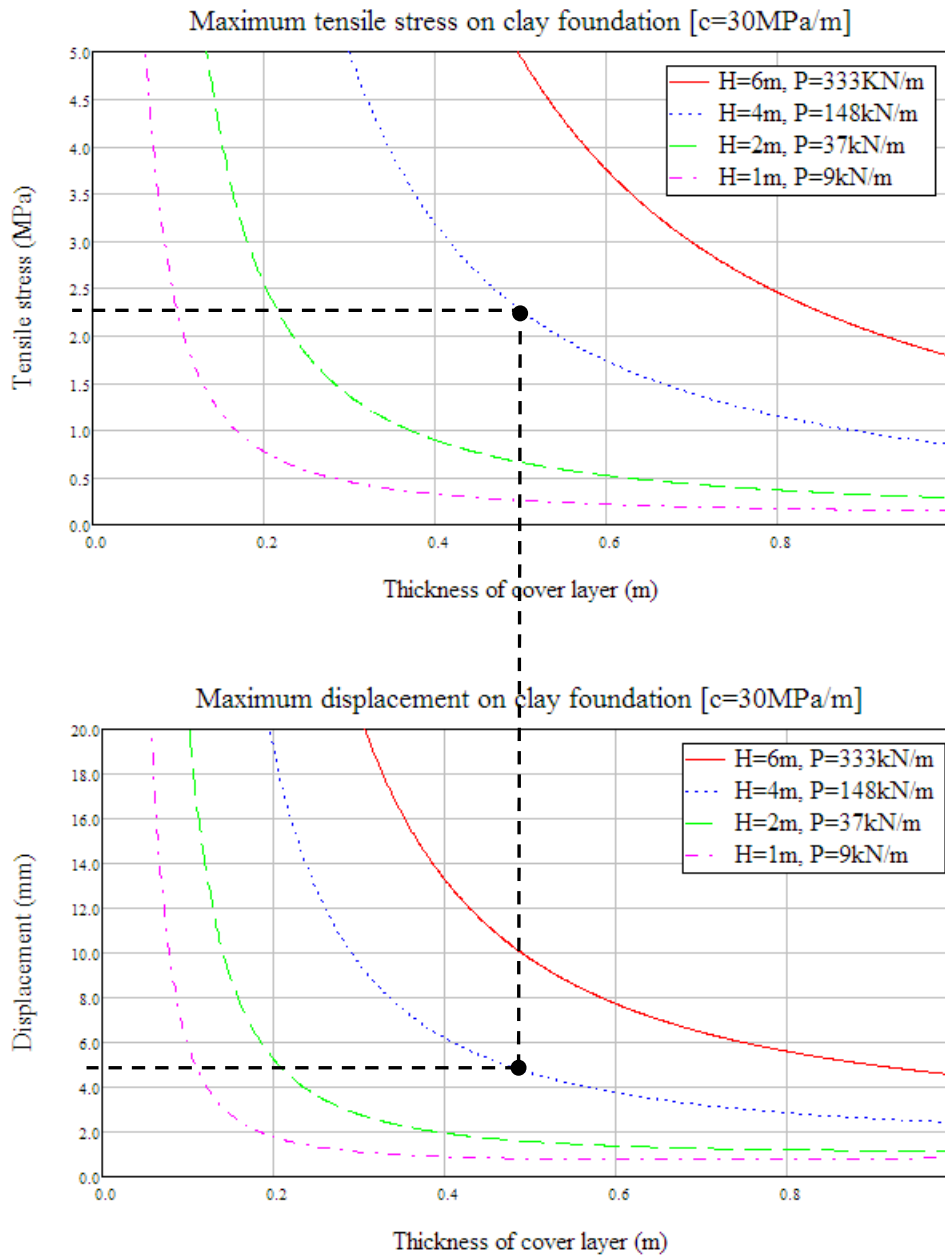
Figure 5.15 Maximum tensile stress and maximum displacement in scenario 2 as functions of the thickness of the cover layer.

The figures can be interpreted as follows. From the upper figure it shows that with a wave height of *H=4 m* and a cover layer thickness of *h=0.5 m* the maximum stress σ_{max} = *2.3 MPa*. This is close to the bending strength of the material. In the lower figure it can be derived that at the same wave height and thickness the displacement under the load is approximately *w_{max}=5 mm*. From this it can be concluded that under these conditions the depth of a cavity that is 2 m wide may not be larger than 5 mm, or breakage will be imminent. If the depth of the cavity is smaller than *d=5 mm*, the displaced cover layer will find support on the bottom of the cavity and material strength will not yet be exceeded.

5.3.6 Evaluation of the model

Wave load schematization

Two methods were used for schematization the same structure under different load cases. However, from the figures above it can be seen that the overall values for σ_{max} in scenario 2 are significantly higher than those in scenario 1. If in scenario 2 the size of the cavity is reduced to zero, $r \to 0$, the difference between the two schematizations becomes clear by comparing the bending moment function as shown in figure 5.16. This appears to be an unwanted effect of the simplification to a line load in scenario 2.
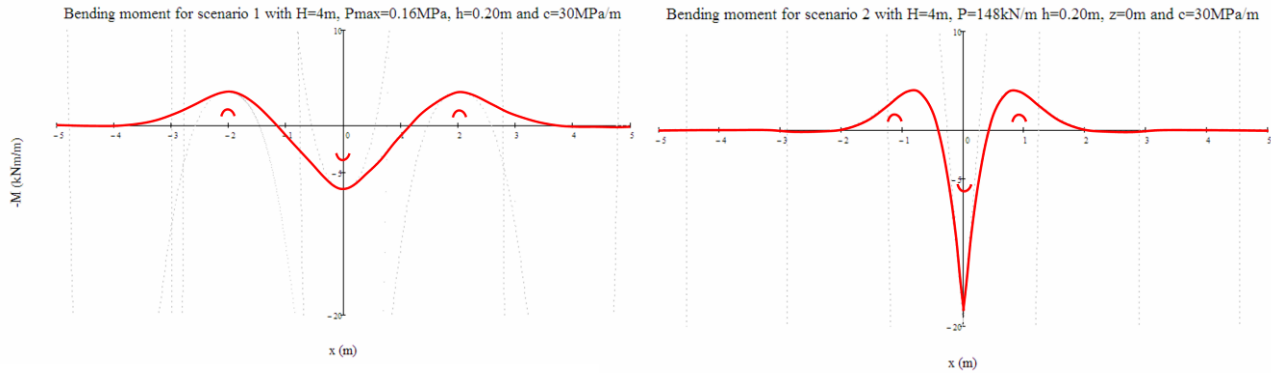
Figure 5.166 Distribution of bending moments in scenario 1 and scenario 2 with cavity size reduced to zero.

In order to assess the consequences of simplifying the distributed load from scenario 1 to a line load in scenario 2, the results for the case above are compared with known solutions to standard cases (figure 5.17).
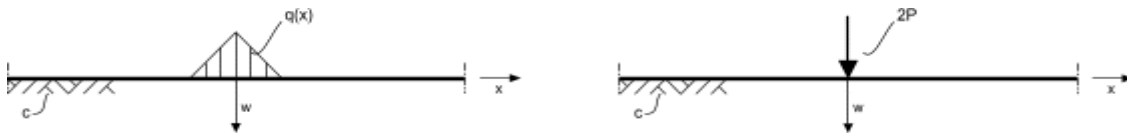
Figure 5.17 Mechanical schematization for both scenarios when the size of the cavity in scenario 2 is reduced to zero.

The solution to the first case (left in figure 5.17) has been presented in the Dutch *Technisch rapport asfalt voor waterkeren* (TAW, 2002). In fact the model is exactly the same as the one presented in this report and should therefore give the same results under input of the same parameters. The report gives the following solution for the maximum tensile stress at $x=0$:

$$\sigma_{max} = \frac{P_{max}}{4\beta^2 \beta z}[1 - e^{(-\beta z)}(\cos(\beta z) + \sin(\beta z))]\frac{6}{h^2}$$

The known solution to the second case can be found in (Bouma, 2000):

$$M_{max} = \frac{P}{2\beta} \quad ; \quad w_{max} = \frac{P\beta}{c}$$

The results from the schematization models presented in this report, the known solutions to the standard cases, and a numerical analysis on a similar case with the software package MATRIXFRAME, are all given in table 5.7.

Table 5.7 Outcomes of the models from the schematization models, compared to known solutions to standard cases and numerical analysis with MATRIXFRAME. In all computations h=0.2m, c=30MPa/m and H=4m.

	Models from this report	Known solution to standard case	Numerical analysis on similar case
Scenario 1			
• Triangular load P_{max}	0.16 MPa	0.16 MPa	0.16 MPa
• M_{mzx} at x=0	7.5 kNm	7.4 kNm	6.9 kNm
• σ_{max} at x=0	1.1 MPa	1.1 MPa	-
• w_{max} at x=0	4.3 mm	-	4.4 mm
Scenario 2 with r = 0m			
• Line load P	148 kN	148 kN	148 kN
• M_{mzx} at x=0	26.2 kNm	26 kNm	26 kNm
• σ_{max} at x=0	3.9 MPa	3.9 MPa	-
• w_{max} at x=0	3.6 mm	3.5 mm	3.6 mm

From the above table it can be concluded that the simplification of the wave load to a line load indeed has a large impact on the results. In reality the stress distribution of a wave impact lies closer to the triangular distribution from scenario 1. The schematization of the wave load to a concentrated line load in scenario 2 apparently leads to an extreme overestimation of the bending moment M_{max} and tension σ_{max}, whereas the displacement w_{max} is underestimated. The schematization as used in scenario 2 is therefore not recommended to be used.

Apparently a different schematization, closer to 'reality', is needed to calculate stresses and deformations in case of a cavity under the cover layer. Therefore in section 5.3.7 a new model is presented, which is, in fact, an extension of the triangular load model from scenario 1 to be used in the case of scenario 2.

Long beam assumption
The schematization as a semi-infinite beam is only valid if the beam is long enough. This is true if the condition $\beta L > \pi$ is satisfied. A layer thickness of *h=0.2 m* and a soil compression constant of *c=30 MPa/m* result in $\beta = 1.4$. If we have a cover layer of say, 5 m wide, then the distance from the middle to the edge is *L= 2.5 m*. Now we find $\beta L = 3.5 > \pi$. The condition is thus satisfied and the long beam assumption is valid.

Bending strength versus shear strength
One of the first assumptions made in the analysis of wave loading, was that the deformation and failure of Elastocoast is governed by bending moment and bending strength only. However it is conceivable that not the bending strength, but the shear strength or a combination of both is normative. In that case the model should be extended with shear deformation and consequently extra material parameters are needed to do so.

Now the question rises whether it is likely or not that the shear strength is normative. The original choice for bending strength was made to simplify the mechanical model and also because the bending strength of Elastocoast was subject of research by Gu (2007). Material parameters concerning bending strength and elastic modulus are therefore readily available.

In the research of Gu a three-point bending test was done. In this test, the maximum bending moment is present in the middle of the beam (figure 5.18). Breakage by exceeding of bending strength should therefore occur near the middle, with some spreading due to material inhomogenity. A constant shear force is present over the entire beam length. Exceeding of the shear strength of the material is therefore not limited to the middle of the beam. Shear breakage should also leave a distinct breakage pattern, where a developing crack will follow the shape of the stress trajectories in the beam (figure 5.19).
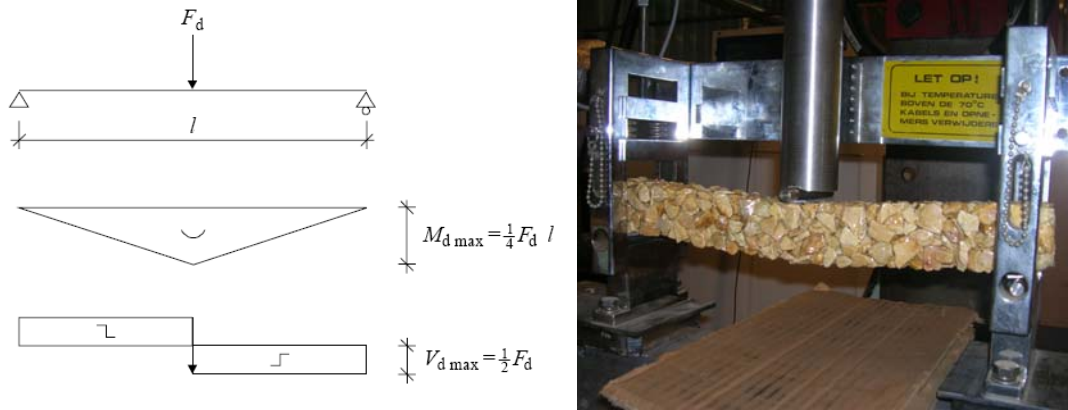
Figure 5.18 Bending moment and shear force in a beam loaded in the middle (left).Three-point bending test on Elastocoast (right) (Gu, 2007b).
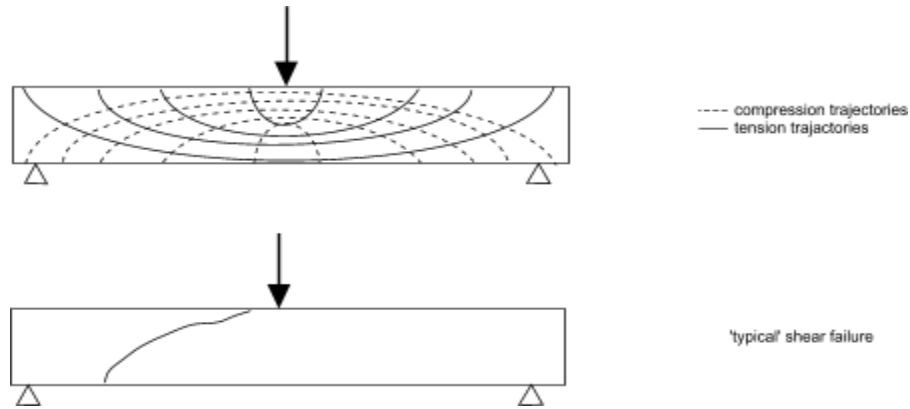
Figure 5.19 Stress trajectories and a typical breakage pattern by exceeding of shear force.

The beams subjected to the three-point bending tests however, all show breakage near the middle of the beam (figure 5.20). Some spreading indeed occurs due to material inhomogenity. Based on these tests, it can be presumed that bending strength is indeed normative, such as was assumed in the schematization of the mechanical models.

Figure 5.20 Breaking positions of beams tested in three-point bending test (Gu, 2007b).

5.3.7   Improved mechanical model

Introduction

From the evaluation of the two mechanical models it was concluded that the simplification of the wave load to a simple line load in scenario 2 (partially supported) leads to pessimistic results. The maximum bending moment and stress were overestimated, whereas the maximum deflection under the load was underestimated. Since the model for scenario 1 (fully supported) makes use of a more realistic shape of the wave load, namely triangular, this model will now be extended to be used in the case of scenario 2. The resulting new model will be more general and consequently applicable in both scenarios.

In finding an analytical model for the situation of a triangular load on a partially supported cover layer, a first problem lies in the size of the cavity relative to the size of the wave load. Whether the cavity is larger or smaller than the base width of the wave load gives different sets of solutions to the differential equation that governs the beam response. Since mechanical breakage by wave impact is expected to play a role only with high waves and we are interested in the lower limits of the cavity size, first the case will be elaborated with a cavity smaller than the base width of the wave load.

Schematization

The schematization will be as follows:
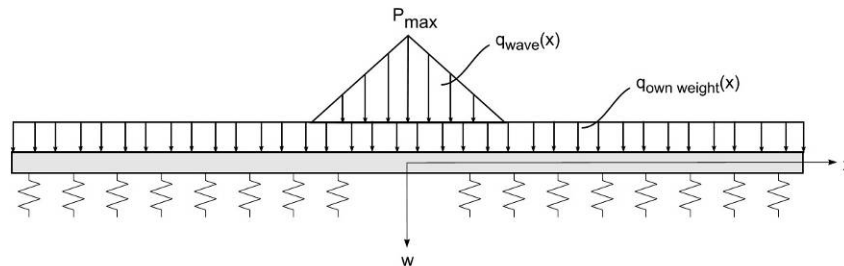
Figure 5.21 Schematization of a triangular wave load on a partially supported cover layer.

The basic differential equation as presented in Section 5.3.2 still holds for this case. Analogue to the previous models, the beam will be considered fully symmetrical around the loading point and infinitely long in the x-direction. The response to the loading will be symmetrical, so that the problem can be simplified by considering one semi-infinite half as shown in the following figure.
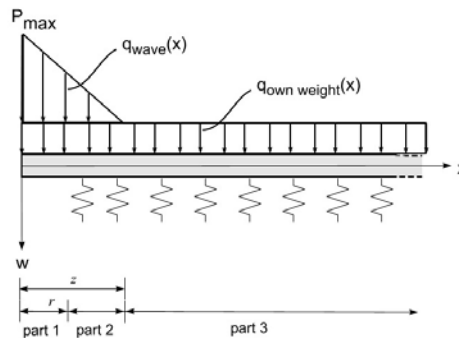
Figure 5.22 Mechanical schematization of the problem as a semi-infinite beam.

Three parts can now be discerned, each with their own loading conditions:

- Part 1: Unsupported part ($x \le r$), loaded by triangular wave load and own weight:

$$c = 0 \quad ; \quad q(x) = \frac{P_{\max}(z - x)}{z} + \rho_{ec} gh$$

- Part 2: Supported part ($r < x \le z$), loaded by triangular wave load and own weight:

$$c \ne 0 \quad ; \quad q(x) = \frac{P_{\max}(z - (x + r))}{z} + \rho_{ec} gh$$

- Part 3: Supported part $x > z$, loaded only by own weight:

$$c \ne 0 \quad ; \quad q(x) = \rho_{ec} gh$$

Choice of the right boundary conditions makes sure that the interface between the different parts is properly defined. A complete elaboration of the schematization and its solution are given in Appendix II.

Calculations
The following calculations represent a case of an Elastocoast cover layer which is only partly supported by a foundation consisting of sand. The structure is loaded by a wave of *H=4 m*. The width of the cavity around *x=0* is taken to be 2 m, so *r=1m*. The figure below shows the deflection of the cover layer along the x-direction.
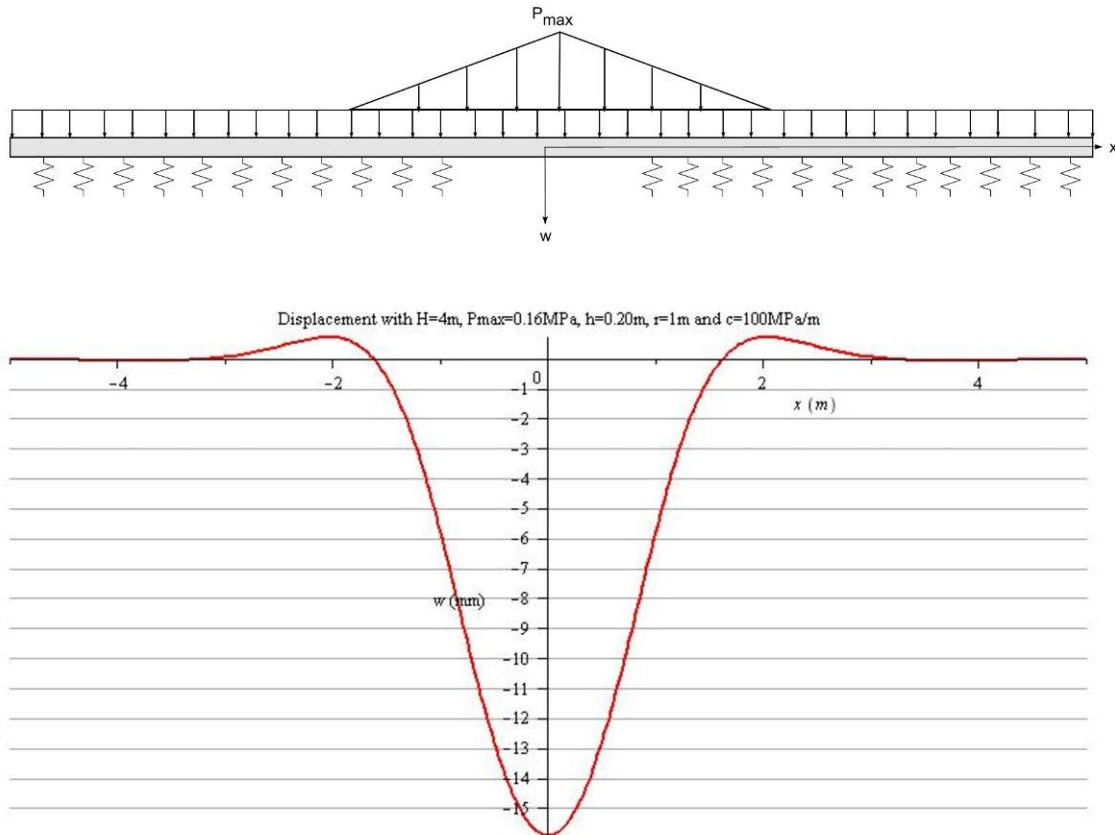
Figure 5.23 Displacement of the cover layer in the improved model for scenario 2.

In the following figures, the maximum tensile stress σ_{max} and the displacement w_{max} at $x=0$ are depicted as a function of the thickness of the cover layer, h. The wave height is fixed at $H=4\ m$. The figures show that the shape of the function varies with the size of the cavity. The figure shows that, if an Elastocoast layer is placed on top of a sand bed and a cavity with a span of $2r=1.0\ m$ occurs, in order to withstand impacting waves with $H=4\ m$, a minimum layer thickness of 30 cm would be required according to the model.

When the cavity is absent, $r=0.00m$, the function gives a local maximum similar to that what was seen with scenario 1 in section 5.3.2. When the cavity increases in size, the exponential behaviour from scenario 2 in section 5.3.2 is seen.
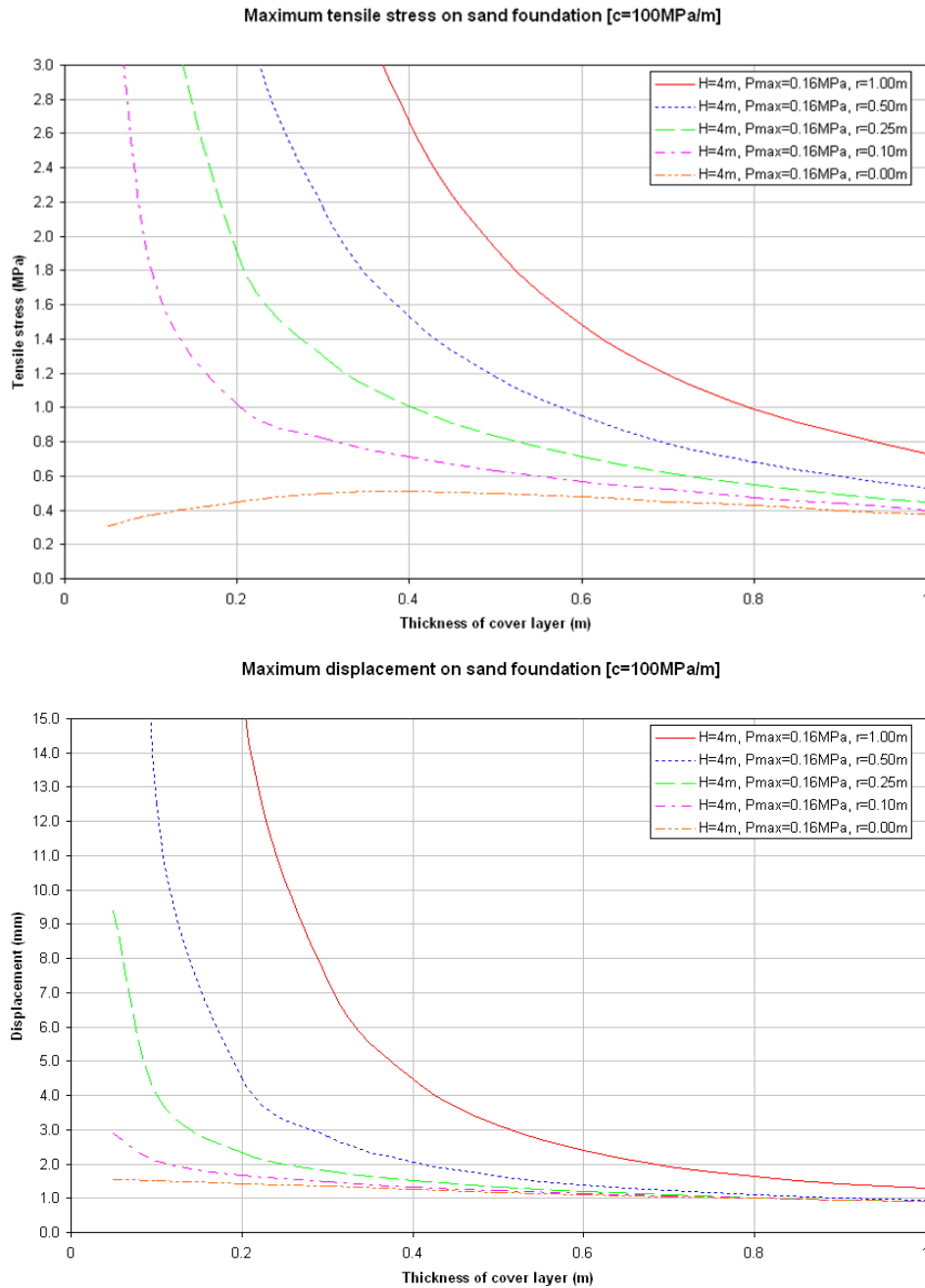
Figure 5.24 Maximum tensile stress and maximum displacement of the cover layer, (partially) supported by a sand foundation, as functions of cover layer thickness.

Now, the same figures, but then with a foundation of clay. A comparison of the figures 5.24 and 5.25 shows that the value for the soil compression constant has significant implications for the required layer thickness. A cover layer placed on a bed of clay is more vulnerable to breakage than one placed on a sand foundation. Note that in case of *r=0.00m*, the function is exactly the same as that seen in figure 5.13 for a wave height of *H=4 m*.
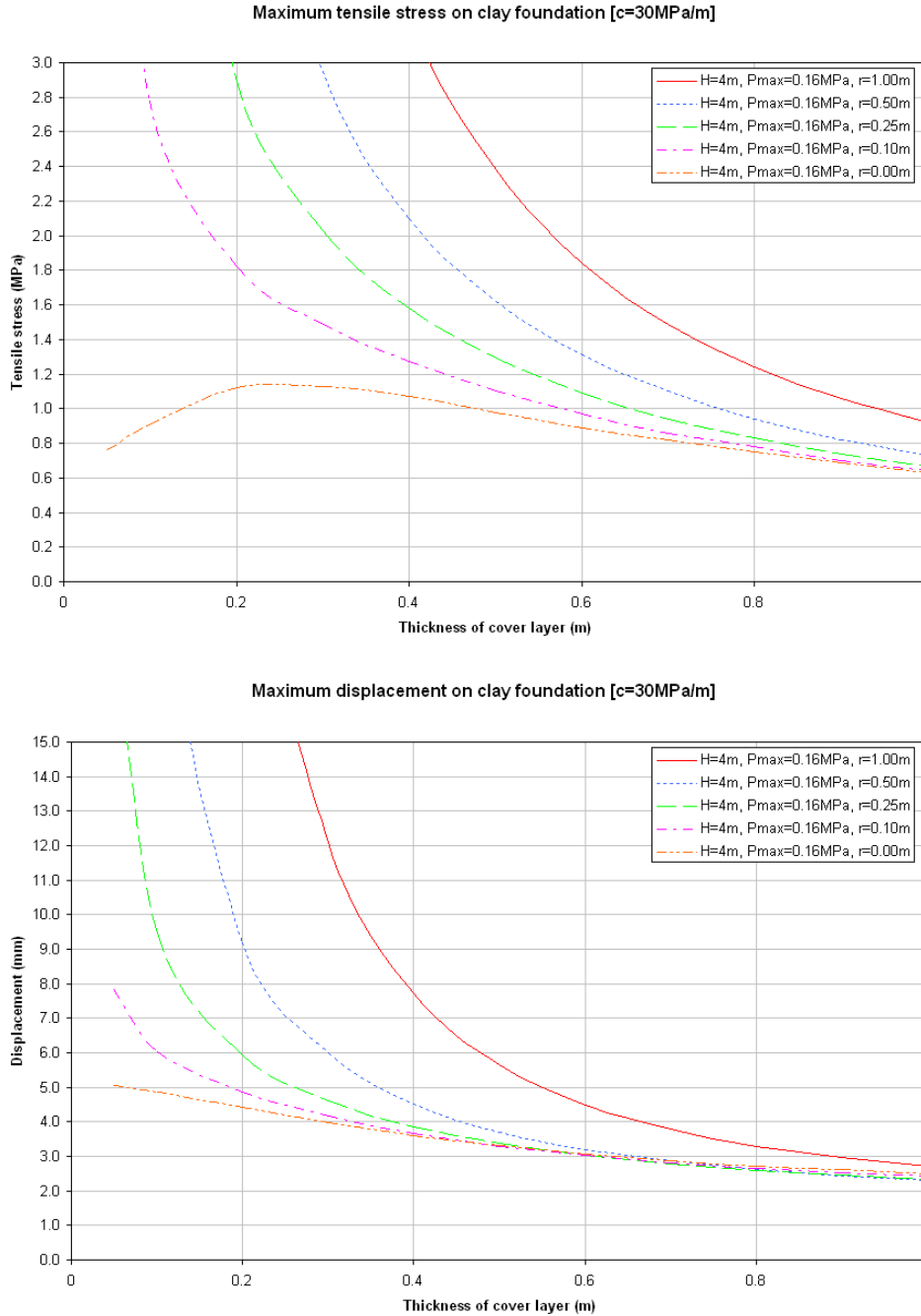
Figure 5.25 Maximum tensile stress and maximum displacement of the cover layer, (partially) supported by a clay foundation, as functions of cover layer thickness.

5.3.8 Conclusion

In this detailed analysis the effect of a wave impact on an Elastocoast cover layer has been determined by schematizing the structure as statically loaded plate on an elastic supporting foundation. Two cases were discerned:

- Scenario 1: wave impact on continuously supported cover layer
- Scenario 2: wave impact on only partially supported cover layer

In case of a continuously supported cover layer, the wave load is schematized as a triangular distributed load and the cover layer itself as an elastically supported bending beam. With this method material stresses and deflections can be calculated. From the calculations it can be concluded that in case of proper continuous support the maximum tension in the bottom of the cover layer will not exceed the bending strength of the material. A lower compression constant of the foundation leads to higher stresses in the cover layer when loaded, but even with a clay foundation the maximum tension does not exceed the bending strength.

In case of a cavity under the cover layer, the wave load was first schematized as a line load and also the structure's own weight was taken into account. The cover layer was then schematized as a bending beam that is only partly supported by an elastic foundation. This simplification however, resulted in an overestimation of the stresses in the cover layer and an underestimation of the displacement.

Therefore the first model is modified to take into account a possible cavity under the cover layer. The new model is a more general form of the first one and is applicable to both scenarios. This is confirmed by the fact that, for the case with *H=4 m* and *r=0.00 m*, exactly the same functions for maximum stress and displacement are found as the model for scenario 1. This is not a coincidence, since both models are based on the same differential equations. A limitation in the model is that the total size of the cavity *2r*, may not exceed the base width of the triangular load, which is equal to the wave height *H*.

An important conclusion that can be drawn from the improved model is that, in case of a cavity, the compression constant of the foundation layer becomes an important factor. A cover layer placed on a bed of clay is more vulnerable to breakage than one placed on a sand foundation.

5.4 System property: Hydraulic conductivity of a clogged porous structure

5.4.1 Introduction

The hydraulic conductivity is a measure for the ease with which water can move through the pore spaces of a material (figure 5.26). Ideally the Elastocoast system has a very open structure; which translates into a high hydraulic conductivity, as presented in Chapter 3. The open structure enables water to flow easily and virtually unobstructed through the cover layer.

Figure 5.26 Water can flow through the pore spaces of a material (BrockUSA, 2008).

It can however be conceived that in some circumstances the open structure can get clogged by sediment or debris. This could strongly reduce the effective hydraulic conductivity of the Elastocoast system. In prototype conditions, significant clogging was observed at the Elastocoast pilot in Petten (Bijlsma, 2008). Therefore the possibility of clogging is important to be taken along in stability calculations.

In this section an existing theoretical model is used to predict the hydraulic conductivity of Elastocoast. Also the possible effect of clogging on the conductivity is examined. In section 5.5 the implications of the hydraulic conductivity on the stability of an Elastocoast cover layer are investigated.

5.4.2 Expected behaviour of Elastocoast

Because the open pore volume of Elastocoast is approximately equal to the natural open pore volume of the used aggregate its hydraulic conductivity should also be equal to that of the granular base material. The hydraulic conductivity of granular material can be predicted theoretically with a model that is normally used for calculations with granular filter layers.

Now the following suppositions are made:

- The hydraulic conductivity of (clean) Elastocoast should approach that of the granular aggregate. Therefore calculation methods for granular material are also applicable to Elastocoast.
- Filling of the open pore structure of Elastocoast will strongly reduce its hydraulic conductivity.

If the first supposition is right, then the results from the calculation model should approach the values known from prototype measurements. Lab measurements of the hydraulic conductivity of Elastocoast were performed by Gu (Gu, 2007a). The results of these measurements were presented in Chapter 3.

A confirmation on the second supposition is not yet possible. No laboratory tests were performed on the hydraulic conductivity of clogged Elastocoast. The results of calculations are used to give a worst case scenario of what is to be expected and will thus be used for stability calculations further on in this report.

5.4.3 Model for hydraulic conductivity of a granular filter

The hydraulic conductivity of a filter layer consisting of granular material depends mainly on its grading, which determines the porosity n and the size of the fine fractions of the material. Also, the conductivity is strongly dependent on the hydraulic gradient through the material.

The hydraulic gradient is defined as (Verruijt, 1999):

$$i = \frac{dh}{ds}$$

In which dh is the hydraulic head difference (m) and ds is the distance (m) over which this head difference works. The gradient i (-) can thus be seen as the slope of the groundwater level in the direction over which the distance is defined. In example, for parallel flow through the filter layer of a dike, the gradient is approximately the same as the dike slope $i \approx\sim 0.25 - 0.50$. The perpendicular gradient through this layer is much larger; it depends on the head difference and the thickness of the cover layer and can be as much as: $i \approx 2.0 - 10$.
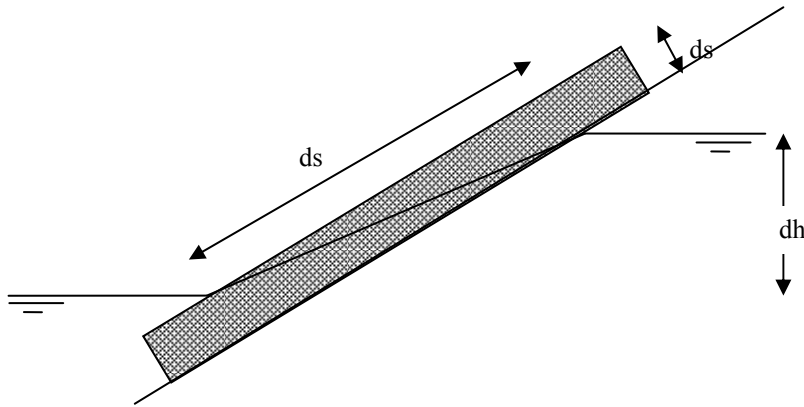
Figure 5.27 Definition sketch of gradients through a filter on a dike slope.

The flow rate q (m/s) through a medium can now be described with Darcy's law (Verruijt, 1999):

$$q = k \cdot i$$

The hydraulic conductivity k (m/s) is a proportionality constant, which relates the amount of water that will flow through the medium with the hydraulic head over that medium. The hydraulic conductivity of a granular filter can be derived with a combination of the theory of Forchheimer and Darcy's Law (TAW, 2003). According to the theory of Forchheimer the relationship between the hydraulic gradient i and the flow through the material q can be characterized with a linear and a quadratic (turbulent) component:

$$i = a_f q + b_f q^2$$

In which, a_f and b_f are coefficients of resistance of the granular material. Together with the Darcy relationship $q = k \cdot i$, the hydraulic conductivity k can be expressed as a function of the hydraulic gradient:

$$k = \frac{-a_f + \sqrt{a_f^2 + 4b_f i}}{2b_f i}$$

For the coefficients a_f and b_f the following values have been obtained from conductivity measurements (TAW, 2003):

$$a_f = 160 \frac{v}{g} \frac{(1-n)^2}{n^3 D_{15}^2} \qquad ; \qquad b_f = \frac{2.2}{gn^2 D_{15}}$$

In which $v=1.2*10^6$ m^2/s is the kinematical viscosity of water, n is the porosity (-) and D_{15} is a measure for the size of the fine fractions in the granular material. The relationship between hydraulic conductivity k, gradient i and the size of the fine fraction D_{15} is given in the figure below:
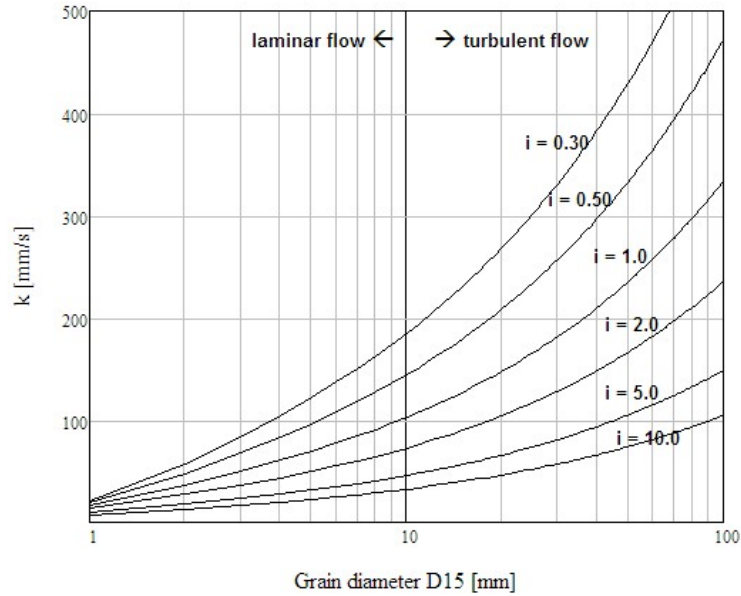
Figure 5.28 Hydraulic conductivity k related to grain size and hydraulic gradient for a filter with a porosity of n=0.5.

5.4.4 Influence of clogging on the permeability of a porous structure

Clogging process

There are two different processes that can each lead to the clogging of a porous structure:

- Clogging from outside
- Clogging from the inside

In the first case sediment is brought in by suspended transport and becomes trapped or settles in the pores of the cover layer. During extreme conditions this sediment is washed away again. In the second case, sediment is transported up from the sand core by wave induced pressure variations. The latter has been observed in geometrically open filters in breakwaters with a sand core (Ockeloen, 2007). Figure 5.29 shows a schematization of this process; between points A and D sand is eroded and transported to below point D where accretion takes place.
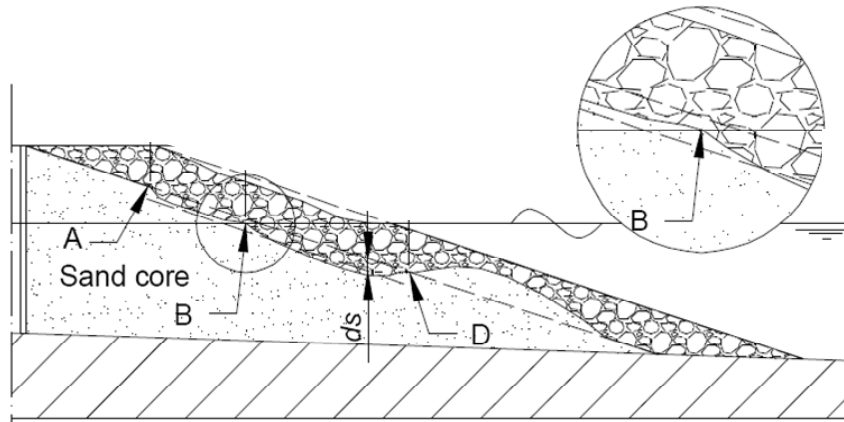
Figure 5.29 Erosion and accretion through an open filter under wave action (Ockeloen, 2007).

Whereas clogging from outside is washed away under extreme conditions, clogging originating from inside may remain in place by arcing of the grains in the pores (figure 5.30). The presence of sand in the pores of the cover layer will have a negative influence on its hydraulic conductivity.
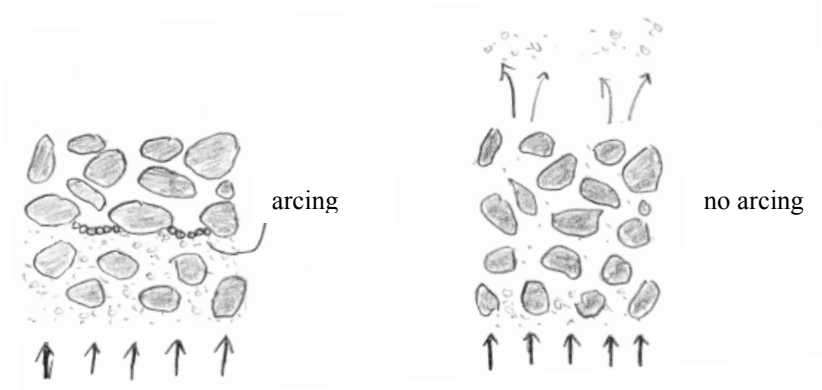
Figure 5.30 Arcing effect for clogging of a granular structure.

Once fine material has collected in the pores of a structure, an interesting habitat for micro-organisms and vegetation is created. These will lead to a further filling of the structure and add organic material. Organic material decreases the hydraulic conductivity and increases the cohesion of the filling material, which in turn increases the resistance of the filling material against being washed away.

Hydraulic conductivity of a clogged porous structure
The hydraulic conductivity of a clogged porous structure will be lower than that of a clean porous structure. The open pore space will be filled with fine material, which has a relatively low hydraulic conductivity. Furthermore the hydraulic conductivity of a clogged porous structure will even be lower than that of the filling material itself. In the following figure this is visualized. The available surface area is reduced and the flow lines are not straight anymore:

$$n=0.5 \qquad \text{'straight' flow lines} \qquad \text{no straight flow lines}$$
$$k=k_{ec} \qquad k=k_z \qquad k<k_z \;!$$
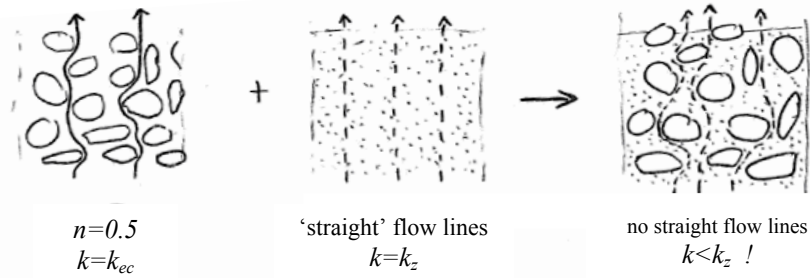
Figure 5.31 Flow lines through a porous structure, through sand and through the combination of both.

To determine the joint hydraulic conductivity an analogy will be made with an electronic circuit containing multiple electrical resistances. Because the hydraulic conductivity factor is a measure of the "ease of flow" through the material, the reciprocal value should be a measure of "resistance". Comparing Darcy's hydraulic conductivity equation with the Ohm's law for electronic circuits shows:

$$Darcy: \quad Q = k \cdot A \cdot i$$

$$Ohm: \quad R = \frac{V}{I} \quad \Leftrightarrow \quad \frac{1}{k \cdot A} = \frac{i}{Q}$$

Where in Darcy's equation Q (m³/s) is the flow rate through the layer, k (m/s) is the hydraulic conductivity of the layer, A (m²) is the surface area of the layer and in Ohm's law R (Ω) is the electrical resistance, V (Volt) is the difference of electrical potential and I (Ampere) is the electric current.

From this we can make the analogy:

$$R \quad \Leftrightarrow \quad \frac{1}{k \cdot A}$$

The combined hydraulic conductivity is now derived by analogy to a serial electrical circuit. The total resistance of a series of resistors is:

$$R_v = R_1 + R_2$$

Now, using R ~ 1/(kA) this relation is rewritten to a hydraulic conductivity formula for a clogged porous structure:

$$\frac{1}{k_v \cdot A_v} = \frac{1}{k_T \cdot A_T} + \frac{1}{k_s \cdot A_s}$$

With:

        k_v = total hydraulic conductivity of clotted system (m/s)
        A_v = surface area of system (m²)
        k_T = hydraulic conductivity of cover layer (m/s)
        A_T = surface area of cover layer (m)
        k_s = hydraulic conductivity of filling material (m/s)
        A_s = surface area of filling material (m²)

And making use of the relations $A_v = A_T$ and $A_S = n_T \cdot A_T$, where n_T is the porosity of the carrying material (-). it follows that:

$$k_v = \frac{k_T \cdot k_s \cdot n_T}{k_T + k_s \cdot n_T}$$

This fully describes the joint hydraulic conductivity of the carrying material and the filling material.

5.4.5   Hydraulic conductivity of (clogged) Elastocoast

Hydraulic conductivity of Elastocoast
The hydraulic gradient is defined as (Gu, 2007a):

$$k = \frac{ql}{AH}$$

In his study, Gu simplified this relation to k=q/A. Therefore, to find the right values for the hydraulic conductivity, his results should be multiplied by *l/H*, or in other words divided by the hydraulic gradient *i*.

The predictions from the model for hydraulic conductivity of a granular filter are in good qualitative agreement with values obtained from the laboratory tests. In the next figure the measured values are plotted against predictions from the model.
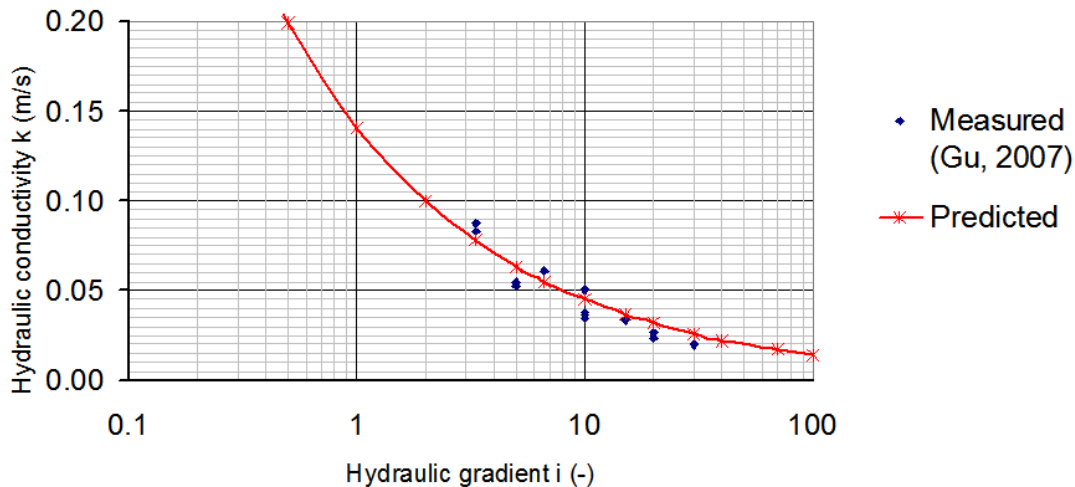
Figure 5.32 Predicted and measured values for the hydraulic conductivity of Elastocoast with D_{15}=22.5 mm and n=0.45.

The laboratory tests were done with Elastocoast placed on top of a geotextile. Consequently it is assumed that the application of geotextile has negligible effect on the permeability of Elastocoast.

Hydraulic conductivity of clogged Elastocoast
Now the hydraulic conductivity of clean Elastocoast is known, the joint conductivity of Elastocoast and a filling material can be derived to find an indication of the conductivity of clogged Elastocoast.

Clogging usually takes place with fine granular material that can be transported in suspension by water. The hydraulic conductivity for several soil types are given in table 5.8.

Table 5.7 Hydraulic conductivity of different soil types (Verruijt, 1999).

Soil type	k (m/s)
Gravel	$10^{-3} - 10^{-1}$
Sand	$10^{-6} - 10^{-3}$
Silt	$10^{-8} - 10^{-6}$
Clay	$10^{-10} - 10^{-8}$

Now it is assumed that in a clogged Elastocoast structure the open pore space is completely filled with sand. Since the conductivity of sand is much smaller than that of Elastocoast, the combined conductivity will be mostly determined by the conductivity of the sand contained in the pores. The following table shows how the hydraulic conductivity of Elastocoast clogged with sand is calculated.

Table 5.8 Hydraulic conductivity of Elastocoast clogged with sand.

Material	Hydraulic conductivity	Joint hydraulic conductivity
Carrying material: Elastocoast D_{15}=21 mm, n_T=0.5	$k_T = 6.8 \cdot 10^{-3}$ m/s	$k_v = \dfrac{k_T \cdot k_s \cdot n_T}{k_T + k_s \cdot n_T} = 0.5 \cdot 10^{-4}$ m/s
Filling material: Sand	$k_S = 1.0 \cdot 10^{-4}$ m/s	

From this calculation it becomes clear that the difference between the conductivities of the carrying and filling material is so large that their joint conductivity is governed only by the porosity of the carrying material and the hydraulic conductivity of the filling material.

So, if $k_s \ll k_T$:

$$k_v = \frac{k_T \cdot k_S \cdot n_T}{k_T + k_S \cdot n_T} \approx k_S \cdot n_T$$

5.4.6 Conclusion

From the results of the calculations the following can be concluded:

- The presented calculation method for hydraulic conductivity of granular filters is also applicable to Elastocoast.
- Clogging of the open structure of Elastocoast strongly reduces its hydraulic conductivity. If the conductivity of the filling material is much smaller than the conductivity of the carrying material (which is the case for Elastocoast filled with sand), the joint hydraulic conductivity can be estimated with $k_v = k_S \cdot n_T$, which is the hydraulic conductivity of the filling material, multiplied by the porosity of the carrying material.

5.5 Failure mechanism: uplift

5.5.1 Introduction

Uplift pressures working on the cover layer of a dike are the result of a pressure gradient by a difference between the outside water level and the water level in the dike body. In Chapter 4, three basic situations were presented in which such a head difference can occur, namely:

- Static
- Dynamic, during maximum wave retreat
- Dynamic, during wave impact

Generally, if the cover layer has some level of permeability there is no danger of uplift by a static head difference. Because of the large timescale over which water level fluctuations occur (several hours), there is enough time for pressures to diminish by seepage through the cover layer.

Dynamic head differences occur on a time scale in the order of the length of a wave period (several seconds) or in case of wave impact even much shorter, in the order of 10-200 ms (Kolkman, 1996). On such a scale the time in which overpressures can diminish by seepage is strongly determined by the rate of flow through the permeable cover layer. Over that short period of time overpressures can cause significant uplift forces of the cover layer.

The actual pressures that exist at the moment of wave impact are very complex to predict and although a lot of research is done, at the moment of writing of this report calculation models are not yet readily available (Klein Breteler, 2007). The situation at the moment of maximum wave retreat is better described. Stability of the cover layer during maximum wave retreat can serve as a good first indication of overall stability under dynamic head differences.

Physical background of uplift

At the moment of maximum wave retreat for a short amount of time the water level at the dike slope is lower than the ground water level in the dike body, which can be assumed to be approximately equal to the still water level. The following figure shows the hydrostatic pressures that are the result of this head difference at the moment of maximum wave retreat. Over a length of x_0 the net water pressure is pushing the cover layer up from the slope.
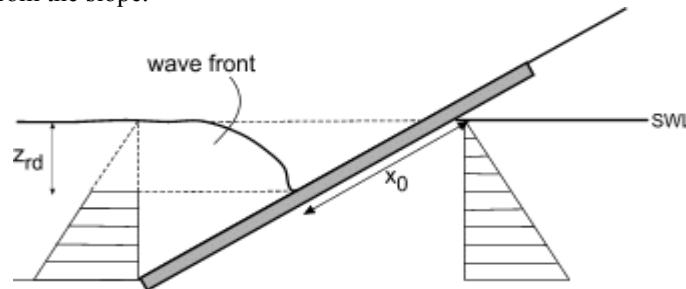
Figure 5.33 Pressures on the inside and outside of a cover layer under maximum wave retreat.

The forces that work on a part of the cover layer are depicted in figure 5.34. If the cover layer consists of individual elements, such as blocks or columns, the uplift pressures are counteracted by:

- Element weight (determined by element size and specific weight)
- Interaction with surrounding elements (friction, wedging or clamping effect)

In case of a continuous cover layer, such as a plate structure, the local uplift pressures are countered by:

- Structure own weight (determined by layer thickness and specific weight)
- Internal forces (shear force and bending moments)
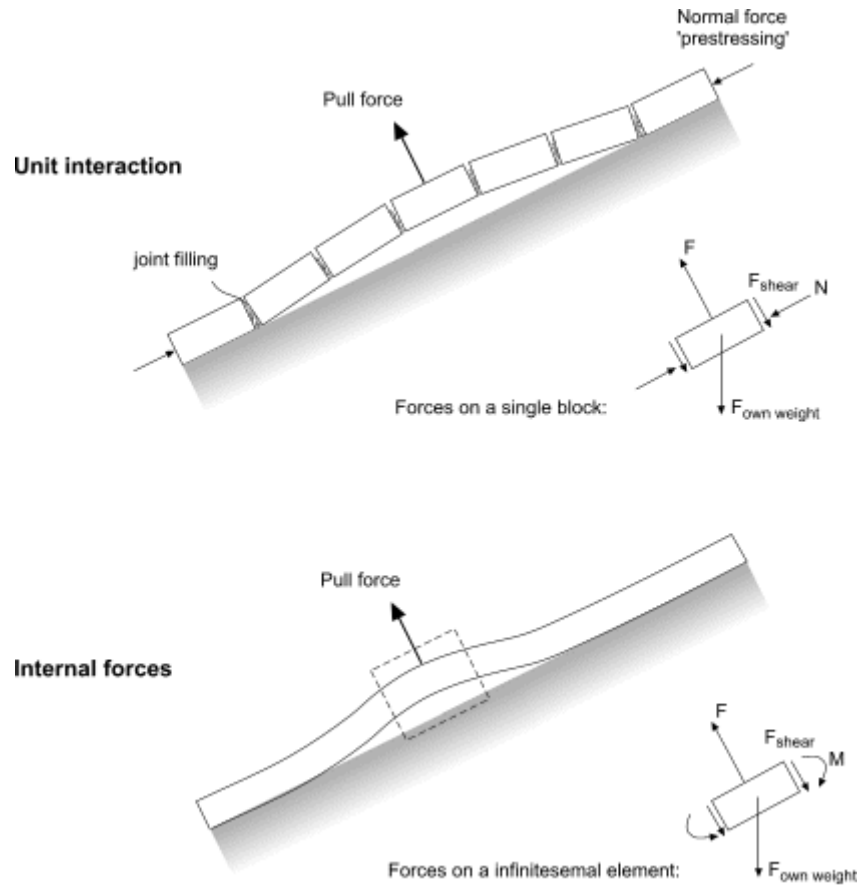
Figure 5.34 Coherence of a cover layer by unit interaction (above) or by internal forces (below).

For a block revetment to derive strength from unit interaction it is necessary that there exists a certain 'prestressing' force. This force is not always present. For simplicity therefore often only the weight is considered in the stability calculation of block revetments. If the weight of the structure is already enough to counter the uplift pressures, than its stability is ensured. Otherwise, a more complex approach is necessary, which also takes along the other effects.

Open versus closed structure: leakage length
The degree of permeability of a revetment plays an important role in its stability under hydraulic loading. Roughly there are three degrees of permeability:

- very open and permeable (i.e. loosely dumped rock)
- semi-permeable (i.e. regularly placed blocks)
- completely impervious (i.e. asphalt plate)

Under the same load structures with different degrees of permeability have an entirely different response and different mechanisms apply that determine the dimensions of the cover layer. For stability calculations an important parameter is introduced: the leakage length, which relates the degree of permeability of the cover layer and that of the underlying (filter) layer:

$$\frac{d_T}{k_T \Lambda} = \frac{\Lambda}{k_F d_F} \quad \Rightarrow \quad \Lambda = \sqrt{\frac{k_F d_F d_T}{k_T}}$$

Where Λ = leakage length (m); d_T = thickness of cover layer (m), d_F = thickness of filter layer (m), k_T = hydraulic conductivity of cover layer (m/s) and k_F = hydraulic conductivity of filter layer (m/s). In words: the leakage length is the length of protection in which the flow resistance through the cover layer and filter layer are the same. The flow through the cover layer is perpendicular and the flow in the filter layer is parallel to the slope. If the filter layer is absent, flow takes place through part of the subsoil (Klein Breteler, 1998).

The leakage length is therefore a measure for the exchange between external and internal loads on the structure. Overpressures under the cover layer may occur if the leakage length is of the same order as or greater than the length scale of the external load, which in the case of waves can be taken as the length of the steep wave front. Table 5.10 shows some typical values for three categories of protection. It shows that for less permeable structures such as placed blocks and asphalt plates there is a risk of overpressures building up under the cover layer that could lead to a resulting uplift force.

Table 5.9 Typical values for permeability and the leakage length parameter for different protection types (adapted from Pilarczyk, 1990).

	d_{top} (m)	d_{filter} (m)	k_{top} (m/s)	k_{filter} (m/s)	Leakage length Λ (m)	External load scale L (m)	
Loose grains (rip-rap, rock)	0.50	0.25	0.5	0.10	0.15	1-2	$\Lambda \ll L$
Coherent (placed blocks)	0.25	0.20	0.001	0.05	1.50	1-2	$\Lambda \approx L$
Cohesive and impervious (asphalt, concrete, clay)	0.30	2.00 (no filter)	"0"	0.0001	"∞"	1-2	$\Lambda \gg L$

5.5.2 Stability of Elastocoast

Ideally the Elastocoast system has a very open structure; this translates into a high hydraulic conductivity, as presented in Chapter 3. This enables water to flow easily and virtually unobstructed through the cover layer if a head difference exists. Overpressures leading to uplift are therefore very unlikely to build up and if so would only result in a higher flow rate through the cover layer instead.

Effect of clogging on stability
It can however be conceived that in some circumstances the open structure can get clogged by sediment or debris. When the open structure of Elastocoast is filled up with small material, the effect on stability is the net result of two factors:

- Increase of stability by added structure weight
- Decrease of stability by reduction of hydraulic conductivity

In prototype conditions, significant clogging was observed at the Elastocoast pilot in Petten (Bijlsma, 2008). It should be noted that this prototype had a very specific structure build up; the Elastocoast cover layer was put directly on top of an existing revetment, namely placed basalt blocks. The low permeability of the supporting basalt layer results in a strong reduction of flow velocities through the cover layer. This in turn enables sediment to settle in the cover layer.

Once sediment has settled in the open pore space of the cover layer and remains in place for a while, there is danger of a more persistent type of clogging. The trapped sediment hold water and the moist conditions in the pores of the cover layer provide excellent growing conditions for algae and other organisms. The introduction and production of organic material further reduces the permeability of the clogging material and increases its cohesion as well. The latter will prevent the material from being washed out again under extreme conditions. Thus, the scenario of clogging can be indeed an important factor in the stability of an Elastocoast cover layer.

On the contrary, it can be argued that clogging will not form a danger for the stability of Elastocoast. This can be illustrated for three possible structure types.

In case of the above pilot situation of Elastocoast on top of an existing revetment:

- Clogging will reduce the hydraulic conductivity of the cover layer, but the supporting layer also has a low conductivity, significant overpressures are therefore not likely to build up.
- Clogging material washed in during calm weather will be washed out again with the next storm and is therefore not present during normative conditions.

← Elastocoast cover layer

← Existing (block) revetment
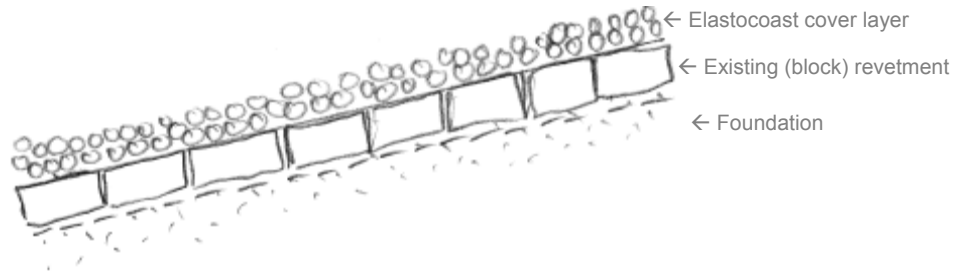
← Foundation

Figure 5.35 Elastocoast applied on top of an existing revetment.

In case of Elastocoast put directly on top of a sand foundation:

- The hydraulic gradient through both layers will prevent sediment from settling in the cover layer.
- Most likely geotextile is present on the interface between the Elastocoast and its foundation. This prevents sand from the foundation to enter into the cover layer and clog it from the inside (see chapter 5.4).

← Elastocoast cover layer
← Geotextile
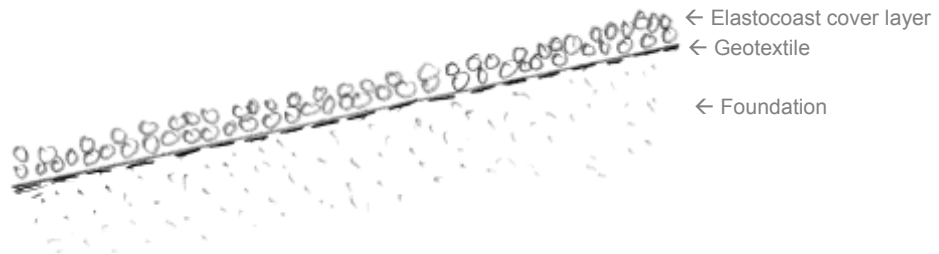
← Foundation

Figure 5.36 Elastocoast applied on top of a sand foundation.

In case of Elastocoast put on a granular filter layer:

- The hydraulic gradient through both layers will prevent sediment from settling in the cover layer.
- If clogging material would be originating from the underlying (sand) foundation, the filter layer is clogged first. This increases the relative permeability of the cover layer and pressure, if anywhere, would be build up under the granular filter instead. This overpressure is then countered by both the weight of the filter layer and the cover layer.

← Elastocoast cover layer

← Granular filter

← Foundation
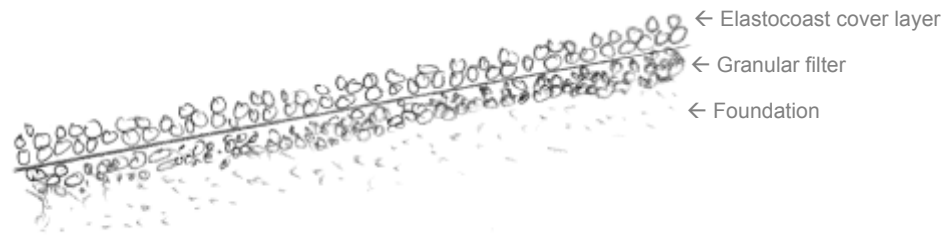
Figure 5.37 Elastocoast applied on top of a granular filter.

The above argumentations are confirmed by the results of an investigation after the clogging phenomenon in placed block revetments (Johanson, 2003). Whether clogging will take place or not was found to be strongly dependent on local conditions and not easy to predict. From in-situ research it showed that at high overpressures the clogging material was (sometimes rapidly) washed away. It was concluded that it is unsure whether clogging is present under normative conditions and negative effects on the stability of the structure are not expected.

Worst case scenario
Despite these arguments against its negative effects, for a better understanding of the effect of clogging on the stability of Elastocoast it is chosen to take the worst case scenario, namely:

- Presence of sand in the pores of the cover layer during extreme conditions. The clogging will also be assumed to be present over the entire thickness of the cover layer.

Leakage length
An important factor in stability calculations for uplift is the leakage length Λ (m). On basis of the comparison of the size of the leakage length and that of the load scale, a prediction can be made whether uplift pressures can be large enough to result in instability. With the leakage length theory and the joint conductivity of clogged Elastocoast (as calculated in section 5.4) a prediction can be made of the stability of Elastocoast in some of its standard applications.

Possible applications proposed for Elastocoast are:

- Placed directly on top of compacted sand or clay (separated with a geotextile).
- Placed on top of a granular filter.
- Placed on top of an existing revetment (i.e. placed blocks, asphalt, clay).

Now the stability can be predicted by calculating the leakage length in the same way as shown in chapter 2. The results are shown in the following table.

Table 5.10 Leakage length related to load scale for different applications of Elastocoast. For both Elastocoast and the filter layer a value of $D_{15}=21$ mm is used for calculation of the hydraulic conductivity.

Application	d_{top} (m)	d_{filter} (m)	k_{top} (m/s)	k_{filter} (m/s)	Leakage length Λ (m)	External load scale L (m)	
Elastocoast + geotextile on sand	0.20	2	0.068	0.0001	0.02	1-2	$\Lambda \ll L$
Elastocoast on granular filter	0.20	0.20	0.068	0.05	0.17	1-2	$\Lambda \ll L$
Clogged Elastocoast + geotextile on sand	0.20	2	0.00005	0.0001	0.9	1-2	$\Lambda \approx L$
Clogged Elastocoast on granular filter	0.20	0.20	0.00005	0.05	6.3	1-2	$\Lambda \approx L$
Elastocoast on existing revetment	0.20	"0"	0.068	"0"	"0"	1-2	$\Lambda \ll L$

For the following two scenarios the Elastocoast cover layer is potentially lifted up by the water pressure if the weight is insufficient:

- Scenario 1: clogged Elastocoast directly on top of compacted sand
- Scenario 2: clogged Elastocoast placed on a granular filter layer

In the next section an analogy is made between the stability of an Elastocoast cover layer and placed block revetments.

5.5.3   Analogy to stability of placed block revetments

During maximum wave run retreat there will be an incoming wave that will later cause an impact on the dike slope. Just before impact this wave causes a high pressure under the point of maximum wave run-down. Above this point the slope is almost dry and there is a low pressure (Klein Breteler, 1998). The pressure difference will result in a flow through the filter layer towards the point of low pressure from above (high ground water level) and below (high wave pressure). This process and the resulting local high pressure are shown in figure 5.38.
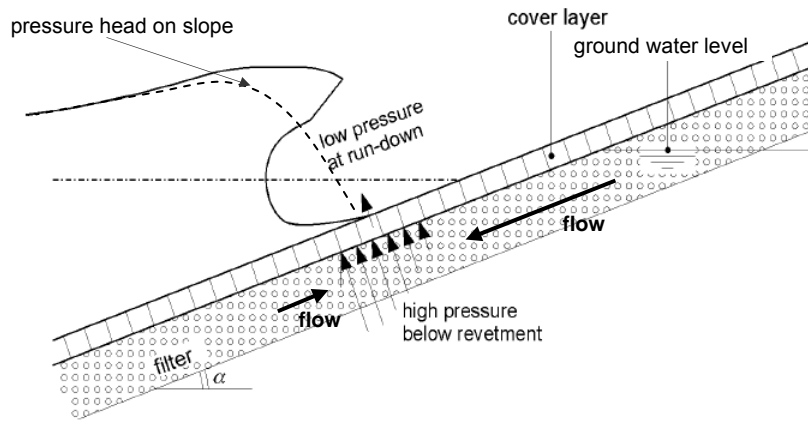
Figure 5.38 Pressure development in a revetment structure (adapted from Klein Breteler, 1998).

Stability according to the leakage length theory
In case of a high pressure behind the cover layer, flow exists through the revetment, if it is porous. From the head differences, resulting in parallel flow through the filter layer and an outward flow through the cover layer, the uplift pressure can be derived. In (TAW, 2003) a complicated calculation method is presented to predict the equilibrium of uplift forces and gravity forces. In this method the wave front is schematized with a curved shape as shown in figure 5.39. The contribution of the internal forces to stability however, is neglected in this method.
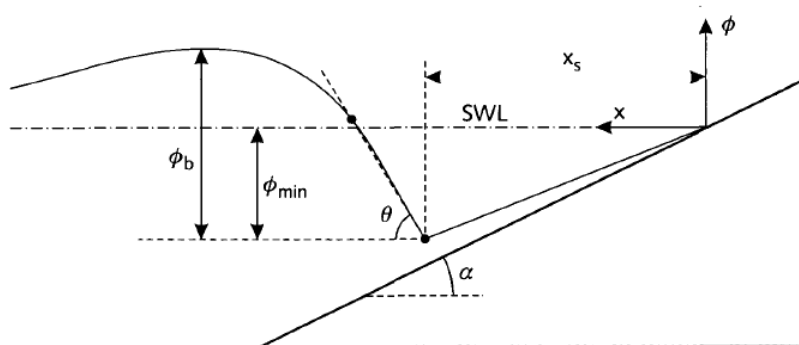
Figure 5.39 Schematization of the wave front as a curve (TAW, 2003).

The calculation method works as follows: it starts by schematization of the wave front with a curved shape (figure 5.39). Then the height of the maximum head of the wave front ϕ_b (m) and the slope of the wave front θ (°) are defined with empirical formulas. From these values and the schematized shape of the wave front, the minimum hydraulic head ϕ_{min} (m) and its location on the slope x_s are calculated. Finally from these values the maximum hydraulic head is calculated in relation to the leakage length parameter Λ (m). This results in a value for the uplift pressure at the given wave conditions.

The schematization of the wave front in the form a curve in (TAW, 2003) is an improvement compared to a more simplistic schematization with a straight wave front presented in the same report. The latter has been implemented in present methods for design and stability assessment in the Netherlands, whereas the improved method is still in an experimental phase. Its fields of application are not yet fully defined. Therefore calculations with this method should primarily be seen as indicative, especially in unique and new applications such as Elastocoast.

Stability according to structural analysis
In 2000 a relatively simple, structural model was proposed that represents the mechanical behaviour of the block revetment under wave loading (Vrijling, 2000). In this model, the contribution of the structure's own weight as well as of the internal forces on the stability of the structure can be incorporated. It is assumed that a hydrostatic water pressure, defined by the still water level, exists behind the revetment (in the filter layer). In the original model for placed block revetments the reduction of pressure due to leakage through the joints between the blocks was neglected.

At the outside of the revetment the water pressure reaches a minimum during wave run-down. The schematized situation at wave run-down is shown in figure 5.40. The expression for the wave run-down proves to be important, because in the end it enables the stability of the revetment to be described as a function of the stability number N_s (see section 5.2.3). The wave run-down z_{rd} is described by the following expression:

$$z_{rd} = \frac{H_s \xi}{3}$$
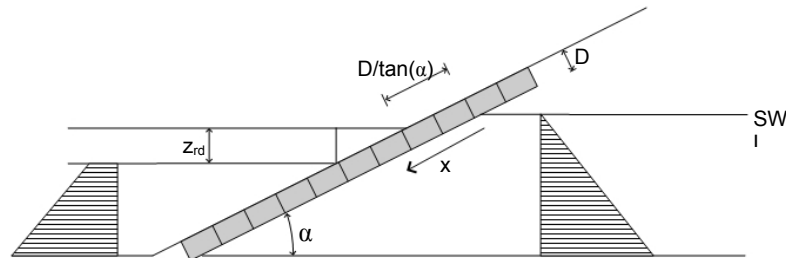
Figure 5.40 Schematization of the block revetment at wave run down (Vrijling, 2000).

Analogy with Elastocoast
In the next sections the stability of Elastocoast will be predicted with the help of the two methods discussed above. First, the stability of Elastocoast is elaborated according to the leakage length theory and the model from (TAW, 2003). This model gives insight in the actual pressures that will occur under the cover layer during maximum wave retreat. However, this method does not take into account the structural coherence contributing to stability. Therefore this method will give safe, but very conservative values for the required layer thickness. Detailed formulas and calculations for the two scenarios are given in Appendix IV. Only the results will be discussed in section 5.5.4.

Then, in section 5.5.5, the structural analysis from (Vrijling, 2000) will be used, which will give an insight into the behaviour of Elastocoast under wave action as a coherent structure with internal forces. The assumption that there is no reduction of pressure due to leakage through the cover layer is a very pessimistic one. In reality, there will be a significant leakage through the Elastocoast revetment, even when its pores are fully clogged with sandy material. Adding a reduction factor to the water pressure makes the algebra and the resulting expressions considerably more complicated. To get a first feeling of the stability, therefore the method will be used in its original form, thus overestimating the uplifting pressures.

Concluding, both methods can be considered conservative. The structural analysis overestimates the existing pressures behind the revetment, whereas the calculations with the leakage length theory do not take into account the contribution of structural coherence to stability.

5.5.4   Calculations with the leakage length theory

Detailed calculations with the leakage length theory from (TAW, 2003) are included in Appendix IV. Only the input and results will be discussed below. In the calculations the wave conditions are assumed to be: wave height $H_s = 2$ m, wave period $T = 4.5$ s. The slope of the dike is set to $tan(\alpha) = 1:3$. For the input wave conditions and dike slope angle the following values are found, describing the shape of the wave front (see also figure 5.39):

Table 5.11 Load parameters which define the shape of the wave front.

Parameter	Value
significant load $\phi_{b.s}$	1.3 m
slope of wave front θ	54 °
minimum head on bank ϕ_{min}	-0.7 m
location of minimum head x_s	3.0 m

The upward pressure is calculated with the schematization of the curved wave front. Stability by weight is guaranteed if the weight of the cover layer is not exceeded by the upward pressure:

$$P < W$$

Where:

$P = \rho_w \cdot g \cdot \phi_w$, is the uplift pressure (kPa)

$W = \rho_v \cdot d_{ec} \cdot \cos(\alpha)$, weight component of the cover layer perpendicular to slope (kPa)

ϕ_w = head difference at maximum wave retreat (m)

$\rho_v = (1 - n_{ec})\rho_{ec} + n_{ec}\rho_s$, is the specific weight of the clogged cover layer (kg/m^3)

n_{ec} = the porosity of the cover layer
d_{ec} = thickness of the cover layer

Scenario 1: clogged Elastocoast directly on top of compacted sand
In this scenario, the revetment structure is build up as shown in the figure below:
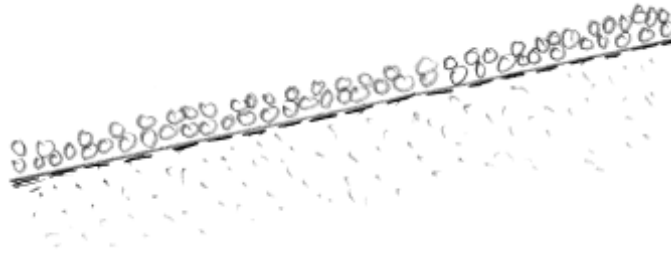
Figure 5.44 Schematization of structure build up in scenario 1: clogged Elastocoast placed directly on top of a compacted sand bed.

In the following figure the upward pressure and weight of the top layer are depicted as functions of the cover layer thickness. It shows that the uplift pressure exceeds the structure weight if the top layer is less than 0.3 m thick.
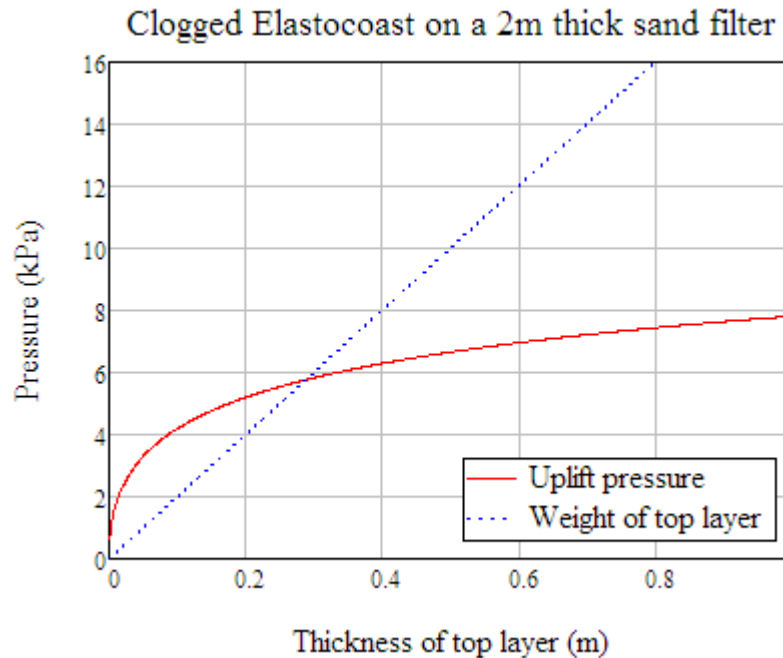
Figure 5.45 Upward pressure and weight of the top layer as a function of layer thickness in case of scenario 1.

At the intersection of the two lines in the above figure, the head difference is equal to approx $\phi_w = 0.58$ m. Both the upward pressure as the structure weight have a value of $P=W= 5.9 \, kPa$.

Scenario 2: clogged Elastocoast placed on a granular filter layer

In this scenario, the revetment structure is build up as shown in the figure below:
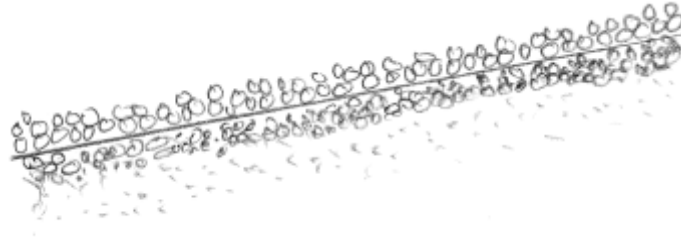
Figure 5.46 Schematization of structure build up in scenario 2: clogged Elastocoast placed on a granular filter.

In the following figure the upward pressure and weight of the top layer are depicted as functions of the cover layer thickness. It shows that the uplift pressure exceeds the structure weight if the top layer is less than 0.6 m thick.
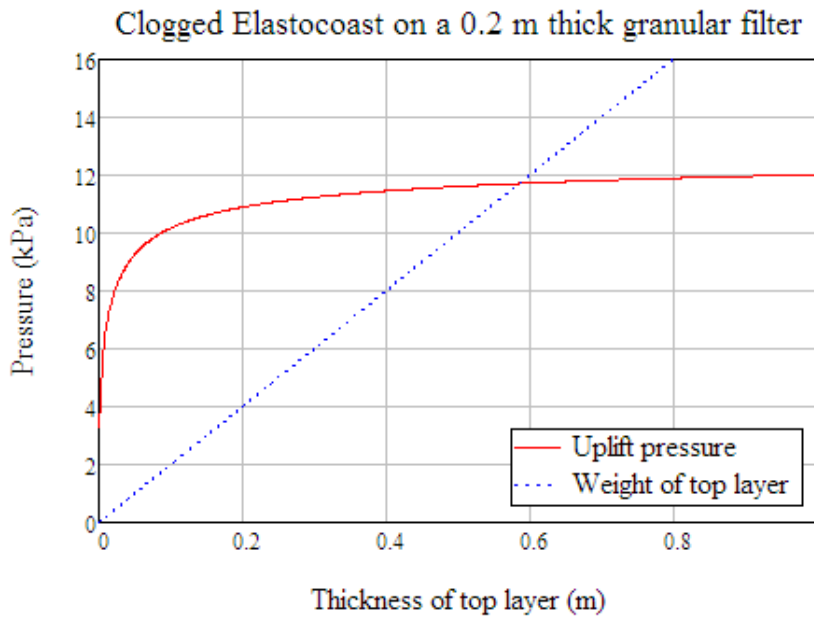
Figure 5.47 Upward pressure and weight of the top layer as a function of layer thickness in case of scenario 2.

At the intersection of the two lines in the figure above, the head difference is equal to approx $\phi_w = 1.17$ m. Both the upward pressure as the structure weight have a value of $P=W= 11.7 \, kPa$.

Discussion of results
The above calculations give a theoretical minimum thickness of the cover layer needed for stability against overpressures. There are several reasons why these values are too pessimistic:

- Clogging of the cover layer is not likely to be present in normative conditions.
- If clogging occurs, the sand in the cover layer will be saturated with water, this adds to the weight and therefore stability of the cover layer (thickness can be reduced with approximately 10%).
- Uplift pressures act locally and are therefore not only countered by structure weight, but also by internal forces that are characteristic for loaded plate structures.

So the overpressures and needed layer thickness are overestimated with these calculations. On the one hand overpressures will in reality be lower, but certainly not higher. On the other hand the structure resistance to these overpressures will be higher, but certainly not lower than calculated. This means that the given values are a safe upper boundary for the needed layer thickness against overpressures.

Nonetheless, the negative effect of a granular filter layer on stability is significant. The use of a granular filter layer is therefore depreciated. If it is necessary for constructive reasons, the thickness of the layer should be kept at a minimum and preferably material should be used with a wide gradation.

5.5.5 Calculations with structural analysis

Using the method of (Vrijling, 2000) discussed above, the situation at wave run-down results in forces working on the revetment as shown in figure 5.41. The structure self weight is, in this case, equal to the weight of Elastocoast, fully clogged with sand in its pores.
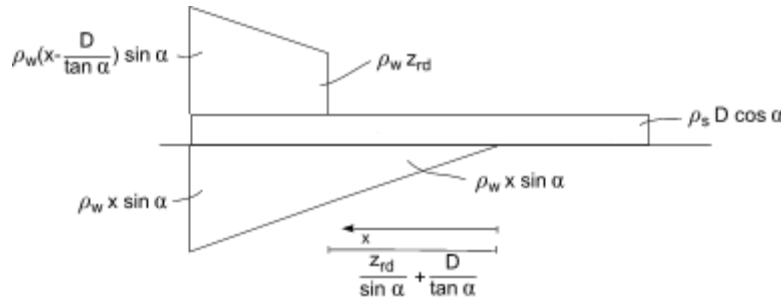
Figure 5.41 Water pressures and self weight acting on the revetment (Vrijling, 2000).

The total loading of the revetment thus becomes:
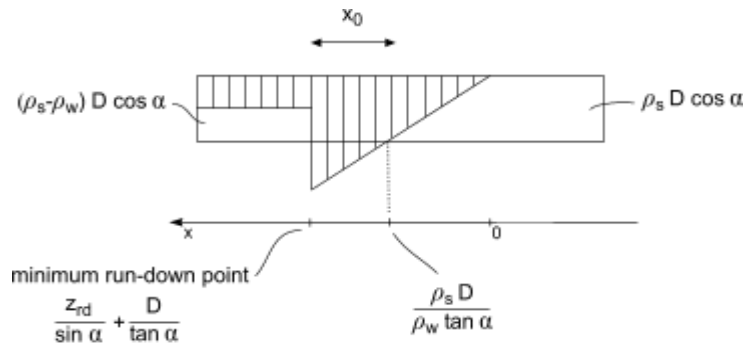
Figure 5.42 Resultant loading of the revetment (Vrijling, 2000).

From figure 5.42 and with the expression for z_{rd} from section 5.5.3 it can be derived that the length over which the total loading becomes negative equals:

$$x_0 = \frac{z_{rd}}{\sin \alpha} - \frac{\Delta D}{\tan \alpha} = \frac{H_s \xi}{3 \sin \alpha} - \frac{\Delta D}{\tan \alpha}$$

The stability of an infinitesimal part of the revetment at the minimum run-down point can be found by equalling the resultant water pressure with the weight of the revetment. With some algebra, the result can conveniently be expressed in the stability number N_s.

$$\rho_s D \cos \alpha = \rho_w x \sin \alpha \qquad \text{for} \qquad x = \frac{z_{rd}}{\sin \alpha} + \frac{D}{\tan \alpha}$$

$$N_{s,own\ weight} = \frac{H_s}{\Delta D} = \frac{3 \cos \alpha}{\xi}$$

Thus, the stability by own weight of the structure is found. Notice the similarity of the expression for the stability number with the Pilarczyk stability-formula discussed in section 5.2.3. In reality, not only the own weight contributes to stability, but also the internal forces delivered by shear and bending moment (see also figure 5.34). In line with the bending beam model of section 5.3, the contribution of shear is now neglected and only the bending moment is taken into account.

From this point, the approach will differ from the original method of (Vrijling, 2000), which was intended for use with block revetments. The Elastocoast revetment has the capability to deform (bend) under loading. The bending moment capacity for an Elastocoast revetment is constant and depends on the bending strength and the thickness of the cover layer:

$$M(x) = \sigma \cdot W = \sigma \cdot \frac{1}{6} D^2$$

To derive the contribution of internal forces to the stability of the infinitesimal part of the revetment, the bending moment resulting from water pressure is equalled with bending moment capacity:

$$\frac{1}{6} x_0^3 g \rho_w \sin \alpha = \sigma \frac{1}{6} D^2$$

In which the gravitational acceleration g is added to achieve the correct units (until know, g was not necessary to include, because it would be cancelled out anyway). After some algebra, the formula that describes the limit imposed by the bending moment is:

$$N_{s,moment\ capacity} = \frac{H_s}{\Delta D} = \frac{3 \cos \alpha}{\xi} \cdot \left(1 + \sqrt[3]{\frac{\sigma_{max} \tan^2 \alpha}{\Delta^3 D g \rho_w \cos \alpha}} \right)$$

Thus the total stability, taking into account structure own weight and bending moment capacity is describe by the following equilibrium:

$$N_{s,total} = \frac{H_s}{\Delta D} = \frac{3 \cos \alpha}{\xi} \cdot \left(2 + \sqrt[3]{\frac{\sigma_{max} \tan^2 \alpha}{\Delta^3 D g \rho_w \cos \alpha}} \right)$$

In the graph on the next page, the stability number is depicted as a function of the surf similarity index ξ for different slope angles and a layer thickness of, respectively, 0.2 m and 1.0 m. The contribution of only the structure weight and the combination of structure weight and moment capacity are depicted separately.
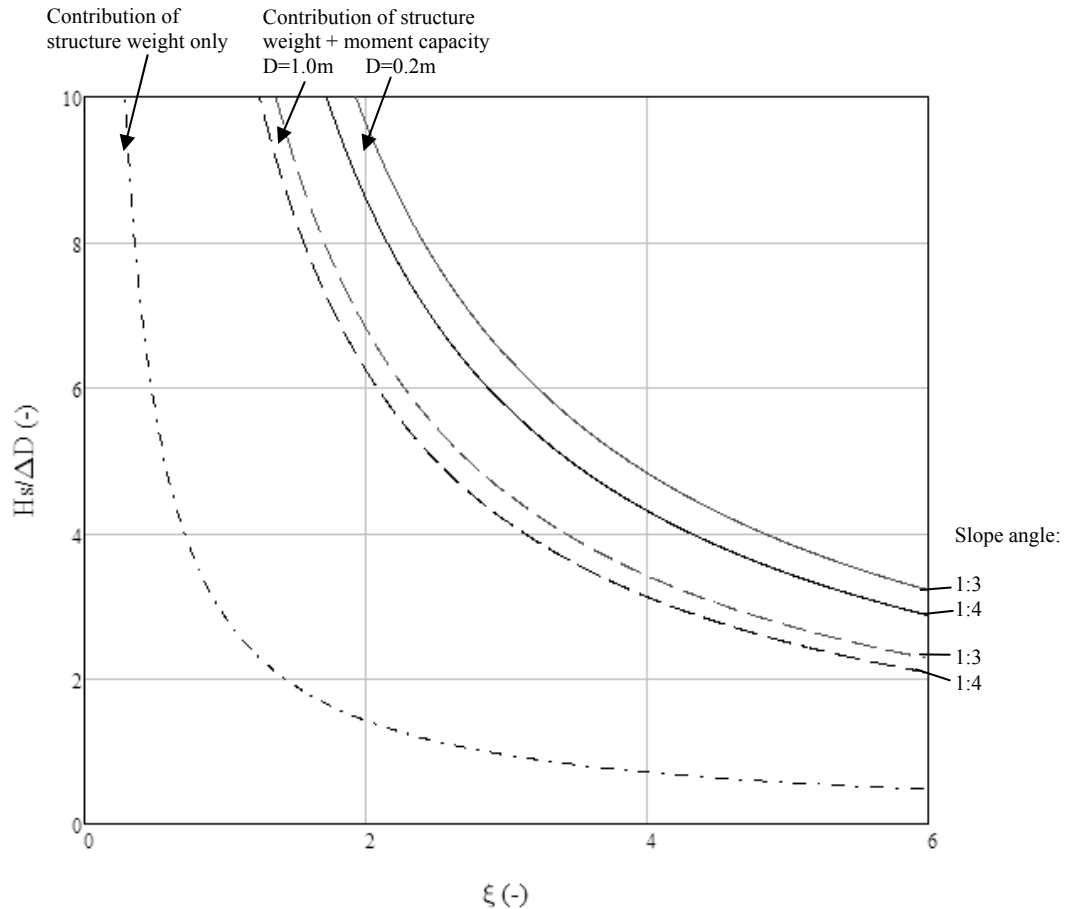
Figure 5.43 Stability parameter as a function of surf similarity index.

Discussion of results
From the above graph several notions can be made:

- The contribution of bending moment to the stability of the structure is (much) larger than that of the structure's weight.
- With increasing layer thickness the stability line approaches slowly towards the line which accounts for structure weight only. It could be argued, that the contribution of the structure weight to stability becomes more important when a thick layer of Elastocoast is placed. However, the stability is stronger influenced by the increase in moment capacity, which is proportional to D^2.
- In a N_s-ξ-diagram, the area under the stability line refers to stable combinations of wave height, layer thickness and breaker type. At first sight, this would imply that the stability of Elastocoast decreases with increasing layer thickness. This is not true, since the layer thickness is present at both sides of the stability function. Though an increase in thickness would lead to a less than proportional lowering of the stability line, the value of N_s would decrease proportional. Thus the stability effectively increases with increasing layer thickness. It should always be kept in mind that the stability curve in this graph is only valid for a specific layer thickness.

Taking pressure leakage into account
In the above method, reduction of pressure due to leakage through the cover layer is neglected. In reality the Elastocoast revetment will have some permeability, which results in a yet unknown reduction of water pressure behind the revetment. To account for this permeability, the reduction of the pressure could, for instance, be assumed proportional by a factor A_p. This reduction would only work on the part of the structure where an effective overpressure exists (figure 5.44). The algebra needed to express the equilibrium into a function of N_s becomes considerably more complex by introduction of the factor A_p.

Considering the already high stability achieved with full pressure, the factor A_p will not be elaborated further in this report.
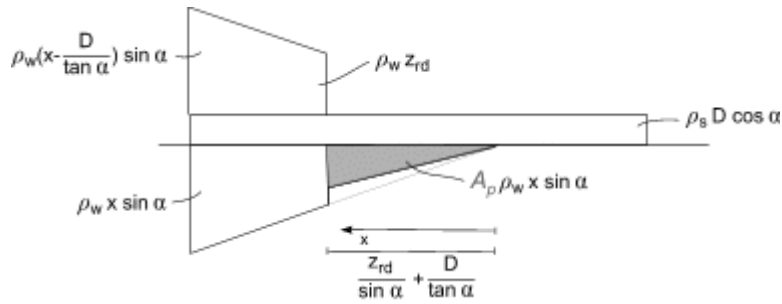
Figure 5.44 Water pressure and self weight acting on the revetment in case of pressure leakage proportional to A_p.

5.5.6   Conclusion

From the calculations and discussion of this chapter it can be concluded that when the Elastocoast structure retains its high permeability, instability by uplift under maximum wave retreat is not expected. Whether clogging will occur strongly depends on the local conditions and structure build-up. Further it is unsure if clogging material will remain present during extreme conditions.

The stability analysis with the leakage length theory according to (TAW, 2003) takes into account the porous flow through the cover layer. Maximum pressured are calculated for the situation at maximum wave retreat. The upward pressures are countered only by the structure's own weight, internal forces are neglected. From this analysis it is concluded that:

- Clogging of the open pore space gives the structure a higher weight but strongly reduces the hydraulic conductivity. The net effect on stability is negative.
- Use of a granular filter layer has a negative effect on stability and should be avoided in cases where clogging can be expected.

Structural analysis according to (Vrijling, 2000) makes a very straightforward schematization of the resulting pressures during maximum wave retreat. Reduction of these pressures by leakage through the porous cover layer is neglected. In this method both the structure's own weight as the moment capacity of the cross section are taken into account as resisting forces. From structural analysis it is concluded that:

- The contribution of bending moment to the stability of the structure is (much) larger than that of the structure's weight.
- Despite neglecting the pressure leakage, high stability is reached.
- Incorporation of pressure leakage in the method results in more complex algebra, but will improve stability.

Both of the above methods underestimate the real stability of the cover layer under maximum wave retreat. The leakage length theory neglects the coherence of the cover layer, whereas the structural analysis neglects the pressure reduction by porous flow through the cover layer. Though the outcomes of these methods can be considered as conservative, their approaches to the problem are entirely different. By using these methods, valuable insight is gained into the behaviour of the structure at maximum wave retreat and the contribution of several system parameters to the structure's stability.

6 Design of an Elastocoast revetment

6.1 Introduction

In this chapter the results from detailed analysis from chapter 5 are combined with knowledge from previous research (Gu, 2007a and 2007b) and experience from the pilot tests (Bijlsma, 2008). By bundling of this information a first suggestion can be made for design guidelines.

First, the result from detailed analysis are compared and discussed. Then several steps in the design process of an Elastocoast revetment are treated. Attention is paid to construction aspects of an Elastocoast cover layer on a dike body, the production of the Elastocoast itself, and the determination of required layer thickness. Where possible, reference is made to relevant sections of this report.

6.2 Results from detailed analysis

6.2.1 Instability of individual rocks (erosion)

From the Dutch pilot tests (Bijlsma, 2008) it was concluded that the Elastocoast revetments suffered only negligible damage during a single storm season. In section 5.2 of this report the stability of individual rocks was further researched. This resulted in a high stability number and the conclusion that loose rock stability formulae are not applicable to an Elastocoast revetment. Damage by erosion of individual rocks is not considered to be normative for the structure design.

6.2.2 Breakage by wave impact

In section 5.3 of this report the effect of wave impact on an Elastocoast plate structure was researched by schematization of the problem by an elastically supported beam under a triangular wave load. From this analysis it was concluded that the maximum tension strength in the bottom of the cover layer will not be exceeded by the bending stresses, as long as the layer is continuously supported over its entire surface. However, if a local cavity is present, breakage may occur. The minimum required layer thickness depends on the size of the load, size of the cavity, the soil elasticity, and the strength of the cover layer. Figure 6.1 shows the minimum required layer thickness depicted as a function of wave height.
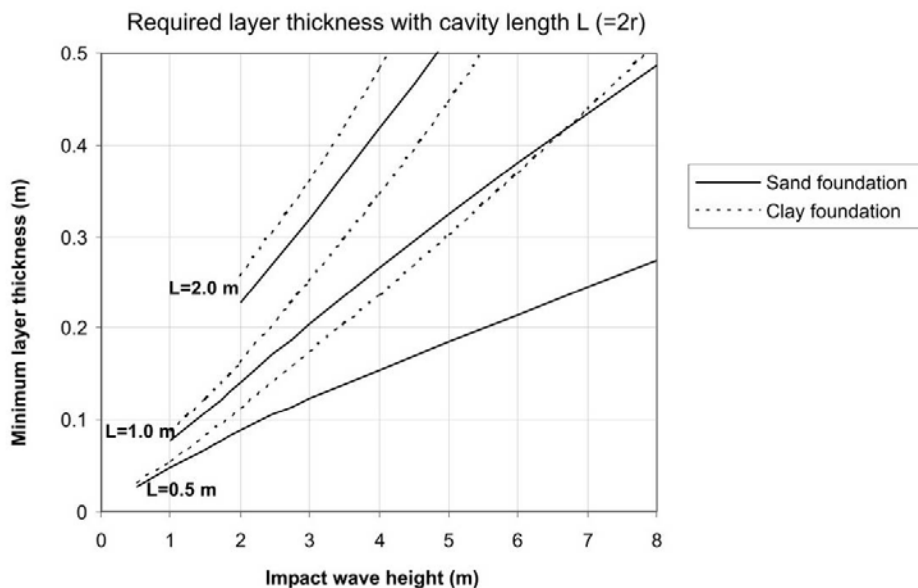
Figure 6.1 Required layer thicknesses as a function of impact wave height. Assumed are a Young's modulus of 2500 MPa and a flexural strength of 2.5 MPa.

6.2.3 Instability by uplift pressures

In section 5.5 the stability of an Elastocoast cover layer under maximum wave retreat was researched. Under 'normal' conditions, there is no danger of instability by uplift because any overpressures behind the cover layer can easily diminish through the pores of the cover layer. However, if the hydraulic conductivity of the cover layer is decreased by clogging, uplift may become a mechanism to consider.

Figure 6.2 compares the results from detailed analysis. The dark line gives the stability curve that resulted from structural analysis. In this analysis pressure leakage through the cover layer are neglected and resulting overpressures are countered by structure weight and coherence by moment capacity. The gray areas give the results from analysis with leakage length theory, in which pressure leakage is accounted for, but structural coherence is not. Pressures are only countered by the structure's own weight.
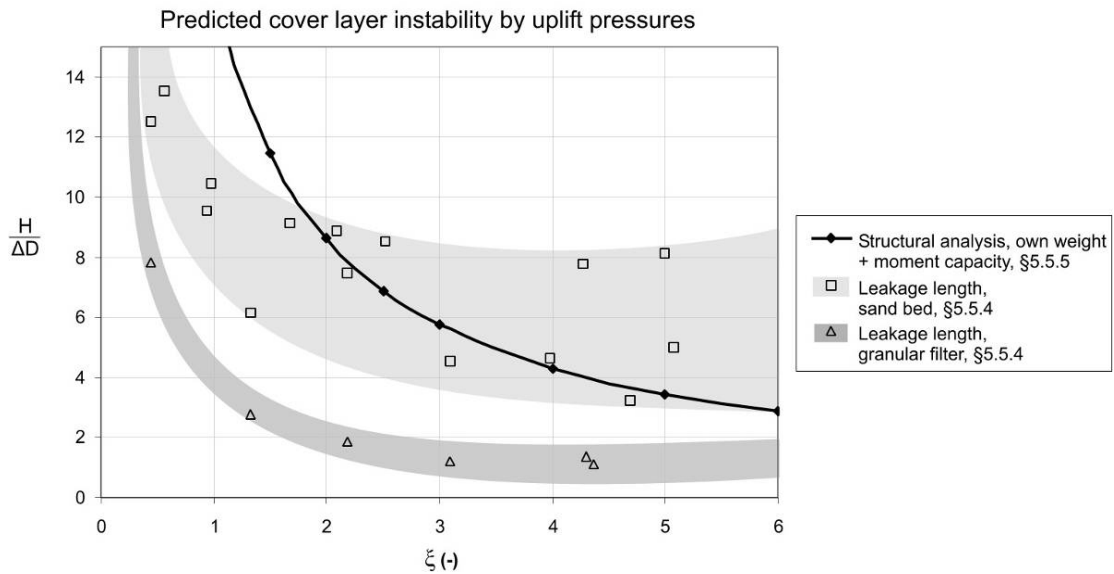
Figure 6.2 Stability of an Elastocoast cover layer under maximum wave retreat according to structural analysis and leakage length theory.

The above figure shows that the spread in the results from the leakage length theory is fairly high, especially for the case in which Elastocoast is placed on top of a sand bed. For design purposes the line described by structural analysis has the most practical value. Though overestimating the overpressures behind the cover layer, this method incorporates both the structure weight as the structure coherence in the stability function of Elastocoast.

6.3 Design of an Elastocoast revetment

6.3.1 Construction on a dike body

Application height and slope:
- Elastocoast is preferably placed on a dike body above the water line, but can also be placed under water. Under water the construction process is less controllable and the strength of the bonding between the rocks is decreased when the hardening process takes place under water (in the order of 50% dependent on the type of aggregate).
- Unhardened Elastocoast has limited stability on steep slopes. In order to remain stable, the material has to be placed on slopes not steeper than 1:3-1:4 (see section 3.3.4).
- In order to decrease risk of macro instability by a shear plane or slip circle, also a slope milder than 1:2.5 is advised (see section 4.4.3).

Compaction and leveling of the subsoil:
- The degree of soil compaction determines a great deal of the carrying capacity of the cover layer. This does not concern specifically the actual bearing strength of the soil, but the uniformity of compaction is important. The compacted application surface does not necessarily have to be level, as long as it is well compacted over the entire surface. Differential settlement could lead to cavities, which negatively influences the local resistance to wave impacts (see section 4.4.2).
- To reduce the chance of subsoil liquefaction by repeated wave impacts, it is also of great importance that the foundation is sufficiently compacted before application of the cover layer.
- When a geotextile is used, special attention has to be paid to the presence of hard objects in the application area. The geotextile could create a hanging surface, resulting in a cavity under the revetment (see section 4.4.2, figure 4.4).
- Clay soil is difficult to compact, because its water content is hard to control. Therefore a supporting layer consisting of sand is preferred.

Filter layers:
- Because of the high porosity of Elastocoast a filter layer is required on the interface when the cover layer is directly placed on a soil foundation. This can either be in the form of a geotextile or a granular filter. A filter is not needed in case the Elastocoast is placed as a cover over an existing revetment.
- The filter must have sufficient hydraulic conductivity. A geometrically open filter is advised against because of exposure through the relatively thin cover layer.

Connections:
- On an existing layer of Elastocoast – clean and dry surface layer for best attachment.
- Between day productions – no overlapping in the seams necessary.
- Between Elastocoast and adjacent structures – pay attention to sand tightness of connection.

6.3.2 Production of Elastocoast

Moisture:
- The aggregate must be dry before it is mixed with the polyurethane. Use of moist aggregate will result in reduced bonding strength (see sections 3.1.2 and 3.4.4) and can often be observed afterwards (figure 6.3).
- Application under water is possible, but for highest strength it is advised to keep at least an hour of hardening between the moment of placing and contact with water.

Temperature:
- Advised working temperature is between 10-30°C. Processing time is temperature dependent (see sections 3.1.2 and 3.4.4).
- Drying of aggregate by heated tumbling is advised against, since this produces extra fine fragments which increase polyurethane consumption. Also, by using hot aggregate, the curing process will be unacceptably accelerated to an extent where the bonding between the rocks is no longer formed.

Quality assessment:
- During construction the condition of the aggregate should be observed and noted down. By ensuring the right conditions during production, the quality of the end product can be guaranteed.
- In-situ cube samples can be taken from every day of production. The compression strength of these samples can then be determined for comparative purposes (see section 3.4.4).
- After a period of time or every few years a drilling core sample can be taken from the revetment. To make use of these samples, it is necessary that standards are developed for testing of Elastocoast cores, in line with the testing of asphalt revetments. Elastocoast has proved to be coherent enough to survive mechanical forces that come with drilling (figure 6.4).

Figure 6.3 Signs of the use of moist aggregate during construction: light discoloration and stripping of the polyurethane film.

Figure 6.4 Drilling of core samples from an Elastocoast revetment (Bijlsma, 2008).

6.3.3 Determination of layer thickness

Construction limitations:

- The minimum layer thickness of Elastocoast is mostly determined by the limitations of the construction material and that of special load requirements. With standard construction equipment where profiling is done by hydraulic crane, it is hard to produce layer thicknesses smaller than 10-15 cm (figure 6.5). Also, a design requirement can be that the cover layer is accessible by construction or maintenance vehicles, which imposes similar loads as described in section 5.3.
- Compaction of the freshly put Elastocoast is not necessary. It is also not necessary to add extra thickness in the design to account for compaction.

Figure 6.5 Profiling of freshly put Elastocoast with a hydraulic crane (photo: BASF Nederland B.V.).

Dimensioning for water overpressures:

- Because of the large hydraulic conductivity of Elastocoast, under normal conditions, uplift by overpressures will be very unlikely. Any existing pressures behind the revetment will quickly diminish by flow through the cover layer (see section 5.5.2).
- If the conductivity of the cover layer is limited by clogging, the danger of uplift may require a minimum layer thickness. The reduction of hydraulic conductivity depends on the type of clogging material (see sections 5.4.4 and 5.5.2). Also blocking or clogging of the geotextile can result in decreased permeability.
- A save way to assess the stability of a cover layer design is by using the following expression from structural analysis (see sections 5.5.5 and 6.2.3):

$$\frac{H_s}{\Delta D} = \frac{3\cos(\alpha)}{\xi} \cdot \left(2 + \sqrt[3]{\frac{\sigma \cdot \tan^2(\alpha)}{\Delta^3 \cdot \rho_w \cdot D \cdot g \cdot \cos(\alpha)}} \right)$$

Dimensioning for breakage by wave impact

- As long as the Elastocoast cover layer is fully supported over its entire surface, no macro scale damage needs to be expected from wave impact. If cavities are observed or expected, the mechanical schematization presented in this report can be used to obtain either minimum layer thickness or maximum acceptable cavity dimensions (see sections 5.3.7 and 6.2.2).

7 Conclusions and recommendations

7.1 Purpose and results of this study

The purpose of this MSc thesis study is to make a first step in the development of design tools for the Elastocoast system (and implicitly for similar polymer bonded revetments). The following objectives were formulated:

- Make an inventory of possible failure mechanisms for Elastocoast revetments.
- Eliminate those mechanisms that are not dominant and quantify those that are.
- Make a proposal for design criteria and construction guidelines where possible.
- Make recommendations for further research into those mechanisms and parameters that could not be quantified.

Below, the results of the first two objectives are summarized. Conclusions and recommendations for further research are then given in the next sections. A proposal for design criteria and construction guidelines was already given in chapter 6.

Inventory of possible failure mechanisms
On basis of theoretical considerations and experience from the field the following failure mechanisms were determined:

- Micro scale instability (erosion)
  - *By tidal flows*
  - *By orbital flow*
  - *By wave breaking combined with wave up- and down-rush*
  - *By overtopping discharge*
- Mechanical failure
  - *Breakage by wave impact*
- Macro scale instability
  - *Uplift by static head difference*
  - *Uplift by dynamic head difference, at maximum wave retreat*
  - *Uplift by dynamic head difference, at wave impact*
  - *Shear plane or circular slip plane*
  - *Soil liquefaction under repeated wave impact*
- Material degradation
  - *Fatigue*
  - *Exposure to aggressive environment*

Elimination of mechanisms that are not dominant
The mechanisms that were found not to be relevant for an Elastocoast revetment are summed up below, together with a short reason why they are considered not to be relevant:

- Micro scale instability (erosion)
  - *By tidal flows:*
    Tidal action results in relatively low flow velocities in shallow water, Elastocoast will mainly be applied in shallow water or above the water line.
  - *By orbital flow:*
    The Dutch pilot tests by ARCADIS and the overtopping test by RWS showed that the

Elastocoast revetment can withstand much higher flow velocities (6-12 m/s) than would occur by orbital flow.

- o *By overtopping discharge*
  In case of overtopping, the same considerations apply as mentioned above.
- Macro scale instability
  - o *Uplift by static head difference:*
    On the timescale in which static head differences are present, even a low permeability of the cover layer is enough for the water pressures to diminish before high uplift pressures can occur.
  - o *Shear plane or circular slip plane:*
    The high permeability of Elastocoast provides good drainage, which reduces the chance of a shear or slip plane forming. Besides, the danger of shear and slip is only likely to be present on steep slopes, whereas Elastocoast is put on relatively mild slopes up to 1:3-1:4.

Quantify mechanisms that are dominant

After elimination of mechanisms that were found not to be relevant the following mechanisms were quantified with detailed analysis:

- Micro scale instability (erosion)
  - o *By wave breaking combined with wave up- and down-rush:*
    The wave conditions that the Elastocoast revetment has proven to be able to withstand in the Dutch pilot tests were used as input for commonly used stability formulas for loose rock. Thus upgrading factors could be back-calculated that take the structure coherence into account.
- Mechanical failure
  - o *Breakage by wave impact:*
    The plate structure at wave impact was schematized in a structural model as a semi-infinite, elastically supported beam under a constant, triangular shaped load. For this problem the static solution if found. The model includes the possibility of a cavity right under the wave load. From the model values for the maximum stress and displacement in the middle under the load can be calculated.
- Macro scale instability
  - o *Uplift by dynamic head difference at maximum wave retreat:*
    First the effect of clogging on the hydraulic conductivity of Elastocoast was investigated and quantified. Then the stability of the cover layer was investigated with two separate approaches: 1) the leakage length theory, which takes into account flow through the cover layer but neglects structural coherence; and 2) a structural analysis, which neglects the reduction of pressure by leakage through the cover layer, but incorporates both the structure weight and moment capacity.

The remaining mechanisms are considered to be relevant but could not be researched or quantified within the scope of the present thesis study. Possible failure mechanisms that have not been eliminated nor quantified in this study are:

- Macro scale instability
  - o *Uplift by dynamic head difference, at wave impact*
    At the moment of wave impact, very short-lived but high pressures can occur behind the revetment. This is a complex phenomenon for which reliable models are not yet available at present. Because of the short loading duration, stability could best be researched with structural analysis instead of the leakage length theory.
  - o *Soil liquefaction under repeated wave impact*
    The open structure of Elastocoast offers a good way for impact pressures to penetrate to the underlying layers. It is conceivable, that repeating wave impact pressures lead to such an increase of saturation and water pressure inside the dike body that liquefaction becomes a danger. This problem can partly be avoided by adequate soil compaction.

- Material degradation
  - *Fatigue*
    Although fatigue is not expected to be relevant for Elastocoast, this assumption is not yet supported by hard results from laboratory research. Thus, the fatigue problem can not yet be definitely eliminated.
  - *Exposure to aggressive environment*
    Research after the durability of Elastocoast and the development of its physical and mechanical properties is subject of research by Elastogran.

7.2 Conclusions

The conclusions from detailed analysis in this report are summarized below.

Micro scale instability by wave breaking (erosion)
The applicability of the stability formulas of Hudson, Van der Meer and Pilarczyk to the erosion of an Elastocoast revetment is very limited. Because of the polyurethane bonding, the stability of individual rocks in an Elastocoast cover layer is extremely high when compared to traditional rock based revetments. The physical processes that lie at the base of stability formulas for rock armours are not adequate to describe the stability of individual rocks in an Elastocoast cover layer. Thus, the use of these formulas for prediction of erosion is advised against.

Based on this analysis, together with results from the Dutch pilot studies, erosion is not considered to be a problem for Elastocoast revetments.

Mechanical failure by wave impact
In case of a continuously supported cover layer, the wave load can be schematized as a triangular distributed load and the cover layer itself as an elastically supported bending beam. Material stresses and deflections can then be calculated. From calculations with this model, it is concluded that, in case of proper continuous support, the maximum tension in the bottom of the cover layer will not exceed the bending strength of the material. A lower compression constant of the foundation leads to higher stresses in the cover layer when loaded, but even on a soft clay foundation the maximum tension will not exceed the bending strength.

In case of a cavity under the cover layer, the elastic support can be considered absent in the model over a specified length. It appears that the maximum tension in the bottom of the loaded cover layer increases significantly when a cavity is present. Stresses increase when the cavity size increases, and also when the soil compression constant is lowered. Tensile strength is then easily exceeded, if the thickness of the layer is not sufficient.

With this model the minimum required thickness and/or the maximum accepted cavity size can be determined, in case of (wave) loading perpendicular to the structure's surface.

The influence of clogging on the Hydraulic conductivity of Elastocoast
A calculation method that is developed for prediction of the hydraulic conductivity of granular filters is found to be also applicable to Elastocoast. Clogging of the open structure of Elastocoast strongly reduces its hydraulic conductivity. If the conductivity of the filling material is much smaller than the conductivity of the carrying material (which is the case for Elastocoast filled with sand), the joint hydraulic conductivity can be estimated with $k_v = k_s \cdot n_T$, which is the hydraulic conductivity of the filling material, multiplied by the porosity of the carrying material.

Macro scale instability by dynamic head difference at maximum wave retreat
When the Elastocoast structure retains its high permeability, instability by uplift under maximum wave retreat is not expected. Clogging of the open pore space gives the structure a higher weight but also strongly reduces the hydraulic conductivity. The net effect on stability is negative. Whether clogging can occur, depends on the local conditions and structure build up.

Stability calculations have been done with two different models. The worst case scenario was taken, namely a fully clogged cover layer. From the first model, according to the leakage length theory, it is concluded that the pressure leakage through the clogged cover layer is significant, so that the structure weight already provides a high stability. From the second model, based on structural analysis, it is concluded that the contribution of structure coherence (in this case defined by moment capacity) to stability is greater than that of structure weight. Of the two models, the structural analysis best describes the mechanisms that contribute to the resistance of an Elastocoast revetment against uplift pressures and is therefore considered to be most suitable for use in design tools.

7.3 Recommendations for further research

After the analysis done in this study, some failure mechanisms remain still to be researched. Also, from the models presented in this report, a suggestion can be done where further research into system and structural parameters is useful.

Elimination or quantification of remaining mechanisms
As mentioned above, the failure mechanisms that need further research are:

- Macro scale instability
  - *Uplift by dynamic head difference, at wave impact*
  - *Soil liquefaction under repeated wave impact*
- Material degradation
  - *Fatigue*
  - *Exposure to aggressive environment*

Further research into material (strength) parameters
In the models presented in this report, both for the resistance to breakage as for the resistance against uplift a structural approach appeared to be valid. In a structural approach material parameters such as the stiffness and flexural strength play a key role in the resistance of the cover layer against loads. This means that it is important that representative values for the material parameters and their uncertainties are correctly described.

In this report material parameters were obtained from research at the Delft University of Technology on model beams with a relatively small aggregate size (10-14mm). Further research is necessary to determine whether these values are still representative for prototype size rocks (20-40mm). It is expected that prototype scale beams will show a lower flexural strength, but also a lower stiffness. A lower stiffness will relieve some of the stresses in the material by allowing more deformation.

Effect of clogging on stability
This report shows that the effect of clogging on the hydraulic conductivity of an Elastocoast revetment can be predicted with relatively simple calculations. It remains unclear however, whether clogging can actually be expected to be present during extreme conditions, or if it will be simply flushed out, leaving the cover layer fully permeable again. Calculations with the worst possible scenario, with full clogging showed that the Elastocoast revetment still retains a fairly high stability. Though further research into the clogging behaviour of porous structures is a very interesting topic, it is not necessarily useful in the development of design tools for Elastocoast.

Improvements can be made to the structural model that predicts the resistance of the (clogged) cover layer against uplift pressures. In the structural model for uplift, the effect of leakage through the cover layer on the hydraulic pressure was neglected. In reality, this leakage will be considerable, even through

a fully clogged Elastocoast cover layer. The incorporation of a pressure leakage factor to the structural model will lead to a quick insight of how a certain amount of pressure reduction translates into increase of stability. Then, it can be determined whether further quantification of this factor is profitable.

Further research into loading parameters
The schematization of hydraulic loading has been very straightforward in this report. For instance, the pressures resulting from impacting waves have been derived from a situation of wave impact on a flat, impermeable surface. In reality, the open structure of the Elastocoast revetment will cause a reduction of these pressures. Little knowledge is available of wave impact pressures on open, permeable revetments. Improved insight would lead to more favorable results for the failure mechanism of breakage by wave impact.

Besides, one has to keep in mind that the wave load in the model for mechanical breakage is a stochastic parameter with a certain probability of occurrence. The choice of a normative impact wave height should therefore be the result of probabilistic considerations.

References

- AKZO NOBEL, (2004). Presentation: Dynamic of oscillatory tests. http://www.cs.akzonobel.com/NR/rdonlyres/E163F416-309D-49DE-ACAC-D69DC9174DE6/9246/Dynamicpropertiessept04.ppt. Accessed on: June 23rd, 2008.
- BASF, (2006). Flexible covering protects imperiled dikes. *In: Science around us, a news service provided by BASF*, P 195/06e.
- BIJLSMA, E., ET AL., (2008). Elastocoast pilots in the Netherlands, storm season 2007/2008. *073890088:0.1, ARCADIS, Hoofddorp*.
- BLAAUWENDRAAD, J., (2006). Plate analysis, theory and application, Volume 1, Theory. *Delft University of Technology, Delft*.
- BOSCH, A., AND VAN DER HARN, W., (1998). Twee eeuwen Rijkswaterstaat. *Europese Bibliotheek, Zaltbommel*.
- BOUMA, A.L., (2000). Mechanica van constructies, elasto-statica van slanke structuren. *Delft University Press, Delft*.
- CEM, BURCHARTH, H. F., AND HUGHES, S. A., (2002). Fundamentals of Design, in Coastal Engineering Manual, Part VI-5, Fundamentals of Design.
- CIRIA, CUR, CETMEF, (2007). The Rock Manual. The use of rock in hydraulic engineering (2nd edition). *C683, CIRIA, London*.
- COEVELD, E.M., (2003). Invloed van golfklappen op stabiliteit: literatuurstudie. *H4134, WL | delft hydraulics, Delft*.
- COMCOAST, (2008). Welcome to ComCoast. http://www.comcoast.org. Accessed on: July 22nd, 2008.
- CUR, (1999). Natuurvriendelijke oevers: oeverbeschermingsmaterialen. *CUR 202, CUR-DWW, Gouda*.
- CUR-VB, (1984). Leidraad cementbetonnen dijkbekledingen, *TAW, CUR-VB*.
- D'ANGREMOND, K., AND VAN ROODE, F.C., (2001). Breakwaters and closure dams. Engineering the interface of soil and water 2. *Delft University Press, Delft*.
- DIBBITS, H.A.M.C., (1950). Nederland-Waterland, een historisch-technisch overzicht. *N.V. A. Oosthoek's uitgeversmaatschappij, Utrecht*.
- DORST, C., (2007). Presentation: Stone Pitchings, for the course CT5314 Flood Defences. *Delft Technical University, Delft*.
- DWW, (2006). Databestand DWW vermoeiingsproeven na 1987. http://www.verkeerenwaterstaat.nl/kennisplein/3/4/348681/VA1987.xls, *data from reports: NPC87069/NPC87070//KOAC88035/KOAC88133/NPC91494*.
- ELASTOGRAN, (2006a). Promotional folder: Elastomeric revetment with Elastocoast. *Elastogran GmbH, Lemförde*.
- ELASTOGRAN, (2006b). Technical data sheet Elastcoast 6551/100. Version 01. October 16th, 2006, *Elastogran GmbH, Lemförde*.
- FÜHRBÖTER, I.A., (1994). Wave loads on sea dikes and sea-walls. In: M.B. Abbot, and Price, W.A. (Editor), Coastal Estuarial and Harbour Engineers' Reference Book. *E & FN Spon, London*, pp. 351-367.
- GAJEWSKI, V., (1990). Chemical degradation of polyurethane. http://www.thefreelibrary.com/Chemical%20degradation%20of%20polyurethane-a09000712. Accessed on: May 19th, 2008. *The Free library*.
- GU, D., (2007a). Hydraulic properties of PUR-revetments compared to those of open stone asphalt revetments. MSc Thesis, *Delft University of Technology, Delft*.
- GU, D., (2007b). Some important mechanical properties of Elastocoast for safety investigation of dikes (VTV 2004). Minor Thesis, *Delft University of Technology, Delft*.
- HOLTHUIJSEN, L.H., (2007). Waves in oceanic and coastal waters. *Cambridge University Press, Cambridge*.
- JOHANSON, (2005). Memo: invloed van inslibbing. October 20th, 2005. *K-05-11-38, RWS Directie Zeeland, Projectbureau Zeeweringen, Middelburg*.

- KLEIN BRETELER, M., (2007a). Black box model voor afschuiving bij steenzettingen. *H4635, WL | delft hydraulics*, *Delft*.
- KLEIN BRETELER, M., AND PILARCZYK, K.W., (1998). Chapter 16. Alternative revetments. In: K.W. Pilarczyk (Editor), Dikes and Revetments. *A.A. Balkema*, *Rotterdam*.
- KLEIN BRETELER, M., (2007b). Toplaagstabiliteit gezette steenbekledingen, Symposium "Onderzoek loont!", December 4th, 2007. *Projectbureau Zeeweringen*, *Utrecht*.
- KOLKMAN, P.A., AND JONGELING, T.J., (1996). Dynamisch gedrag van waterbouwkundige constructies, Deel B: constructies in golven. *DWW-RWS*, *Delft*.
- LOCK, M., (2008). Early colonization of littoral communities on polyurethane coated substrates: a field and laboratory study, *ARCADIS*, *Hoofddorp*.
- METRIKINE, A.V., (2006). Dynamics, slender structures and an introduction to continuum mechanics, CT4145 module Dynamics of mechanical systems and slender structures. *Delft University of Technology*, *Delft*.
- MICHEALIS, P., (1997). Stabilization strategies for weatherable PU. http://www.thefreelibrary.com/Stabilization%20strategies%20for%20weatherable%20PU.%20(polyurethanes)-a019393698. Accessed on: May 19th, 2008. *The Free library*.
- OCKELOEN, W.J., (2007). Open filters in breakwaters with a sand core. MSc Thesis, *Delft University of Technology*, *Delft*.
- OERTEL, G., (1985). Polyurethane Handbook. *New York*.
- PASCHE, E., AND EVERTZ, T., (2007). Presentation: Elastomeric Revetments with Elastocoast, Conference on Elastocoast, June 12-13th, 2007, *Holm Gröde*.
- PILARCZYK, K.W., (1990). Coastal Protection, proceedings of the short course on coastal protection. *A.A. Balkema*, *Rotterdam*.
- PROVOOST, Y., (2008). Personal communication: Preliminary results on the overtopping tests at Kattendijke (NL). June 23rd, 2008, *Rotterdam*.
- SCHIERECK, G.J., (2001). Introduction to bed, bank and shore protection. Engineering the interface of soil and water. *Delft University Press*, *Delft*.
- SIMONE, A., (2007). Analysis of slender structures, lecture notes for CT3110. *Delft University of Technology*, *Delft*.
- TAW, (1984). Leidraad voor de toepassing van asfalt in de waterbouw. *TAW, Staatsuitgeverij*, *'s-Gravenhage*.
- TAW, DWW, (2002). Technisch Rapport Asfalt voor Waterkeren. *DWW-2002-121*, *TAW-DWW*, *Delft*.
- TAW, (1988a). Leidraad Keuzemethodiek Dijk- en Oeverbekledingen, Deel I, *TAW*, *Delft*.
- TAW, (1988b). Leidraad Keuzemethodiek Dijk- en Oeverbekledingen, Deel II, *TAW*, *Delft*.
- TAW, DWW, (2003). Technisch Rapport Steenzettingen, Deel Achtergronden. *DWW-2003-097*, *TAW-DWW*, *Delft*.
- VAN DER MEER, J.W., (2002). Technisch Rapport Golfoploop en golfoverslag bij dijken, *TAW-DWW*, *Delft*.
- VAN DER MEER, M.T., (1990). Schadecatalogus voor dijkbekledingen, *RWS-DWW*, *Delft*.
- VERHAGEN, H.J. (2008). Presentation on the course CT5308 Bed, bank and shore protection. *Delft University of Technology, Delft*.
- VERRUIJT, A. (1999). Grondmechanica. *Delft University Press*, *Delft*.
- VNC, (1986). Betonnen bekledingen op dijken en langs kanalen. *VNC*, *'s-Hertogenbosch*.
- VRIJLING, J.K., ET AL., (2000). The structural analysis of the block revetment on the dutch dikes. In: B.L. Edge (Editor), Coastal Engineering 2000 conference proceedings. *ASCE, Sydney, Australia*, pp. 1991-2003.
- VTV, (2007). Voorschrift Toetsen op Veiligheid Primaire Waterkeringen, *Ministerie van Verkeer en Waterstaat, RWS-DWW*, *Delft*.
- VUGREK, D., (2007). Festigkeit Proben Ouwerkerk Petten, *Elastogran GmbH*, *Lemförde*.
- WIKIPEDIA, (2008). Viscoelasticity. http://en.wikipedia.org/wiki/Viscoelastic. Accessed on: June 23rd, 2008.

Appendix I
Prototype pilots in the Netherlands

A detailed report of the Dutch pilot tests with Elastocoast can be found in the following document:

- BIJLSMA, E., ET AL., (2008). Elastocoast pilots in the Netherlands, storm season 2007/2008. *073890088:0.1*, *ARCADIS*, *Hoofddorp*.

Below an abstract and, conclusions from this report are given.

Abstract
In September 2007 two prototype pilot tests were constructed along the Dutch coast with an experimental, polymer based revetment: Elastocoast. An area of 490 m^2 was put on a dike slope in the Eastern-Scheldt basin, and another 385 m^2 on the horizontal surface of a beach groyne near the Pettemer Zeewering along the North-Sea coast.

The revetment consists of polyurethane bonded aggregate. A two-component polyurethane adhesive is added to and mixed with narrow graded mineral aggregate. The mixture is then cast in-situ on the dike surface, where hardening takes place. The individual rocks are fixed together only at their contact points, so that the natural porosity of the aggregate is maintained.

During the storm season of 2007-2008 the two pilot locations were inspected on a regular basis. Damage observations were done visually and material loss out of several control areas was quantified. Though the storm season counted several periods with strong winds and high waves, both pilots survived with only negligible and superficial damage. During the most extreme conditions, the Eastern-Scheldt pilot was persistently subjected to high flow velocities and the most unfavourable form of wave loading on a dike slope, namely plunging and collapsing waves. The pilot along the North-Sea coast was mostly submerged, resulting in attack by strong bed flow velocities, with water containing high concentrations of abrasive material (sand and shell fragments).

With the pilots, the polymer revetment proved able to withstand typical Dutch storm conditions and also valuable experience in constructing with this new material was gained.

Chapter 5 "Conclusions and recommendations" from (Bijlsma, 2008)

<u>**Conclusions from storm analysis**</u>

Pilot location Zuidbout
In the storm season of 2007/2008 six periods were observed in which sustained wind speeds of above 17.2 m/s (8 Bft) were measured. From these periods, two storms with wind blowing from the West were the most extreme, namely the storm of February 2nd and that of March 12th. During both storms a significant wave height of 1.4 m was measured and a peak wave period of around 5 s. During the most extreme conditions, the Elastocoast revetment at the Zuidbout pilot was persistently subjected to high flow velocities and the most unfavourable form of wave loading on a dike slope; namely plunging and collapsing waves.

Pilot location Petten
From the storm season of 2007/2008 only limited data is available due to instrument failure. No data is available for the month of December and beyond February 12th. In the remaining periods five storms were observed in which wind speeds were measured of above 17.2 m/s (8 Bft). Beyond February 12th another two storms occurred, but no data is available from these storms. During the most extreme conditions, the Elastocoast revetment at the Petten pilot was completely submerged the largest part of the time, especially when the highest waves were measured. Therefore there was no direct wave impact loading on the structure during the most extreme conditions. However, when submerged, the Elastocoast structure was persistently subjected to strongly varying near bed flow velocities.

Conclusions from site monitoring

Pilot location Zuidbout

From the results of the monitoring period October 2007 to April 2008 the following conclusions can be drawn:
- Microscopic damage to the Zuidbout Elastocoast revetment after the storms of October 2007 to April 2008 is negligible and of no influence on the structure's performance;
- The polyurethane contact points in between rocks are the weakest parts of the structure;
- There is no abrasion damage to the Zuidbout Elastocoast revetment;
- There is no clotting of the open structure of Elastocoast at the Zuidbout.

Pilot location Petten

From the results of the monitoring period October 2007 to February 2008 the following conclusions can be drawn:
- Microscopic damage to the Petten Elastocoast revetment after the storms of October 2007 to February 2008 is negligible and of no influence on the structure's performance;
- There is only superficial abrasion damage to the Petten Elastocoast revetment;
- There is significant clotting of the open structure of Elastocoast at Petten, due to high amounts of sediment, shells and organic material in the coastal water of the North Sea.

General

From the total of the two Dutch pilot locations the following conclusions can be drawn:
- At neither of the two pilot locations signs of macroscopic failure were observed. This is structure related and on basis of these results no conclusions be drawn whether the Elastocoast system is susceptible to macroscopic failure mechanisms.
- In contrast to the Zuidbout, the Petten pilot showed excessive amounts of sediment and dirt clogging the open structure and weathering its surface. However, this fine abrasive material does not seem to have any influence on the damage development of the Elastocoast structure.
- Although the length of the record is limited, it can be concluded on the basis of visual observations that the damage development rate is not progressive, meaning that initial damage does not initiate the development of larger damage. From the visual observations at the pilot locations, the burn-in scenario seems likely. Under this scenario, the rate of erosion diminishes over time as initially poorly bonded stones are eroded from the revetment.

Lessons that can be learned from the pilots

In general, the Dutch pilots were very successful. Two stretches of good quality were produced and performed well during the tempestuous storm season of 2007/2008. Still, important lessons can be learned to assure the quality and performance in future Elastocoast applications.

With analysis of the monitoring data it became clear that the erosion damage to the 20 cm and 30 cm layers of Elastocoast was significantly higher than that of the 10 cm layer. The reason for this is expected to be the small scale of the production process. With batches of only 0.5 m3 it takes a relatively long time before enough material is dumped for a layer of 20-30 cm thick to be finished and brought to profile. Thus:

The handling time of 20 minutes from the moment of mixing can lead to time shortage when applying thick layers of Elastocoast with small scale production equipment. Consequently, the exceeding of handling time before profiling leads to a decreased bonding strength of the aggregate.

Also, with the construction of the two Dutch pilots the importance of quality monitoring during construction is emphasized:
- The use of moist aggregate as a base material reduces the strength of the Elastocoast significantly; the structure becomes more vulnerable to material loss through erosion and stripping of the polyurethane film from the rocks.

- The tumble-heating of aggregate to reduce moist content has two implications:
  - presence of more fine fragments in the aggregate on the one hand increases the strength of the Elastocoast system, but on the other hand increases polyurethane consumption and produces a 'dirty' looking end product;
  - the high temperature of the aggregate accelerates the curing process of the polyurethane adhesive, resulting in a reduction of the already short handling time. This could be problematic for the application.

Recommendations

From the research and conclusions of this report the following recommendations can be done:
- Further model or prototype research for macroscopic failure mechanisms of a sloping Elastocoast cover layer placed on top a filter layer or directly on a sand bed. Special attention could be given to the clogging of Elastocoast and its influence on macro stability.
- Assurance of quality of the end product can be further improved by development of a standardized on-site quality control system. In this system, for instance, moist content, temperature and processing time should be regularly set to record.

Appendix II
Bending of elastically supported beams under wave load

Breakage by wave impact: Scenario 1

Scenario 1: wave load on continuously supported cover layer
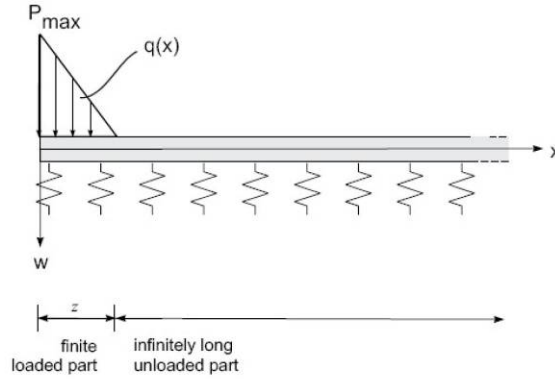
System described by differential equation

$$K \frac{\delta^4 w}{\delta \cdot x^4} + c \cdot w = q(x)$$

with homogeneous counterpart

$$\frac{\delta^4 w}{\delta \cdot x^4} + \beta^4 \cdot w = 0 \qquad \beta^4 = \frac{c}{4K}$$

Part 1: finite, elastically supported bending beam with distributed load

Distributed load

$$q(x) := \frac{P \cdot (z - x)}{z}$$

General solution for situation where displacement approaches zero at infinite distance

displacement

$$w_1(x) := e^{\beta \cdot x} \cdot \left(C_1 \cdot \cos(\beta \cdot x) + C_2 \cdot \sin(\beta \cdot x) \right) + e^{-\beta \cdot x} \left(C_3 \cdot \cos(\beta \cdot x) + C_4 \cdot \sin(\beta \cdot x) \right) + \frac{P \cdot (z - x)}{z \cdot c}$$

rotation

$$\theta_1(x) := \frac{d}{dx} w_1(x)$$

bending moment

$$M_1(x) := K \cdot \left(\frac{d}{dx} \theta_1(x) \right)$$

shear force

$$V_1(x) := \frac{d}{dx} M_1(x)$$

Page 1 of 7

Part 2: semi-infinite, elastically supported bending beam

General solution for situation where displacement approaches zero at infinite distance

displacement $\qquad w_2(x) := e^{-\beta \cdot x}\left(C_7 \cdot \cos(\beta \cdot x) + C_8 \cdot \sin(\beta \cdot x)\right)$

rotation $\qquad \theta_2(x) := \dfrac{d}{dx} w_2(x)$

bending moment $\qquad M_2(x) := K \cdot \left(\dfrac{d}{dx} \theta_2(x)\right)$

shear force $\qquad V_2(x) := \dfrac{d}{dx} M_2(x)$

Solution for two parts combined at x = z

Given

Boundary conditions at x = 0

$$\theta_1(0) = 0$$

$$V_1(0) = 0$$

Transitional conditions at x = z

$$w_1(z) = w_2(z)$$

$$\theta_1(z) = \theta_2(z)$$

$$M_1(z) = M_2(z)$$

$$V_1(z) = V_2(z)$$

Solution

$$\begin{pmatrix} C_1 \\ C_2 \\ C_3 \\ C_4 \\ C_7 \\ C_8 \end{pmatrix} := \text{Find}\left(C_1, C_2, C_3, C_4, C_7, C_8\right)$$

Breakage by wave impact: Scenario 1

$$
\begin{pmatrix} c_1 \\ c_2 \\ c_3 \\ c_4 \\ c_7 \\ c_8 \end{pmatrix} \text{ simplify } \rightarrow
\begin{bmatrix}
\dfrac{e^{-\beta \cdot z} \cdot (P \cdot \cos(\beta \cdot z) - P \cdot \sin(\beta \cdot z))}{4 \cdot \beta \cdot c \cdot z} \\[2ex]
\dfrac{P \cdot e^{-\beta \cdot z} \cdot (\cos(\beta \cdot z) + \sin(\beta \cdot z))}{4 \cdot \beta \cdot c \cdot z} \\[2ex]
\dfrac{P \cdot \left(e^{-\beta \cdot z} \cdot \sin(\beta \cdot z) - e^{-\beta \cdot z} \cdot \cos(\beta \cdot z) + 2\right)}{4 \cdot \beta \cdot c \cdot z} \\[2ex]
\dfrac{P \cdot \left(e^{-\beta \cdot z} \cdot \cos(\beta \cdot z) + e^{-\beta \cdot z} \cdot \sin(\beta \cdot z) - 2\right)}{4 \cdot \beta \cdot c \cdot z} \\[2ex]
\dfrac{P \cdot e^{\beta \cdot z} \cdot \cos(\beta \cdot z) - 2 \cdot P + P \cdot e^{-\beta \cdot z} \cdot \cos(\beta \cdot z) + P \cdot e^{\beta \cdot z} \cdot \sin(\beta \cdot z) - P \cdot e^{-\beta \cdot z} \cdot \sin(\beta \cdot z)}{4 \cdot \beta \cdot c \cdot z} \\[2ex]
\dfrac{P \cdot e^{\beta \cdot z} \cdot \cos(\beta \cdot z) - 2 \cdot P + P \cdot e^{-\beta \cdot z} \cdot \cos(\beta \cdot z) - P \cdot e^{\beta \cdot z} \cdot \sin(\beta \cdot z) + P \cdot e^{-\beta \cdot z} \cdot \sin(\beta \cdot z)}{4 \cdot \beta \cdot c \cdot z}
\end{bmatrix}
$$

Extremes at x = 0

Maximum values are found at $x = 0$

$$M_{max}(P, \beta, z, c) := -K \cdot \left(2 \cdot C_2 \cdot \beta^2 - 2 \cdot C_4 \cdot \beta^2\right)$$

$$w_{max}(P, \beta, z, c) := C_1 + C_3 + \frac{P}{c}$$

Maximum tensile stress at $x = 0$

$$W := \frac{1}{6} \cdot h^2$$

$$\sigma_{max}(M_{max}, h) := \frac{M_{max}(P, \beta, z, c)}{W} \rightarrow \frac{6 \cdot M_{max}(P, \beta, z, c)}{h^2}$$

$$\sigma_{max}(P, \beta, z, h, c) := \frac{6}{h^2} \cdot M_{max}(P, \beta, z, c)$$

Page 3 of 7

Breakage by wave impact: Scenario 1

Loading parameters

$H_{max} := 0m, 0.5m .. 6m$

$\rho_w := 1025 \dfrac{kg}{m^3}$ $\qquad$ $q := 4.0$ $\qquad$ $g := 9.81 \dfrac{m}{s^2}$

$P_{indicatie}(H_{max}) := \rho_w \cdot g \cdot q \cdot H_{max}$

$P_{indicatie}(1m) = 0.04 \cdot MPa$

$z(H_{max}) := \dfrac{1}{2} \cdot H_{max}$

Relation wave height and schematized load
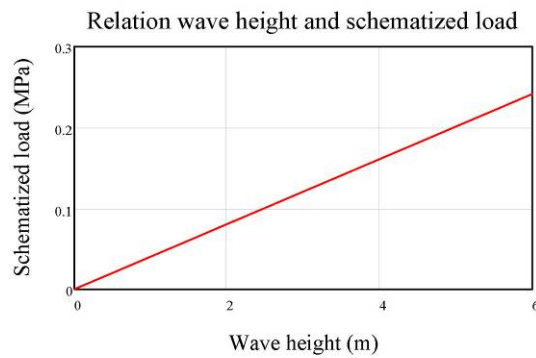
Strength and material parameters

$E := 2500 MPa$ — Bending stiffness of cover layer (2500-3000MPa for Elastocoast)

$c := 100 \dfrac{MPa}{m}$ — Compression coefficient for subsoil (100 MPa/m for sand)

$v := 0.35$ — Poisson ratio (assumption)

$h \rightarrow h$ — Thickness of cover layer

Definitions

$K(h) := \dfrac{E \cdot h^3}{12 \cdot \left(1 - v^2\right)}$ — Stiffness for a thin plate

$\beta(h, c) := \sqrt[4]{\dfrac{c}{4 \, K(h)}}$ — Parameter used for differential equation

$W(h) := \dfrac{1}{6} \cdot h^2$ — Shape parameter ("weerstandsmoment" per m)

Page 4 of 7

116

Breakage by wave impact: Scenario 1

Maximum tensile stress on sand foundation [c=100MPa/m]

Maximum displacement on sand foundation [c=100MPa/m]

Page 5 of 7

Breakage by wave impact: Scenario 1

Maximum tensile stress on clay foundation [c=30MPa/m]

Maximum displacement on clay foundation [c=30MPa/m]

Page 6 of 7

Breakage by wave impact: Scenario 1

Displacement with H=4m, Pmax=0.16MPa, h=0.20m and c=30MPa/m

x (m)
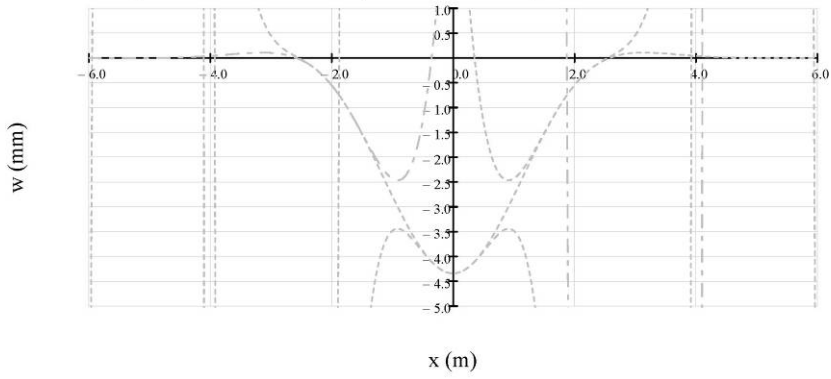
Bending moment with H=4m, Pmax=0.16MPa, h=0.20m and c=30MPa/m

x (m)
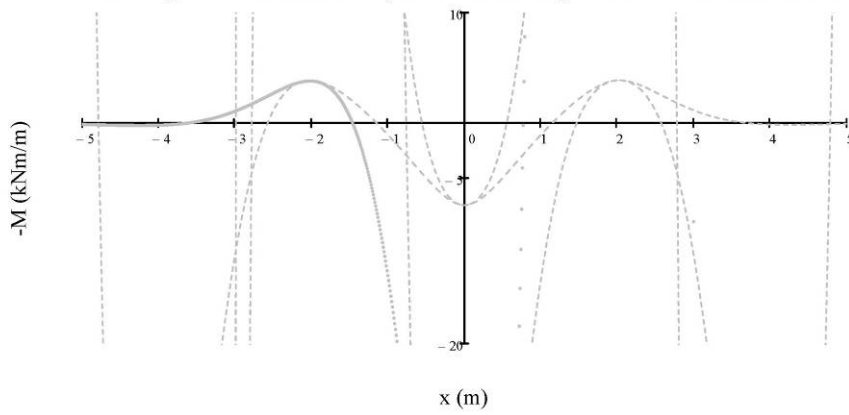
Scenario 2: wave load on partly unsupported cover layer
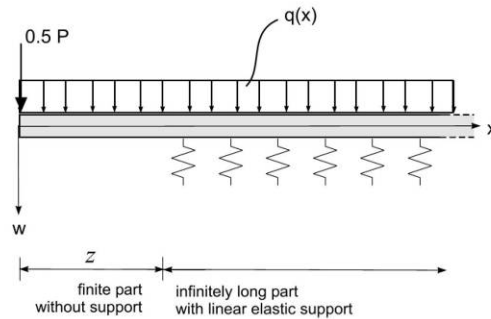
Part 1: finite, elastically unsupported bending beam with distributed load

System described by differential equation

$$K \frac{\delta^4 w}{\delta \cdot x^4} = q(x)$$

Distributed load

$$q(x) := \rho_{ec} \cdot g \cdot h$$

General solution for situation where displacement approaches zero at infinite distance

displacement

$$w_1(x) := \frac{-1}{K} \cdot \left[\frac{-1}{24} \cdot (\rho_{ec} \cdot g \cdot h) \cdot x^4 + \frac{1}{6} C_1 \cdot x^3 + \frac{1}{2} C_2 x^2 + C_3 \cdot x + C_4 \right]$$

rotation

$$\theta_1(x) := \frac{d}{dx} w_1(x)$$

bending moment

$$M_1(x) := K \cdot \left(\frac{d}{dx} \theta_1(x) \right)$$

shear force

$$V_1(x) := \frac{d}{dx} M_1(x)$$

Breakage by wave impact: scenario 2

Part 2: semi-infinite, elastically supported bending beam with distributed load

$$K_2 \frac{\delta^4 w}{\delta \cdot x^4} + c \cdot w = q(x) \qquad \text{with homogeneous counterpart} \qquad \frac{\delta^4 w}{\delta \cdot x^4} + \beta^4 \cdot w = 0 \qquad \beta^4 = \frac{c}{4K_2}$$

General solution for situation where displacement approaches zero at infinite distance

displacement $\qquad w_2(x) := e^{-\beta \cdot x} \left(C_7 \cdot \cos(\beta \cdot x) + C_8 \cdot \sin(\beta \cdot x) \right) + \frac{\rho_{ec} \cdot g \cdot h}{c}$

rotation $\qquad \theta_2(x) := \frac{d}{dx} w_2(x)$

bending moment $\qquad M_2(x) := K_2 \cdot \left(\frac{d}{dx} \theta_2(x) \right)$

shear force $\qquad V_2(x) := \frac{d}{dx} M_2(x)$

Solution for two parts combined at x = z

Given

Boundary conditions at x = 0

$$\theta_1(0) = 0$$

$$V_1(0) = \frac{-1}{2} P$$

Transitional conditions at x = z

$$w_1(z) = w_2(z)$$

$$\theta_1(z) = \theta_2(z)$$

$$M_1(z) = M_2(z)$$

$$V_1(z) = V_2(z)$$

Solution $\qquad \begin{pmatrix} C_1 \\ C_2 \\ C_3 \\ C_4 \\ C_7 \\ C_8 \end{pmatrix} := \text{Find}(C_1, C_2, C_3, C_4, C_7, C_8)$

Page 2 of 8

Breakage by wave impact: scenario 2

C_1 simplify $\rightarrow \dfrac{P}{2}$

C_2 simplify $\rightarrow \dfrac{24 \cdot K \cdot g \cdot h \cdot \rho_{gc} \cdot \beta^3 \cdot z^2 + 24 \cdot K \cdot P \cdot \beta^3 \cdot z + 24 \cdot K \cdot g \cdot h \cdot \rho_{gc} \cdot \beta^3 \cdot z + 12 \cdot K \cdot P \cdot \beta^3 + 2 \cdot c \cdot g \cdot h \cdot \rho_{gc} \cdot z^3 + 3 \cdot P \cdot c \cdot z^2}{12 \cdot \left(4 \cdot K \cdot \beta^3 + c \cdot z\right)}$

C_3 simplify $\rightarrow 0$

C_4 simplify $\rightarrow \dfrac{96 \cdot g \cdot h \cdot \rho_{gc} \cdot K^2 \cdot \beta^4 + 48 \cdot P \cdot K^2 \cdot \beta^4 + 96 \cdot g \cdot h \cdot \rho_{gc} \cdot K^2 \cdot \beta^3 + 20 \cdot g \cdot h \cdot \rho_{gc} \cdot K^2 \cdot \beta^3 \cdot c \cdot z + 16 \cdot P \cdot K \cdot \beta^3 \cdot c \cdot z + 40 \cdot g \cdot h \cdot \rho_{gc} \cdot K \cdot \beta^3 \cdot c \cdot z + 24 \cdot P \cdot K \cdot \beta^3 \cdot c \cdot z + 48 \cdot g \cdot h \cdot \rho_{gc} \cdot K \cdot \beta \cdot c \cdot z^2 + 24 \cdot g \cdot h \cdot \rho_{gc} \cdot K \cdot \beta \cdot c \cdot z^2 + 24 \cdot P \cdot K \cdot \beta \cdot c \cdot z^2 + 2 \cdot g \cdot h \cdot \rho_{gc} \cdot c^2 \cdot z^4 + P \cdot c^2 \cdot z^4}{24 \cdot c \cdot \left(4 \cdot K \cdot \beta^3 + c \cdot z\right)}$

C_7 simplify $\rightarrow \dfrac{12 \cdot K \cdot P \cdot \beta^4 \cdot \cos(\beta \cdot z) - 12 \cdot K \cdot P \cdot \beta^4 \cdot \sin(\beta \cdot z) + 3 \cdot P \cdot \beta^2 \cdot c \cdot z^2 \cdot \cos(\beta \cdot z) + 3 \cdot P \cdot \beta^2 \cdot c \cdot z^2 \cdot \sin(\beta \cdot z) + 6 \cdot P \cdot \beta \cdot c \cdot z \cdot \cos(\beta \cdot z) + 12 \cdot \beta \cdot c \cdot h \cdot \rho_{gc} \cdot z \cdot \sin(\beta \cdot z) + 12 \cdot \beta \cdot c \cdot g \cdot h \cdot \rho_{gc} \cdot z^2 \cdot \cos(\beta \cdot z) - 24 \cdot K \cdot \beta^4 \cdot g \cdot h \cdot \rho_{gc} \cdot z^2 \cdot \sin(\beta \cdot z) + 12 \cdot \beta \cdot c \cdot g \cdot h \cdot \rho_{gc} \cdot z^2 \cdot \cos(\beta \cdot z) + 4 \cdot \beta^3 \cdot c \cdot g \cdot h \cdot \rho_{gc} \cdot z^3 \cdot \cos(\beta \cdot z) + 4 \cdot \beta^3 \cdot c \cdot g \cdot h \cdot \rho_{gc} \cdot z^3 \cdot \sin(\beta \cdot z)}{6 \cdot c^2 \cdot z \cdot e^{-\beta z} + 24 \cdot K \cdot \beta^3 \cdot c \cdot e^{-\beta z}}$

C_8 simplify $\rightarrow \dfrac{12 \cdot K \cdot P \cdot \beta^4 \cdot \cos(\beta \cdot z) + 12 \cdot K \cdot P \cdot \beta^4 \cdot \sin(\beta \cdot z) - 3 \cdot P \cdot \beta^2 \cdot c \cdot z^2 \cdot \cos(\beta \cdot z) + 3 \cdot P \cdot \beta^2 \cdot c \cdot z^2 \cdot \sin(\beta \cdot z) + 6 \cdot P \cdot \beta \cdot c \cdot z \cdot \sin(\beta \cdot z) - 3 \cdot P \cdot \beta^2 \cdot c \cdot z^2 \cdot \cos(\beta \cdot z) + 12 \cdot \beta \cdot c \cdot g \cdot h \cdot \rho_{gc} \cdot z \cdot \sin(\beta \cdot z) + 12 \cdot \beta \cdot c \cdot g \cdot h \cdot \rho_{gc} \cdot z^2 \cdot \cos(\beta \cdot z) + 24 \cdot K \cdot \beta^4 \cdot g \cdot h \cdot \rho_{gc} \cdot z^2 \cdot \sin(\beta \cdot z) - 4 \cdot \beta^3 \cdot c \cdot g \cdot h \cdot \rho_{gc} \cdot z^3 \cdot \cos(\beta \cdot z) + 4 \cdot \beta^3 \cdot c \cdot g \cdot h \cdot \rho_{gc} \cdot z^3 \cdot \sin(\beta \cdot z)}{6 \cdot c^2 \cdot z \cdot e^{-\beta z} + 24 \cdot K \cdot \beta^3 \cdot c \cdot e^{-\beta z}}$

Page 3 of 8

Breakage by wave impact: scenario 2

Extremes at x = 0

Maximum values are found at x = 0

$$M_{max}(P, h, K, \beta, z, c, \rho_{ec}) := C_2$$

$$w_{max}(P, \beta, z, h, \rho_{ec}, c, K) := \frac{-C_4}{K}$$

Maximum tensile stress at x = 0

$$W(h) := \frac{1}{6} \cdot h^2$$

$$\sigma_{max}(M_{max}) := \frac{M_{max}(P, h, K, \beta, z, c)}{W(h)}$$

$$\sigma_{max}(P, \beta, z, h, K, c, \rho_{ec}) := \frac{6}{h^2} \cdot M_{max}(P, h, K, \beta, z, c, \rho_{ec})$$

Loading parameters

$$H_{max} := 0m, 0.5m .. 5m \qquad\qquad \rho_w := 1025 \frac{kg}{m^3} \qquad\qquad q := 2.3$$

$$P_{indicatie}(H_{max}) := \rho_w \cdot g \cdot q \cdot H_{max} \cdot 0.4 H_{max}$$

$$P_{indicatie}(4m) = 147.963 \cdot \frac{kN}{m}$$

Relation wave height and schematized load

Schematized load (kN/m) vs Wave height (m)
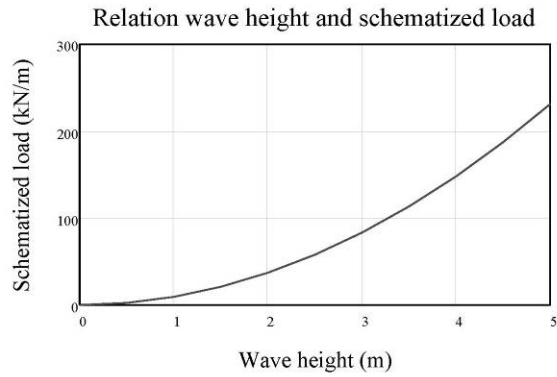
Breakage by wave impact: scenario 2

Strength parameters

$E := 2500 \, \text{MPa}$ — Bending stiffness of cover layer (2500-3000MPa for Elastocoast)

$c := 100 \dfrac{\text{MPa}}{\text{m}}$ — Compression coefficient for subsoil (100 MPa/m for sand)

$v := 0.35$ — Poisson ratio (assumption)

$\rho_{ec} := 1350 \dfrac{\text{kg}}{\text{m}^3}$ — Bulk specific weight of Elastocoast

$h \rightarrow h$ — Thickness of cover layer

Definitions

$K(h) := \dfrac{E \cdot h^3}{12 \cdot \left(1 - v^2\right)}$ — Stiffness for a thin plate

$\beta(h, c) := \sqrt[4]{\dfrac{c}{4 \, K(h)}}$ — Parameter used for differential equation

$W(h) := \dfrac{1}{6} \cdot h^2$ — Shape parameter ("weerstandsmoment" per m)

Breakage by wave impact: scenario 2

Maximum tensile stress on sand foundation [c=100MPa/m]

Maximum displacement on sand foundation [c=100MPa/m]

Breakage by wave impact: scenario 2

Maximum tensile stress on clay foundation [c=30MPa/m]

Maximum displacement on clay foundation [c=30MPa/m]

Breakage by wave impact: scenario 2

Displacement with H=4, P=148kN/m, h=0.20m, z=1m and c=100MPa/m

Bending moment with H=4m, P=148kN/m h=0.20m, z=0m, c=30MPa/m

Page 8 of 8
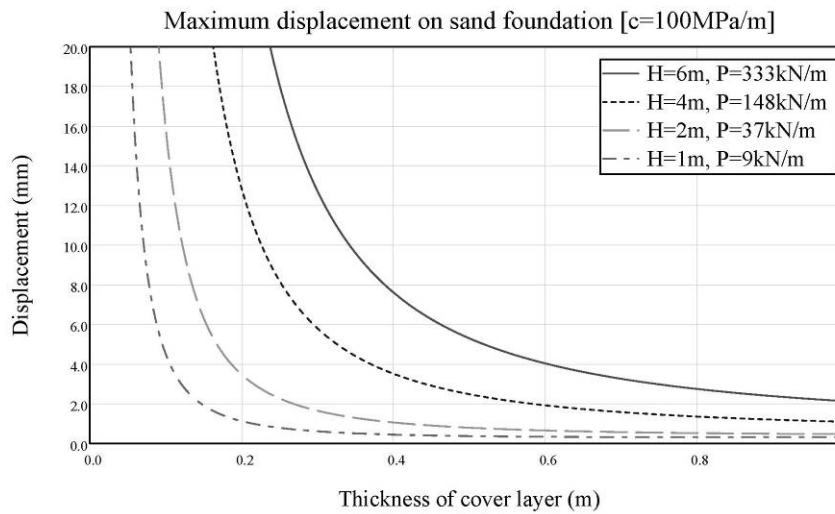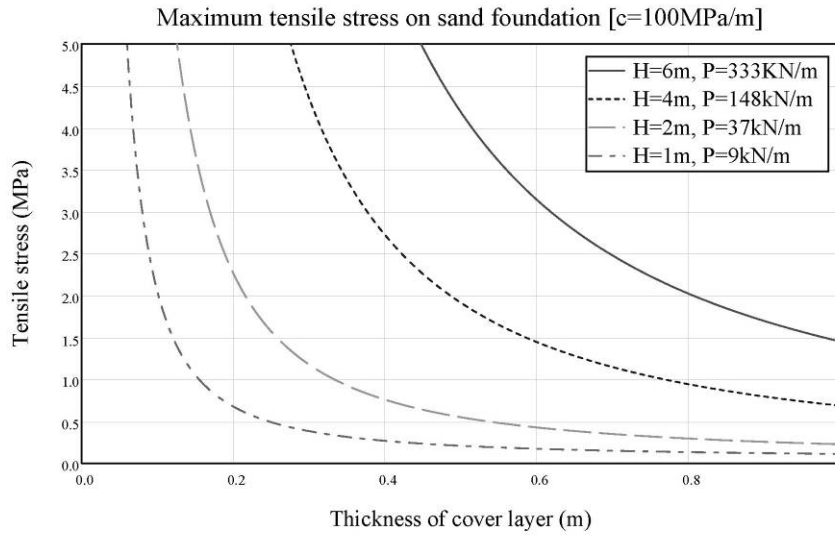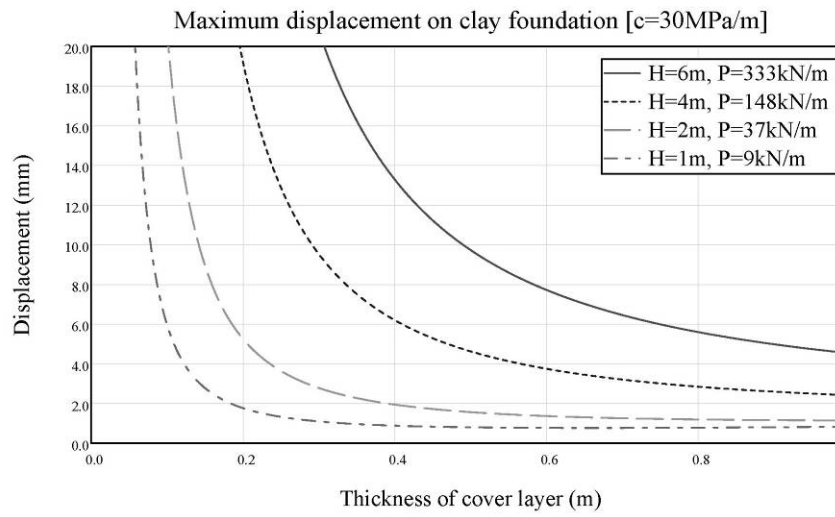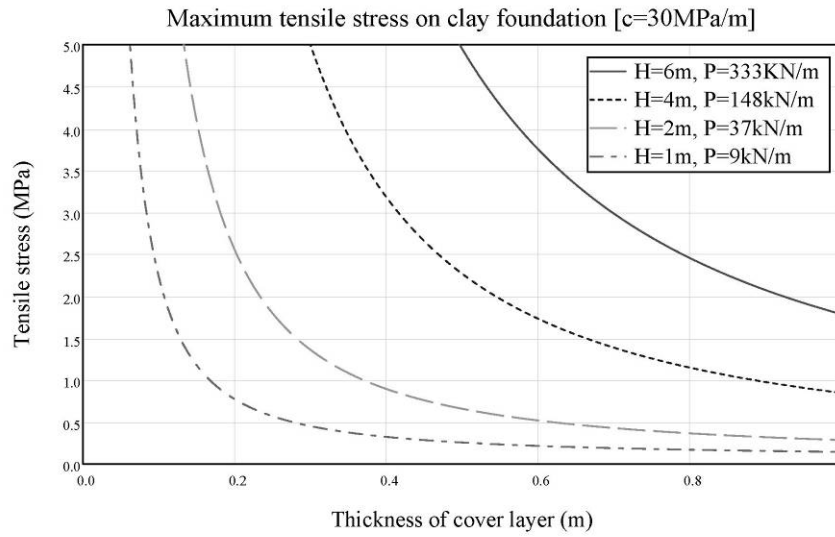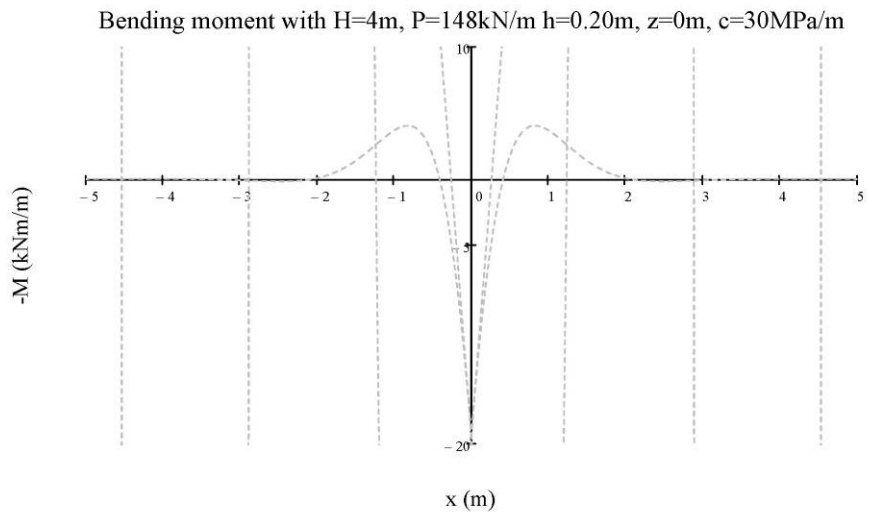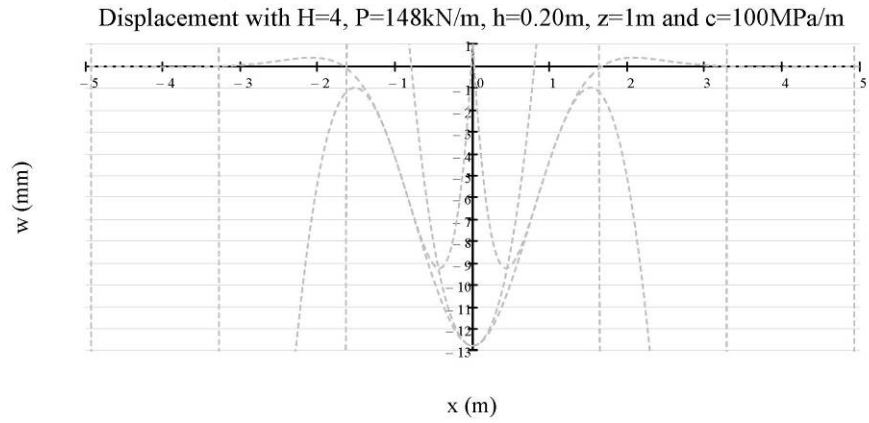
```
> restart;
```

Breakage by wave impact: enhanced model

Beam stiffness and shape property.

```
> W:=1/6*h^2;
```

$$W := \frac{1}{6} h^2 \qquad (1)$$
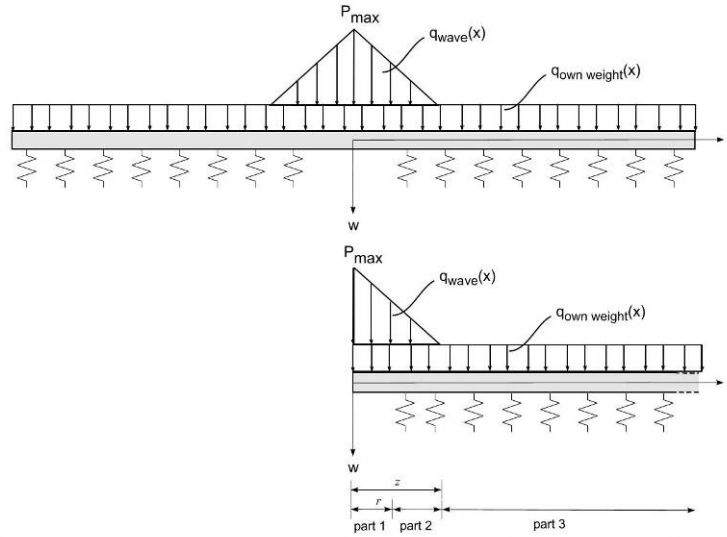
Part 1: Finite, unsupported beam loaded by triangular waveload and own weight

```
> Q1:=rho*g*h+Pmax*(z-x)/z;
```

$$Q1 := \rho\, g\, h + \frac{Pmax\,(z-x)}{z} \qquad (2)$$

```
> w1:=(rho*g*h*x^4)/(24*K)+(Pmax*x^4)/(24*K)-(Pmax*x^5)/(120*K*z)+
  (C1*x^3)/6+(C2*x^2)/2+C3*x+C4;
  theta1:=-diff(w1,x):
  M1:=K*diff(theta1,x):
  V1:=diff(M1,x):
```

$$w1 := \frac{1}{24}\frac{\rho\, g\, h\, x^4}{K} + \frac{1}{24}\frac{Pmax\, x^4}{K} - \frac{1}{120}\frac{Pmax\, x^5}{K z} + \frac{1}{6}C1\, x^3 + \frac{1}{2}C2\, x^2 + C3\, x + C4 \qquad (3)$$

Part 2: Finite, elastically supported beam loaded by triangular waveload and own weight.

```
> Q2:=rho*g*h+Pmax*(z-(x+r))/z;
```

$$Q2 := \rho\, g\, h + \frac{Pmax\,(z-x-r)}{z} \qquad (4)$$

```
> w2:=exp(beta*x)*(C5*cos(beta*x)+C6*sin(beta*x))+exp(-beta*x)*(C7*
```

Page 1 of 4

```
    cos(beta*x)+C8*sin(beta*x))+Q2/c;
    theta2:=-diff(w2,x):
    M2:=K*diff(theta2,x):
    V2:=diff(M2,x):
```

$$w2 := e^{\beta x} \left(C5 \cos(\beta x) + C6 \sin(\beta x) \right) + e^{-\beta x} \left(C7 \cos(\beta x) + C8 \sin(\beta x) \right) \tag{5}$$

$$+ \frac{\rho\, g\, h + \dfrac{Pmax\,(z-x-r)}{z}}{c}$$

Part 2: Semi-infinite, elastically supported beam loaded own weight.

```
> Q3 := rho*g*h;
```

$$Q3 := \rho\, g\, h \tag{6}$$

```
> w3:=exp(-beta*x)*(C11*cos(beta*x)+C12*sin(beta*x))+Q3/c;
    theta3:=-diff(w3,x):
    M3:=K*diff(theta3,x):
    V3:=diff(M3,x):
```

$$w3 := e^{-\beta x} \left(C11 \cos(\beta x) + C12 \sin(\beta x) \right) + \frac{\rho\, g\, h}{c} \tag{7}$$

Boundary conditions at x=0.

```
> x:=0:
    eq1:=theta1=0:
    eq2:=V1=0:
```

Transitional conditions between part 1 and part 2 at x=r.

```
> x:=r:
    eq3:=w1=w2:
    eq4:=theta1=theta2:
    eq5:=M1=M2:
    eq6:=V1=V2:
```

Transitional conditions between parts 2 and 3 at x=z.

```
> x:=z:
    eq7:=w2=w3:
    eq8:=theta2=theta3:
    eq9:=M2=M3:
    eq10:=V2=V3:
```

Bending moment, deflection, stress in x=0.

```
> x:=0;
    Mmax:=simplify(M1);
    wmax:=simplify(w1);
    sigma:=Mmax/W;
```

$$x := 0$$

$$Mmax := -K\, C2$$

$$wmax := C4$$

$$\sigma := -\frac{6\,K\,C2}{h^2} \tag{8}$$

Solution to the integration constants.

```
> solution:=solve({eq1,eq2,eq3,eq4,eq5,eq6,eq7,eq8,eq9,eq10},{C1,C2,
  C3,C4,C5,C6,C7,C8,C11,C12}):assign(solution);
```

Parameters.

```
> r:=1; Half span width of cavity (m)
  H:=4; Wave height (m)
  rho_water:=1025: Density of water (kg/m3)
  g:=9.81: Gravitational acceleration (m/s2)
  q:=4: Empirical wave impact factor (-)
  Pmax:=rho_water*g*q*H; Maximum wave impact pressure (N/m2)
  z:=1/2*H; Half base width of triangular load (m)
  c:=100*10^6: Soil compression constant (N/m2/m)
  v:=0.35: Poisson's constant (-)
  E:=2500*10^6: Stiffness of cover layer (N/m2)
  rho:= 1350: Density of cover layer (kg/m3)
  h:=0.2: Thickness of cover layer (m)
  beta:=root[4]((3*c*(1-v^2))/(E*h^3)); Calculation parameter
  K:=(E*h^3)/(12*(1-v^2)); Stiffness of beam element
```

$$r := 1$$

$$H := 4$$

$$Pmax := 1.6088400\,10^5$$

$$z := 2$$

$$\beta := 1.904735149$$

$$K := 1.899335233\,10^6 \tag{9}$$

Extreme values at x=0 (in kNm/m, MPa, and mm).

```
> Mmax/(10^3);
  sigma/(10^6);
  wmax*(10^3);
```

$$50.72513273$$

$$7.608769908$$

$$15.91060854 \tag{10}$$

Deflection:

```
> x:='x':with(plots):
  F:=plot(-w1,x=0..r):
  G:=plot(-w2,x=r..z):
  H:=plot(-w3,x=z..z+4):
```

```
w4:=subs(x=-x,w1):
w5:=subs(x=-x,w2):
w6:=subs(x=-x,w3):
J:=plot(-w4,x=-r..0):
K:=plot(-w5,x=-z..-r):
L:=plot(-w6,x=-z-4..-z):
display({F,G,H,J,K,L});
```
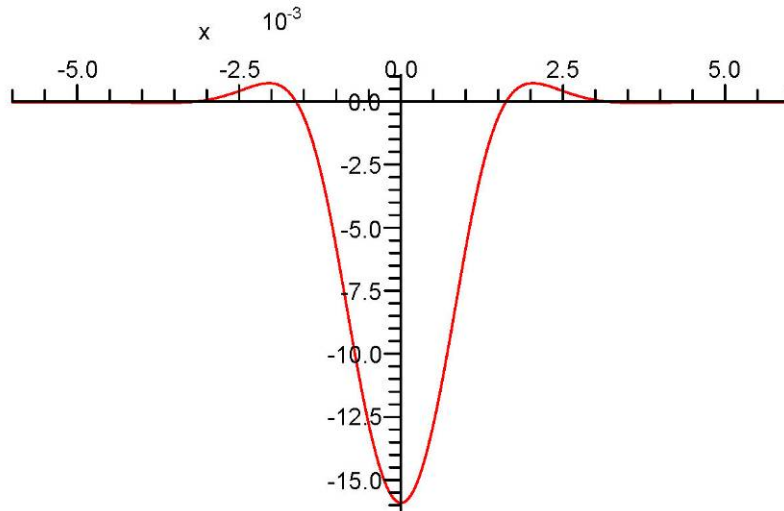
Appendix III
Hydraulic conductivity of
Elastocoast

In 2007, Gu performed laboratory tests on Elastocoast samples to determine the hydraulic conductivity (in his study referred to as permeability).

The grading width of *Big Yellow Sun* used in Gu's research was used in another project as well. For the grading width was referred to the report of that project (Ockeloen, 2007). The grading width of *Big Yellow Sun* is given in the graph below (Gu, 2007). From this graph it can be determined that D_{15}=22.5 mm.
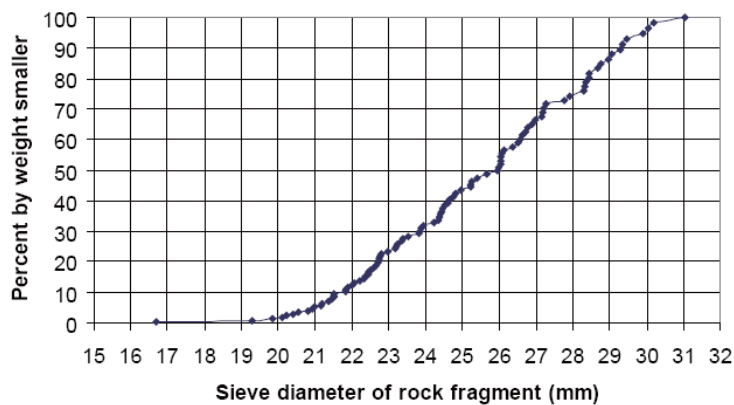
Figure III.1 Grading of the Big Yellow Sun rocks

Normally, the permeability test is carried out under a constant water pressure and then the volume of water passing through the specimen is measured to fill in the formula:

$$k = \frac{ql}{AH}$$

In which:
k = permeability coefficient
q = water discharge
l = flow path, namely the thickness of specimen
A = the cross section area of flow
H = water head, namely the difference of the water pressure

Then the permeability coefficient can be calculated, the unit is cm/s or m/day. In his study, the calculation of permeability coefficient was simplified to be 'k=q/A' for the convenience of comparisons among different specimens. The results from Gu are given in the following figure.

Water head (m)	Permeability of 10 cm (m/s)	Permeability of 20 cm (m/s)	Permeability of 30 cm (m/s)
0	0	0	0
1	0.341	0.272	0.292
2	0.476	0.376	0.406
3	0.582	0.501	0.497
Water head (m)	Calibration of 10 cm (m/s)	Calibration of 20 cm (m/s)	Calibration of 30 cm (m/s)
0	0	0	0
1	0.366	0.261	0.275
2	0.529	0.370	0.407
3	0.616	0.502	0.510

Figure III.2 Results for the permeability of Big Yellow Sun specimens (Gu, 2007).

In order to find the correct values for the hydraulic conductivity k, therefore the results from Gu should be multiplied by l/H, which is the same as dividing by the hydraulic gradient i. By doing so, the following values are found:

Table III.I Hydraulic conductivity of Big Yellow Sun, based on Gu's experiments.

Hydraulic head H (m)	Thickness of specimen l (m)	Hydraulic gradient i (-)	Permeability found by Gu k (m/s)	Hydraulic conductivity k (m/s)
1	0.1	10	0.341	0.0341
2	0.1	20	0.476	0.0238
3	0.1	30	0.582	0.0194
1	0.2	5	0.272	0.0544
2	0.2	10	0.376	0.0376
3	0.2	15	0.501	0.0334
1	0.3	3.33	0.292	0.0876
2	0.3	6.66	0.406	0.0609
3	0.3	10	0.497	0.0497
1	0.1	10	0.366	0.0366
2	0.1	20	0.529	0.0265
3	0.1	30	0.616	0.0205
1	0.2	5	0.261	0.0522
2	0.2	10	0.37	0.0370
3	0.2	15	0.502	0.0335
1	0.3	3.33	0.275	0.0825
2	0.3	6.66	0.407	0.0611
3	0.3	10	0.51	0.0510

In this study the values in the last column of the table above are used for calculations.

Appendix IV
Uplift pressures on a clogged structure

Scenario 1: clogged Elastocoast placed directly on sand bed

Material properties

Elastocoast 20-40mm

Porosity $\quad n_{ec} := 0.5$

Fine grading $\quad D_{15.e^{\wedge}} := 21mm$

Specific mass $\quad \rho_{ec} := 2720 \frac{kg}{3}$

Bulk mass $\quad \rho_{ec.bulk} := n_{ec} \cdot \rho_{ec} = 1.36 \times 10^3 \frac{kg}{m^3}$

Granular filter: sand

Hydraulic conductivity $\quad k_f := 0.0001 \frac{m}{s}$

Filling material: sand

Hydraulic conductivity $\quad k_s := 0.0001 \frac{m}{s}$

Bulk mass $\quad \rho_s := 1600 \frac{kg}{m^3}$

Hydraulic conductivity of Elastocoast

Forchheimer Theory: $\quad i := a_f \cdot q + b_f \cdot q^2$

Linearized form with Darcy's Law:

$$k := \frac{-a_f + \sqrt{a_f^2 + 4b_f i}}{2b_f i}$$

Gradient: $\quad i := 5$

Gravitational acceleration: $\quad g := 9.8 \frac{m}{s^2}$

Kinematic viscosity: $\quad \nu := 1.2 \cdot 10^{-6} \frac{m^2}{s}$

Grain diameter: $\quad D_{15} := 1mm, 2mm .. 100mm$

Uplift pressure: scenario 1

Linear coefficient of resistance: $\quad a_f(D_{15}, n) := 160 \cdot \dfrac{\nu}{g} \cdot \dfrac{(1-n)^2}{n^3 D_{15}^2}$

Turbulent coefficient of resistance: $\quad b_f(D_{15}, n) := \dfrac{2.2}{g \cdot n^2 D_{15}}$

Hydraulic conductivity of a granular layer:

$$k(D_{15}, i, n) := \dfrac{-a_f(D_{15}, n) + \sqrt{a_f(D_{15}, n)^2 + 4\, b_f(D_{15}, n) i}}{2\, b_f(D_{15}, n) i}$$
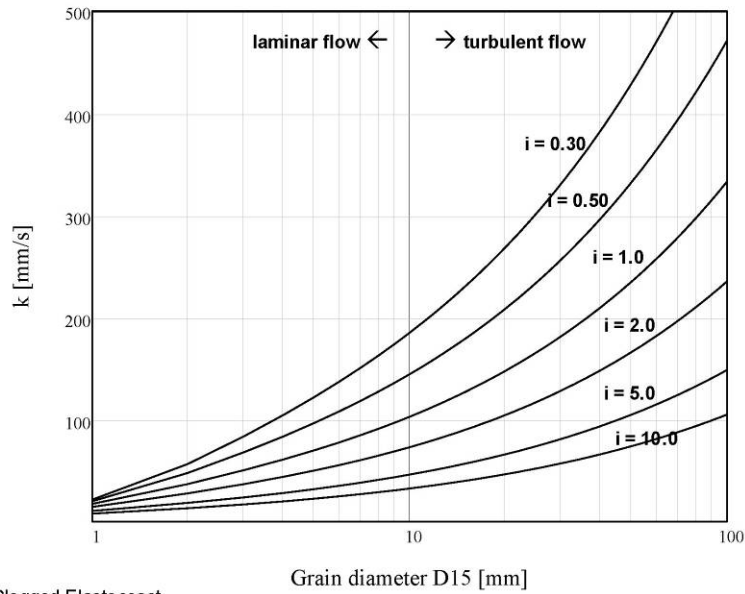
Clogged Elastocoast

$$k_{ec} := k(D_{15.ec}, i, n_{ec}) = 0.068 \, \dfrac{m}{s}$$

$$k_v := \dfrac{k_{ec} \cdot k_s \cdot n_{ec}}{k_{ec} + k_s \cdot n_{ec}} = 4.996 \times 10^{-5} \, \dfrac{m}{s}$$

$$\rho_v := (1 - n_{ec}) \cdot \rho_{ec} + n_{ec} \cdot \rho_s = 2.16 \times 10^3 \, \dfrac{kg}{m^3}$$

Leakage length

$$\Lambda(d_{ec}, d_f) := \sqrt{\dfrac{k_f \cdot d_f \cdot d_{ec}}{k_v}} \qquad\qquad \Lambda(0.2, 2) = 0.895$$

Page 2 of 4

138

Uplift pressure: scenario 1

Hydraulic head under maximum wave retreat

Schematization in the form of a curved wave front:
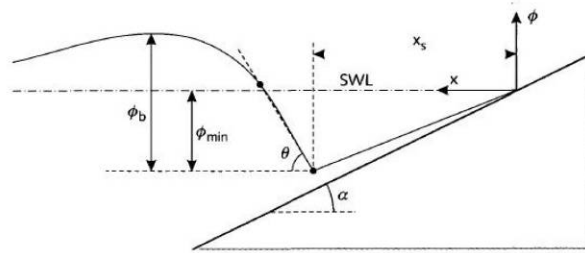
$H_s := 2.0\,m$ $\qquad$ $T_p := 4.5\,s$ $\qquad$ $L_{0p} := \dfrac{g \cdot T_p^{\,2}}{2 \cdot \pi} = 31.584\,m$

$\alpha := atan\left(\dfrac{1}{3}\right)$ $\qquad\qquad$ $\xi_{0p} := \dfrac{tan(\alpha)}{\sqrt{\dfrac{H_s}{L_{0p}}}} = 1.325$

$\rho_w := 1025\,\dfrac{kg}{m^3}$

$\gamma_{\phi b} := 1.0$ $\qquad$ $\gamma_{\phi min} := 1.0$ $\qquad$ $\gamma_x := 1.0$

Significant load:
$$\phi_{b.s} := min\left[0.22 \cdot \frac{\gamma_{\phi b} \cdot \xi_{0p}}{(tan(\alpha))^{0.75}}, 2.0 \cdot \gamma_{\phi b}\right] \cdot H_s = 1.329\,m$$

Slope of wave front:
$$\theta_s := atan\left[\frac{1.5}{\left(\dfrac{1}{3}\right)}\right] = 53.79 \cdot deg$$

Minimum head on bank:
$$\phi_{min.s} := max\left[-0.13 \cdot \gamma_{\phi min} \cdot \left(\frac{\xi_{0p}}{\sqrt{tan(\alpha)}}\right)^{1.25}, \frac{-2.0 \cdot \gamma_{\phi min}}{1 + \dfrac{0.9}{\sqrt{\xi_{0p}}}}\right] \cdot H_s$$

Location of minimum head on bank: $x_s := min\left[\gamma_x \cdot \left(0.4 + 0.16 \cdot \dfrac{\xi_{0p}}{tan(\alpha)^{1.5}}\right), 1.5 \cdot \dfrac{\gamma_x}{tan(\alpha)}\right] \cdot H_s = 3.003\,m$

Level of freatic line above toe of wave front $z_f := \phi_{b.s} = 1.329\,m$

Uplift pressure: scenario 1

Maximum head difference:

$$c := \frac{\tan\left(\theta_s\right) \cdot \cos(\alpha)}{3 \cdot \phi_{b.s} + 2.4 \cdot \phi_{min.s}}$$

$$\phi_{w.s}\left(d_{ec}, d_f\right) := \Lambda\left(d_{ec}, d_f\right) \frac{1}{2} \cdot \left[\frac{-c \cdot \phi_{min.s}}{1 + c \cdot \Lambda\left(d_{ec}, d_f\right)} + \frac{\tan\left(\theta_s\right) \cdot \cos(\alpha)}{\left(1 + c \cdot \Lambda\left(d_{ec}, d_f\right)\right)^2} + \sin(\alpha) \right] \cdot \left(1 - \exp\left(\frac{-2 \cdot z_f}{\Lambda\left(d_{ec}, d_f\right) \cdot \sin(\alpha)}\right) \right)$$

Clogged Elastocoast on a 2m thick sand filter

Legend:
— Uplift pressure
---- Weight of top layer

Thickness of top layer (m)

Page 4 of 4
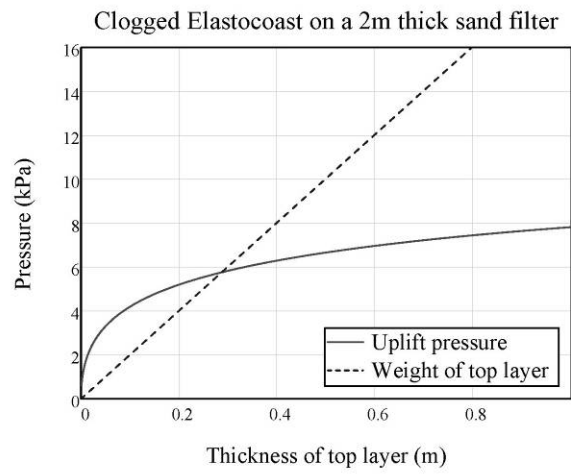
Uplift pressure: scenario 2

Scenario 2: clogged Elastocoast on top of a granular filter

Granular filter

Hydraulic conductivity $\qquad k_f := 0.05 \dfrac{m}{s}$

Thickness of filter layer $\qquad d_f := 0.2m$

Leakage length

$$\Lambda\left(d_{ec}, d_f\right) := \sqrt{\frac{k_f \cdot d_f \cdot d_{ec}}{k_v}} \qquad\qquad \Lambda(0.2, 0.2) = 6.327$$

Maximum head difference:

$$c := \frac{\tan\left(\theta_s\right) \cdot \cos(\alpha)}{3 \cdot \phi_{b.s} + 2.4 \cdot \phi_{min.s}}$$

$$\phi_{w.s}\left(d_{ec}, d_f\right) := \Lambda\left(d_{ec}, d_f\right) \frac{1}{2} \left[\frac{-c \cdot \phi_{min.s}}{1 + c \cdot \Lambda\left(d_{ec}, d_f\right)} + \frac{\tan\left(\theta_s\right) \cdot \cos(\alpha)}{\left(1 + c \cdot \Lambda\left(d_{ec}, d_f\right)\right)^2} + \sin(\alpha) \right] \cdot \left(1 - \exp\left(\frac{-2 \cdot z_f}{\Lambda\left(d_{ec}, d_f\right) \cdot \sin(\alpha)}\right) \right)$$

Clogged Elastocoast on a 0.2 m thick granular filter

Page 1 of 1